1989

Ultrasonic attenuation estimation for tissue characterization

Viren R. Amin
Iowa State University

Ultrasonic attenuation estimation for tissue characterization

by

Viren R. Amin

A Thesis Submitted to the

Graduate Faculty in Partial Fulfillment of the

Requirements for the Degree of

MASTER OF SCIENCE

Interdepartmental Program: Biomedical Engineering
Major: Biomedical Engineering

Iowa State University
Ames, Iowa
1989

TABLE OF CONTENTS

LIST OF TABLES

LIST OF FIGURES

CHAPTER 1. INTRODUCTION

Ultrasound applications to the fields of medicine, agriculture, and food are relatively recent developments which parallel rapid growth in electronic and signal processing technologies. After the piezoelectric effect (upon which the generation and detection of an ultrasound signal depend) was noted by Pierre and Jacques Curie in 1880, it was only in early 1940s when the first use of ultrasound in medical imaging was reported. Since then, in last 45 years, ultrasonic techniques have become an integral part of diagnostic imaging.

Ultrasound imaging techniques non-invasively obtain information about size and structure of the tissues, and functions of the organs of the body. The interactions of transmitted ultrasound with tissue structures give rise to the information which can be visually displayed. This information is therefore directly related to acoustic properties of the tissues and is essentially different from that supplied by other diagnostic tools such as an x-ray or isotope imaging. Because of its marked superiority (particularly for safety, size and cost) over x-ray for soft-tissue visualization, ultrasonography is rapidly supplementing, and in some instances, replacing x-ray for soft-tissue visualization. Many applications in obstetrics, gynecology, hepatic, breast, cardiac, renal, pancreatic, neurological, and vascular imaging are now standard. Work is in progress to apply improvements in resolution and tissue differentiation to ultrasonic images,

and even to find parameters for pathology differentiation.

In recent years, many ultrasonic parameters have been found to have potential for tissue characterization. These include attenuation, velocity, reflection, and scattering. Advanced signal processing and pattern recognition techniques are applied to extract information about particular parameters. Attenuation has been found to have potential for characterizing the tissues because tissues differ in their attenuation values for ultrasound. These might be used to differentiate the tissues, to diagnose various pathologies, or to improve the ultrasonic images. In the meat industry, this could be applied to differentiate (and ultimately, to grade) samples with varying contents and distribution of fat and muscle tissues.

The purpose of this research was to develop a personal computer based system by which the ultrasonic attenuation parameter for different tissue samples could be estimated, and its potential for tissue characterization/differentiation could be determined. Specifically, this involved the following objectives:

- Set up a simple hardware system that can take several A-scans of a tissue sample at varying angles, digitize the signal at varying depths of the sample and at high MHz sampling rate, and store it in a computer.
- Find an appropriate method for estimating attenuation of ultrasound in the tissue sample from the stored signal, and develop appropriate signal processing routines.
- Analyze the attenuation results in order to determine their correlations, if any, with relative fat/muscle contents in different tissue samples.
- Determine effects of bandwidth and center frequency of the transducer, on accuracy and consistency of the attenuation results, by using two different transducers (a narrow-band and a wide-band). Also, an effort is made to compare the results using two spectral estimation techniques.

Chapter 2 reviews the basics of ultrasonics and describes some parameters useful for tissue characterization. The attenuation as a tissue characterizing parameter is discussed, in detail, in Chapter 3. It also reviews the attenuation data for normal and pathological tissues, and their clinical significance. Recently developed techniques for estimating attenuation in tissues is reviewed in detail, since finding the best suitable method for fat/muscle differentiation was the first and perhaps crucial step in this research.

The development of the personal computer based data-acquisition system is described in Chapter 4. It also describes the developed software, implementing the log-spectral difference method of attenuation estimation. The results of this study are presented in and discussed in Chapter 5. The attenuation was found to be an useful parameter for differentiating tissues, depending upon their fat/muscle contents.

CHAPTER 2. BASICS OF ULTRASONICS

The phenomenon of ultrasound is the same as that of normal audible sound. It occurs when mechanical vibrations in one region of a medium are transmitted to another region by the mechanical interaction of the atoms and molecules of the medium. Ultrasound is the term used to describe the sound when pitch is too high for human ears to hear. The lower limit of the ultrasonic spectrum is usually taken as about 20 KHz. The frequency range of ultrasound for medical applications is usually between 1 MHz and 20 MHz.

Generation and Detection of Ultrasound

There are several types of devices that can be used to generate and detect ultrasonic waves. The most common type of transducer used in medical ultrasound employs the **piezoelectric effect** (Greek word *piezein* means *to press*). This is the property of certain materials where an application of an electric field causes a change in physical dimensions and vice versa. Commonly used (natural and synthetic) piezoelectric materials are quartz, barium titanate, lead zirconate titanate (PZT), or poly(vinylidine fluoride) (PVDF).

As shown in Figure 2.1a, two opposite faces of the transducer disc are plated with conductive metal films; a voltage V is applied to produce an electric field E_z across

the thickness l of the transducer, whose magnitude is given by $E_z = V/l$ (assuming the diameter is much larger than l).

The expansion or contraction of the transducer, (for this so called *thickness mode* of orientation,) depends on the polarity of the signal. Oscillating signals cause the transducer to vibrate, resulting in propagation of sound waves into the medium with which the crystal is in contact. The most efficient transduction of energy occurs at natural resonance frequency. This is determined by thickness of the piezoelectric element; the thinner the element, the higher the frequency.

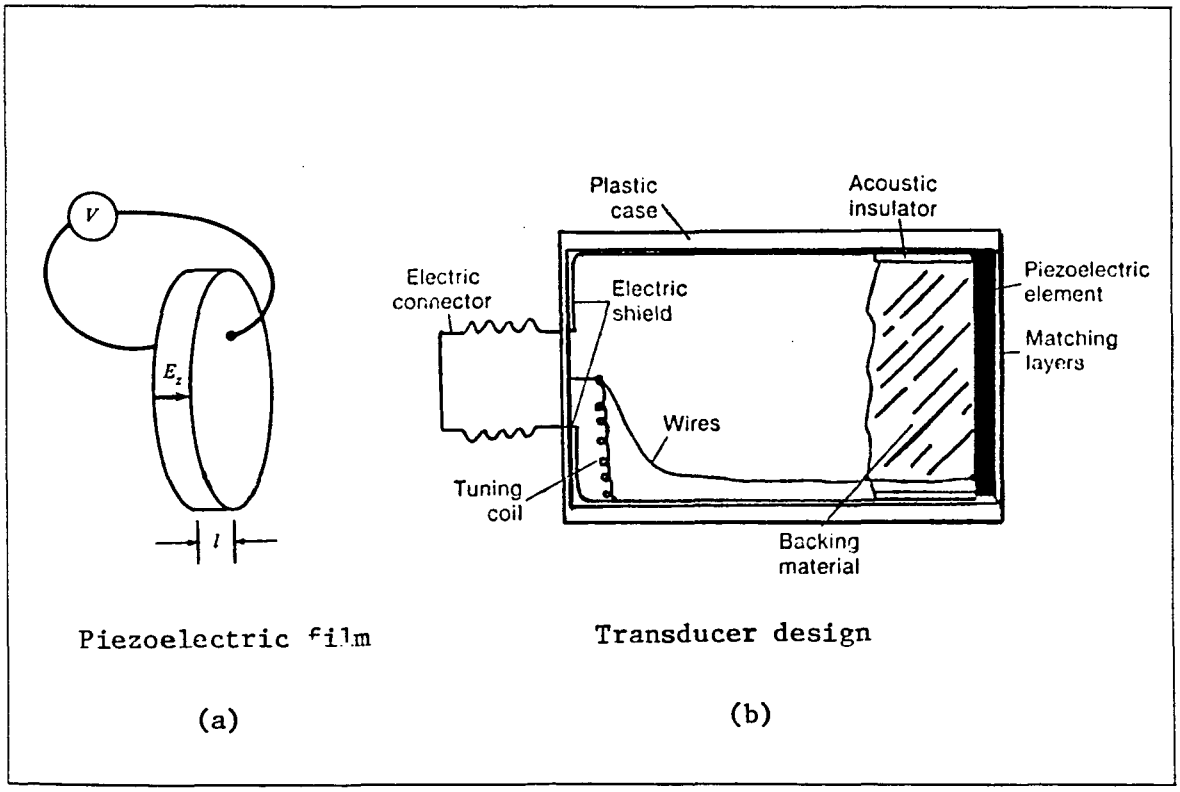

Figure 2.1: Basic transducer design for ultrasonic pulse-echo applications [(a) simplified sketch of a piezoelectric material used as a transducer with opposing electrodes, and (b) schematic of a single-element nonfocused transducer used in pulse-echo applications]

Figure 2.1b shows the basic design of a single-element non-focused transducer. Such a transducer is used both as transmitter and receiver. A flat, circular disc of piezoelectric material is mounted coaxially in a cylindrical case. The backing material plays a major role in *damping out* the transducer oscillations when excited by a pulse. Acoustic impedance of the backing material is matched to that of the piezoelectric element to reduce reflections at the interface. Also, it is filled with special sound-absorbing material (e.g., aluminum-filled epoxy or tungsten-filled epoxy) to damp the oscillations, resulting in the transmission of short duration acoustic impulses into the medium. Attachment of impedance-matching layers to the front face of the transducer provides more efficient transmission of sound waves from the transducer element to soft tissue and vice versa.

Frequency Characteristics of the Transducer

The frequency response of a transducer system is sometimes described by a term called *quality factor* or **Q-factor.** It is defined as a ratio of resonance frequency to bandwidth (for -3 dB power). As shown in Figure 2.2a, higher Q means narrow bandwidth. The magnitude of Q is mainly determined by the losses encountered in the transducer.

For pulse-echo system, the bandwidth depends upon the pulse duration; the shorter the pulse, the wider the bandwidth (Figure 2.2b).

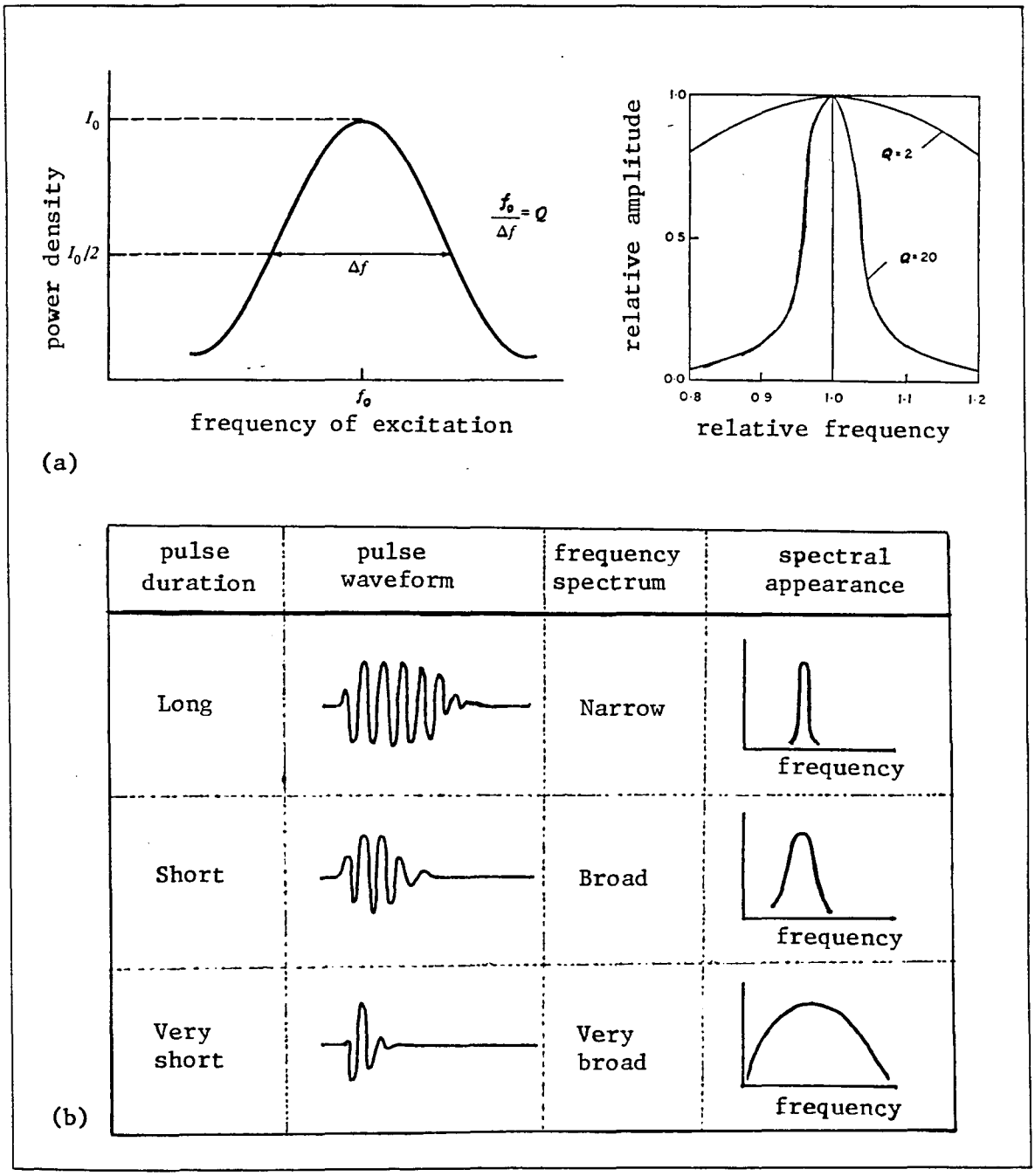

Figure 2.2: Frequency characteristics of the transducer and pulsed ultrasound [(a) the resonance curve for a transducer with center frequency f_1 and quality factor Q. The larger the Q, the narrower the frequency response. (b) the relationship between pulse duration and frequency characteristics of pulse-echo system]

Axial Resolution

The transducer frequency characteristics are closely related to the axial resolution of pulse-echo system. Axial resolution is limited by the pulse duration; the shorter the pulse duration, the better is the axial resolution (Figure 2.3).

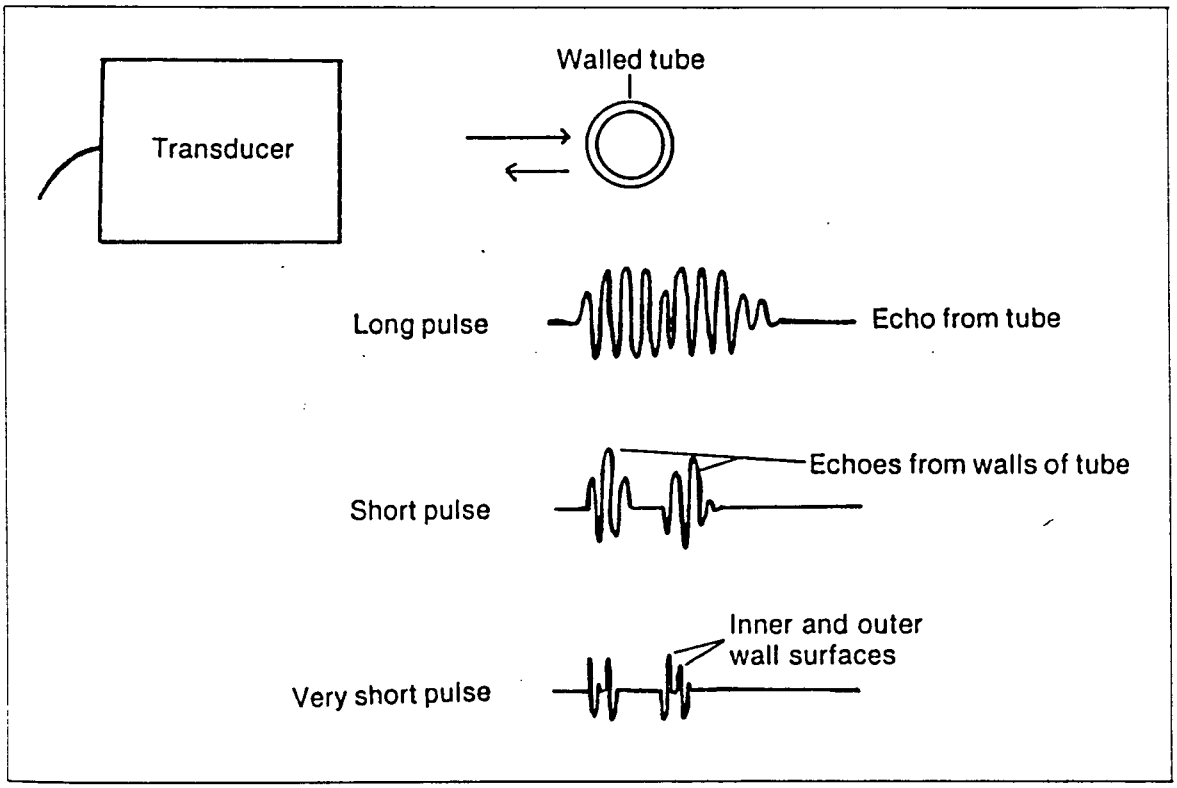

Figure 2.3: Relationship between pulse duration and axial resolution for the pulsed ultrasound (the shorter the pulse duration, the better the axial resolution)

Beam Pattern and Lateral Resolution

The sound beam produced by an unfocused circular transducer maintains the approximate lateral dimensions of the transducer for a certain distance, referred to

as *near field* or *Fresnel zone*. At larger distances, the natural divergence begins to spread the transverse extent of the beam, referred to as *far field* or *Fraunhofer zone* (Figure 2.4).

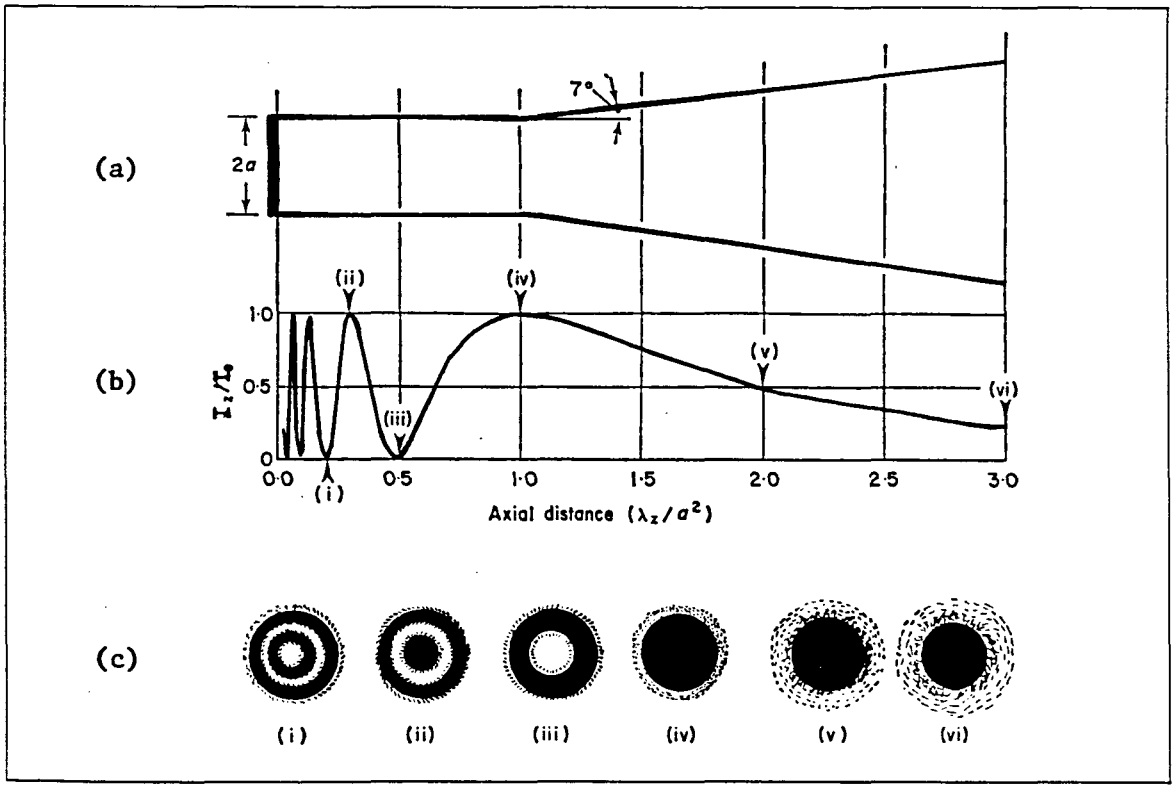

Figure 2.4: The ultrasonic field of a plane disc transducer [(a) conventional *textbook* representation of the field, (b) relative intensity distribution along the central axis of the beam, and (c) ring diagrams showing the energy distribution of the beam sections at positions indicated in (b)]

The **lateral resolution** for pulse-echo system is most closely related to the transducer beam width at the depth of interest. The beam width from an unfocused transducer is generally too wide to give adequate lateral resolution. Therefore, a lens or other focussing scheme (such as a spherical reflector or focused annular array of transducers) is sometimes employed to converge the radiating beam into a relatively

small spot at the focal plane. The size (i.e., lateral dimensions) and the depth (i.e., axial distance over which the beam maintains its approximate focused size) of focus are important parameters determining lateral resolution. Recently the approach has been to generate a moving focus for transmitter and receiver, using complex electronic circuits, for maximum possible resolution.

Transducer Selection

We have seen that the transducers vary in frequency characteristics, focal zone, and face diameter. Choosing the correct transducer for a specific scanning situation is essential. The selection of the center frequency of the transducer is a trade off between the penetration depth of ultrasonic beam and axial resolution. Visualizing deep structures requires more penetration; therefore, a lower frequency transducer is desired which, in turn, gives less axial resolution. *As a general rule, it is best to use the highest frequency that allows adequate penetration.*

The focal zone of the transducer is the distance range at which the lateral resolution is best. It is selected according to the depth of the structure to be scanned. The diameter of the transducer face is an important factor when the window, through which the transducer scans the structure, is small; e.g., intercostal spaces. In such situations, it may not be possible to achieve proper focal zone. For abdominal scanning, an array of transducers is widely used.

Thus, the transducer selection is a matter of compromise: frequency vs. penetration, and focal zone vs. face size. It may be helpful to examine the same area with different transducers to obtain the most information.

Ultrasound/Tissue Interactions

When an ultrasonic pulse travels through the tissues of the body, it undergoes continuous modifications, which depend on characteristics of sound waves as well as tissues. This section describes some important parameters of ultrasound/tissue interactions.

Velocity

The speed at which ultrasound travels through a medium depends on the density and compressibility of the material. The more solid the material, the greater is the velocity of sound. Table 2.1 shows the values for biological tissues.

As seen from values for water at different temperatures, the velocity increases with the temperature. It also depends on condition of the tissue, e.g., dead or living. In ultrasonics for tissue characterization, there are a few situations, listed below, in which the knowledge of the velocity is relevant.

1. For conversion of pulse-return time into the depth of tissue.
2. To calculate the acoustic impedance of tissue, which allows echo size to be estimated.
3. Refraction (deviation of ultrasonic beam) occurs at tissue interfaces when velocity differs in two tissues.
4. To produce B-scan images of tissues, an average value for the velocity of sound in the examined tissue, rather than the exact velocity for each individual tissue, is taken. This can create errors, typically about 2mm in range of 20 cm for abdominal scanning (McDicken, 1976, p. 44). Using this fact, velocity profile imaging techniques have recently emerged, producing tomograms of spatial distribution of velocities in tissues from their time-of-flight properties (Greenleaf and Johnson, 1975).

Table 2.1: Mean velocity values for selected biological tissues (data selected from Wells, 1977, p. 125; McDicken, 1976, p. 43; and Christensen, 1988, p. 61)

Tissue/material	Mean velocity (m/sec)
Air	330
Aqueous humour	1500
Blood	1570
Bone (skull)	4080
Brain	1540
Breast	1510
Fat	1450
Kidney	1561
Lens of eye	1620
Liver	1550
Lung	658
Muscle (skeletal)	1585
Soft tissues (average)	**1540**
Vitreous humour	1520
Water (20^{O} C.)	1480
Water (50^{O} C.)	1540

Acoustic Impedance and Reflection

Acoustic impedance of tissue is the resistance exerted by tissue to the sound propagation; it is given by the product of tissue density (ρ) and the velocity of sound (c) for the tissue, $\rho\ c$. An echo is generated at a tissue interface if the acoustic impedances of two tissues on either side are different. Echo size is determined by magnitude of the difference in the impedance. The ease with which any mass, e.g., a tumor, is detected in diagnostic ultrasonics is highly dependent on its acoustic impedance relative to that of the surrounding tissue.

Specular reflector is the term used for a large, flat surface reflecting a perpendicularly (or normally) incident beam. Here, the reflected beam is also perpendicular to the surface, so the same transducer can receive it. Specular reflection is very common in abdominal scanning; examples are capsules of the liver and kidney, the gall bladder, and the aorta.

The size of echo due to reflection at a particular interface is expressed as the ratio of reflected wave amplitude to the incident wave amplitude. This ratio is also known as **reflection coefficient** (R).

$$R = \frac{P_r}{P_i} = \frac{Z_1 - Z_2}{Z_1 + Z_2}$$

where P_i, P_r = pressure amplitudes of the incident and the reflected beams,
Z_1, Z_2 = impedances of the tissues making the interface.

Amplitude ratios for boundaries of interest are shown in Table 2.2. The values from the table explain why scanning through lung or gas in the bowel, or through bone is difficult, and also why water is used as a coupling medium.

Refraction

For non-perpendicular sound beam incidence, the beam bends at the interface if the speed of sound changes across the interface; this causes the transmitted beam to emerge in a direction different from the incident beam. This is refraction and is illustrated in Figure 2.5.

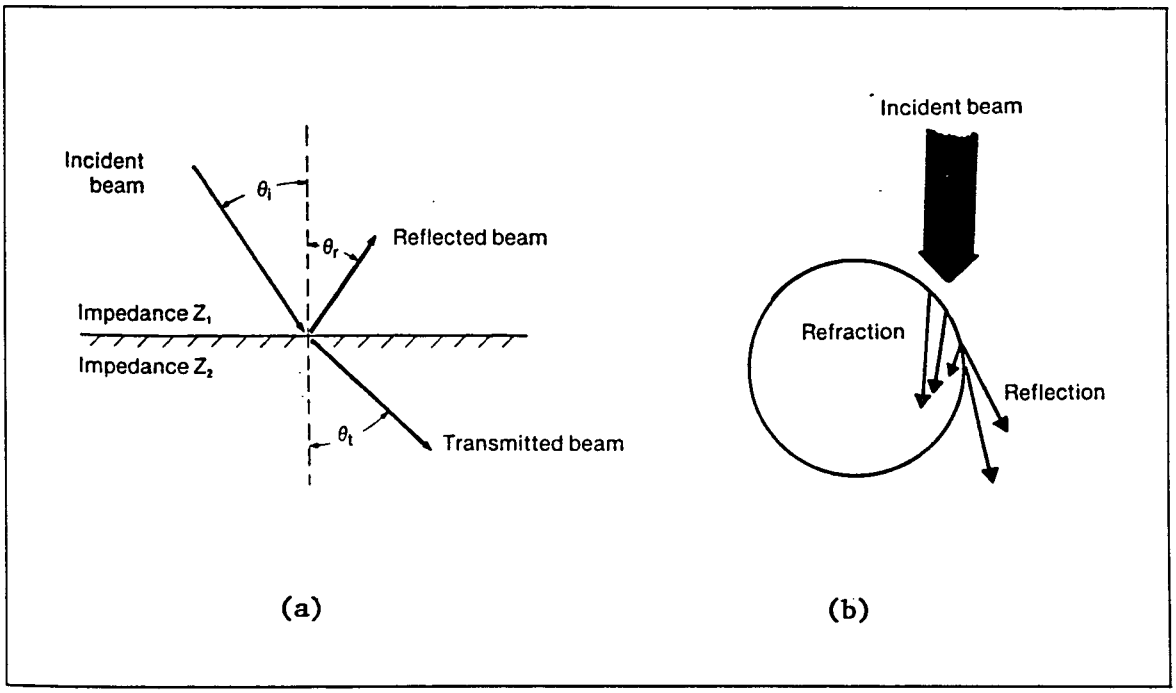

Figure 2.5: Reflection and refraction for non-perpendicular incidence of an ultrasound beam [(a) note that the transmitted beam angle θ_t is different than the incident beam angle θ_i (b) an example of refraction near an edge of a circular or tubular structure]

Table 2.2: Reflection coefficients (or amplitude ratios) and percentage energies reflected for normally incident waves at typical tissue interfaces (from McDicken, 1976, p. 47)

Reflecting interface	Amplitude ratio	Percentage energy reflected
Fat-Muscle	0.10	1.08
Fat-Kidney	0.08	0.64
Muscle-Blood	0.03	0.07
Bone-Fat	0.69	48.91
Bone-Muscle	0.64	41.23
Lens-Aqueous Humor	0.10	1.04
Soft tissue-Water	0.05	0.23
Soft tissue-Air	0.9995	99.90
Soft tissue-PZT5 crystal	0.89	80.00

Scattering

For smaller dimensions (about the magnitudes of wavelength of incident ultrasonic pulse) of interfacing surface, the incident wave is reflected in all directions and is said to be scattered (Figure 2.6). When the dimensions of scattering objects are very much less than the wavelength, it is known as **Rayleigh scattering**. Since the scattered wave spread in all directions, echo signals detected from a volume containing small scatterers are not highly dependent on the orientation of individual scatterers. This is in contrast to the strong orientation dependence seen for specular reflectors.

For very small scatterers, the scattering usually increases with increasing frequency; this can be used to an advantage in ultrasound imaging. Since specular reflection is frequency independent and scattering increases with frequency, it is often possible to enhance scattered signals over specular echo signals by utilizing higher

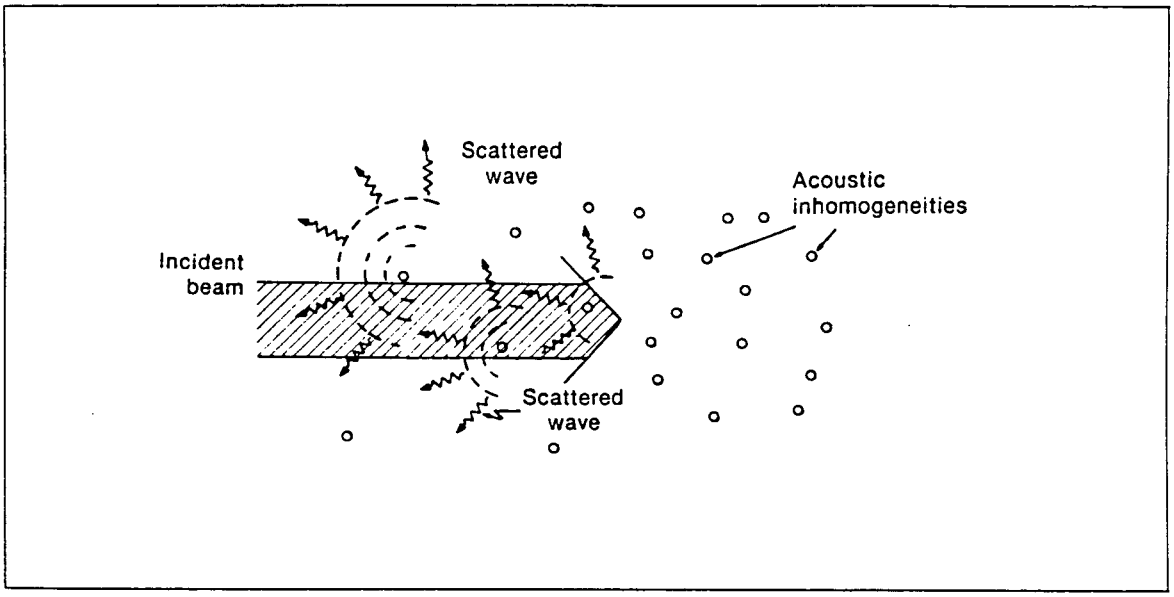

Figure 2.6: Scattering of sound at small interfaces (Hagen-Ansert, 1983, p. 8)

ultrasonic frequencies.

Backscatter coefficient is the term used to describe the ratio of energy scattered back through 180 degrees to incident energy, per unit area. Examples of small scatterers are red blood cells and multiple air-filled alveoli of lung tissue (where the scattering is so severe that 1 MHz ultrasound wave is considered non-penetrating to lung regions).

Absorption

Absorption of ultrasound is the process by which a portion of originally organized acoustic energy is transferred to subsequent heat. (Under ordinary circumstances with diagnostic ultrasound, the amount of heat produced is too small to cause a temperature change measurable by ordinary instruments.) Absorption increases with

frequency of sound; therefore it is said to exhibit dispersion.

Absorption and its mechanisms are rarely considered in isolation in routine clinical techniques. Total attenuation, which includes a number of other factors as well, is a more relevant quantity.

Attenuation

As a sound beam traverses through a medium, its amplitude and intensity are reduced as an exponential function of distance; this is referred to as attenuation. It is the result of interactions between ultrasound and tissue including absorption, reflection, and scattering. Mathematically, attenuation is defined in terms of attenuation coefficient (α), in the expressions

$$A = A_O \, e^{-\alpha l}$$

$$\alpha = \alpha_O \, f^n$$

where l = acoustic path length in attenuating medium
A_O = amplitude at $l = 0$
n = power of frequency dependence of α
α_O = a constant.

As seen from these equations, attenuation increases with increasing frequency, which limits the maximum frequency that can be used to scan the particular depth of tissue or region of body; the working frequency range is typically 1-5 MHz for scanning the abdomen, heart, or head, and 5-20 MHz for eyes. Thus, by limiting the maximum frequency, attenuation also limits the range resolution indirectly. Since attenuation is the parameter of interest in this study, it is discussed in detail in Chapter 3.

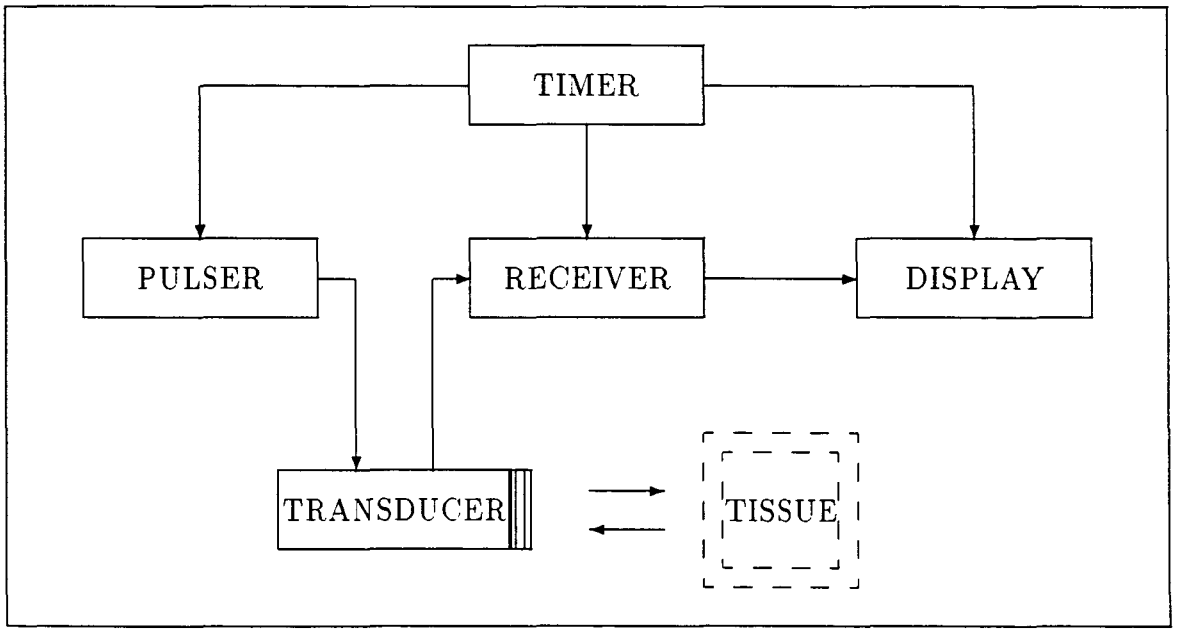

Figure 2.7: Block diagram of simplified pulse-echo instrument

Ultrasonic Instrumentation

Pulse echo ultrasound is widely used to localize and image structures in the body. The basic principle is that the distance between transmitter and reflector, d, is $c/2t$ where c is average speed of sound in the tissue and t is delay between transmitted pulse and received echo. The simplified block diagram of pulse echo instrument is shown in Figure 2.7.

Pulser

The pulser provides an impulse for driving the piezoelectric transducer. This is done at a fixed rate, called pulse repetition rate (prf). The pulse duration affects the

bandwidth of the transducer as mentioned earlier. The acoustic power is determined by amplitude of the pulser output.

Receiver

The receiver detects and amplifies the echoes. If only one transducer is used, the fraction of time that the transducer is actually emitting or receiving is indicated by *duty factor*, which is the dimensionless product of the prf (pulses/sec) and the time duration of each pulse (sec/pulse). Sound beam attenuation in tissue is compensated by using swept gain (also called TGC for time gain compensation) in the receiver.

Signal Processing

Besides amplification, the echo signals are often processed by rectification, compression and rejection to *condition* them for effective display. These basic steps are illustrated in Figure 2.8.

Display

A-mode is a one-dimensional display of echo amplitude, as shown in Figure 2.9a. This was widely used to diagnose midline shifting of brain (due to edema, hematoma, etc.) by comparing the distance of midline of brain (i.e., echo from Fax cebrii) from either sides of the skull.

Figure 2.8: The sequence of signal conditioning steps often implemented in processing of the received ultrasonic echoes (Modified from Christensen, 1988, p. 134)

(a) unprocessed, amplified echoes;

(b) after demodulation (rectification and smoothing), yielding the pulse envelop;

(c) time gain control (TGC) amplification;

(d) logarithmic compression;

(e) elimination of signals below threshold setting;

(f) sweeped B-scope; and

(g) triggered B-scope

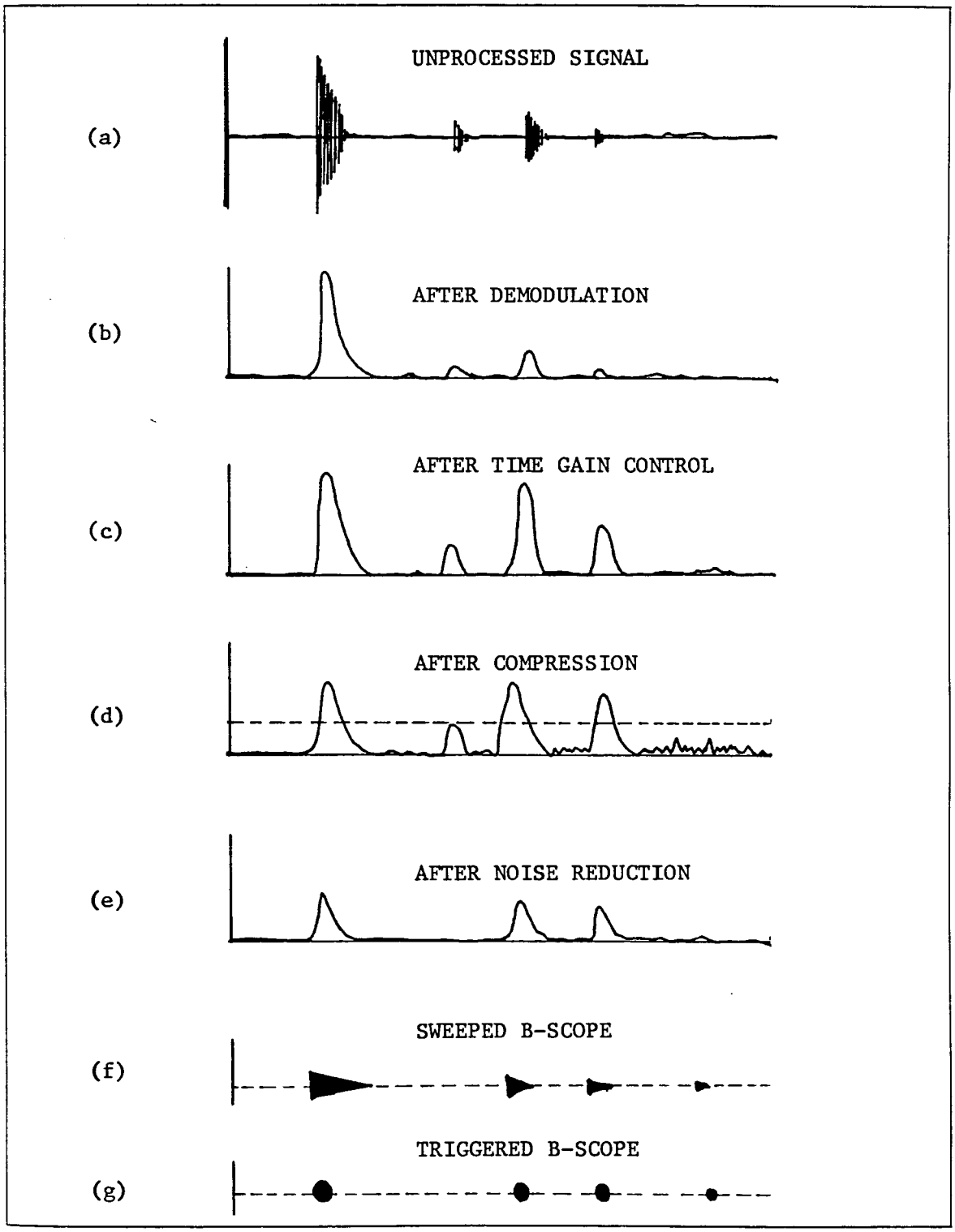
(a)
UNPROCESSED SIGNAL
(b)
AFTER DEMODULATION
(c)
AFTER TIME GAIN CONTROL
(d)
AFTER COMPRESSION
(e)
AFTER NOISE REDUCTION
(f)
SWEEPED B-SCOPE
(g)
TRIGGERED B-SCOPE

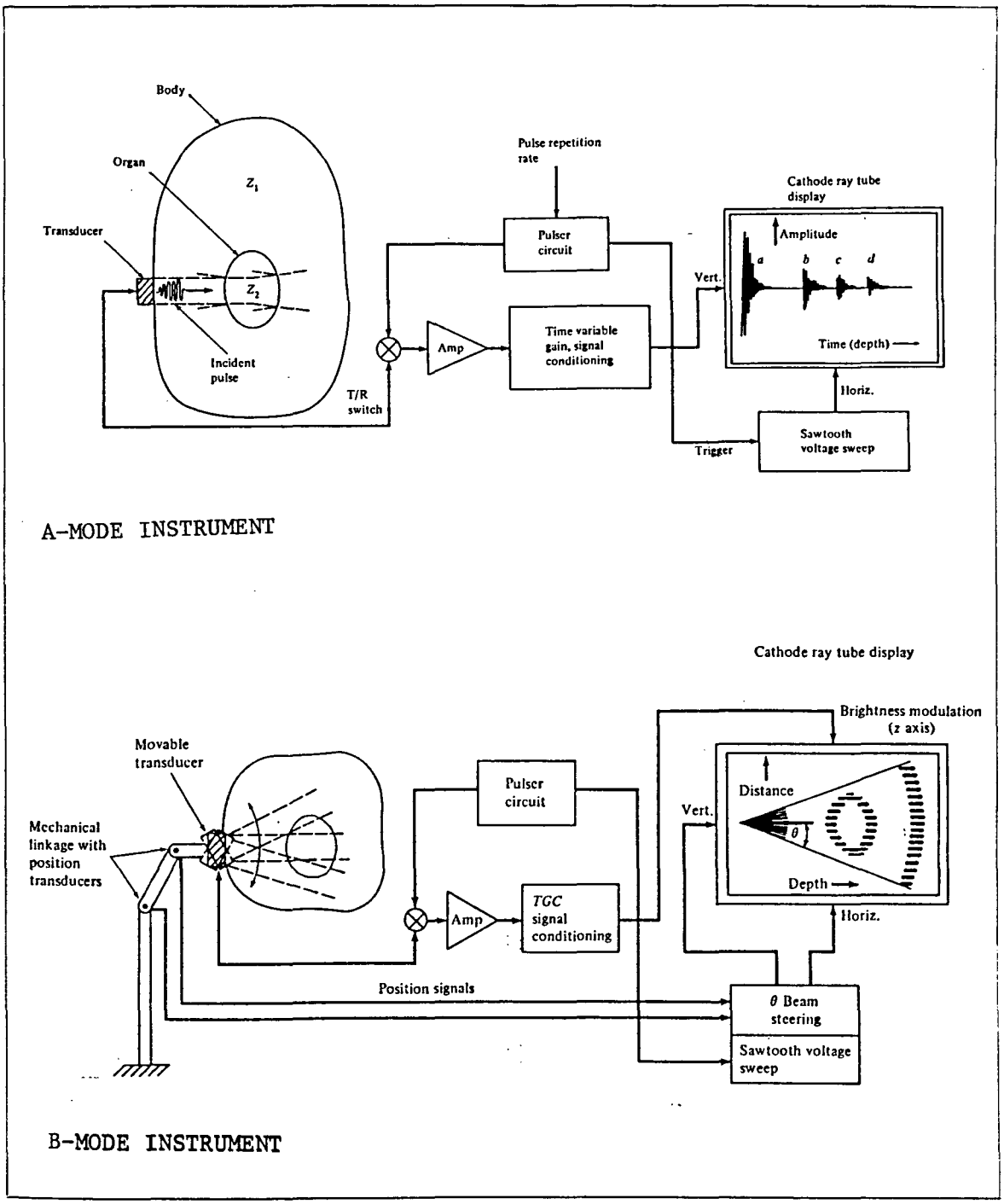

Figure 2.9: Elements of A-mode and B-mode pulse-echo instruments (Christensen, 1988, pp. 126 and 136)

B-mode is two dimensional display where the echo amplitude is modulated into brightness of the displayed beam (also called gray scale or z-axis modulation). This is shown in Figure 2.9b. The image is constructed from several A-mode signals taken at different angles. Most commercially available ultrasonic imaging systems use a variety of scanning methods. These include mechanical (rotating, oscillating, etc.) and electronic (linear array, phased array and annular array) scanners. Some examples are illustrated in Figure 2.10. The advantages of these complex arrangements are real time (therefore, also called real time scanner), precision scanning of larger area of tissues with better axial, and in case of annular array, lateral resolution.

C-mode refers to through-transmission imaging in which the ultrasound pulse is transmitted from one side of the body through to receiving transducers on the opposite side. Attenuation and velocity data may be obtained by this method.

Ultrasound Applications for Tissue Characterization

Ever since the use of ultrasound for tissue characterization began, it has grown tremendously, almost as a separate discipline. It is the second most widely used imaging technique, being next only to radiology. Ultrasonic tissue characterization involves the determination of propagation characteristics (velocity, attenuation, backscatter, etc.) of ultrasonic energy in various tissues. In the medical field, tissue characterization applications range from detecting a fetus in the uterus to differentiating pathologies of liver, breast, eye, etc., which can not be easily diagnosed by other methods.

Javanaud (1988) has reviewed applications of ultrasound to agricultural and food

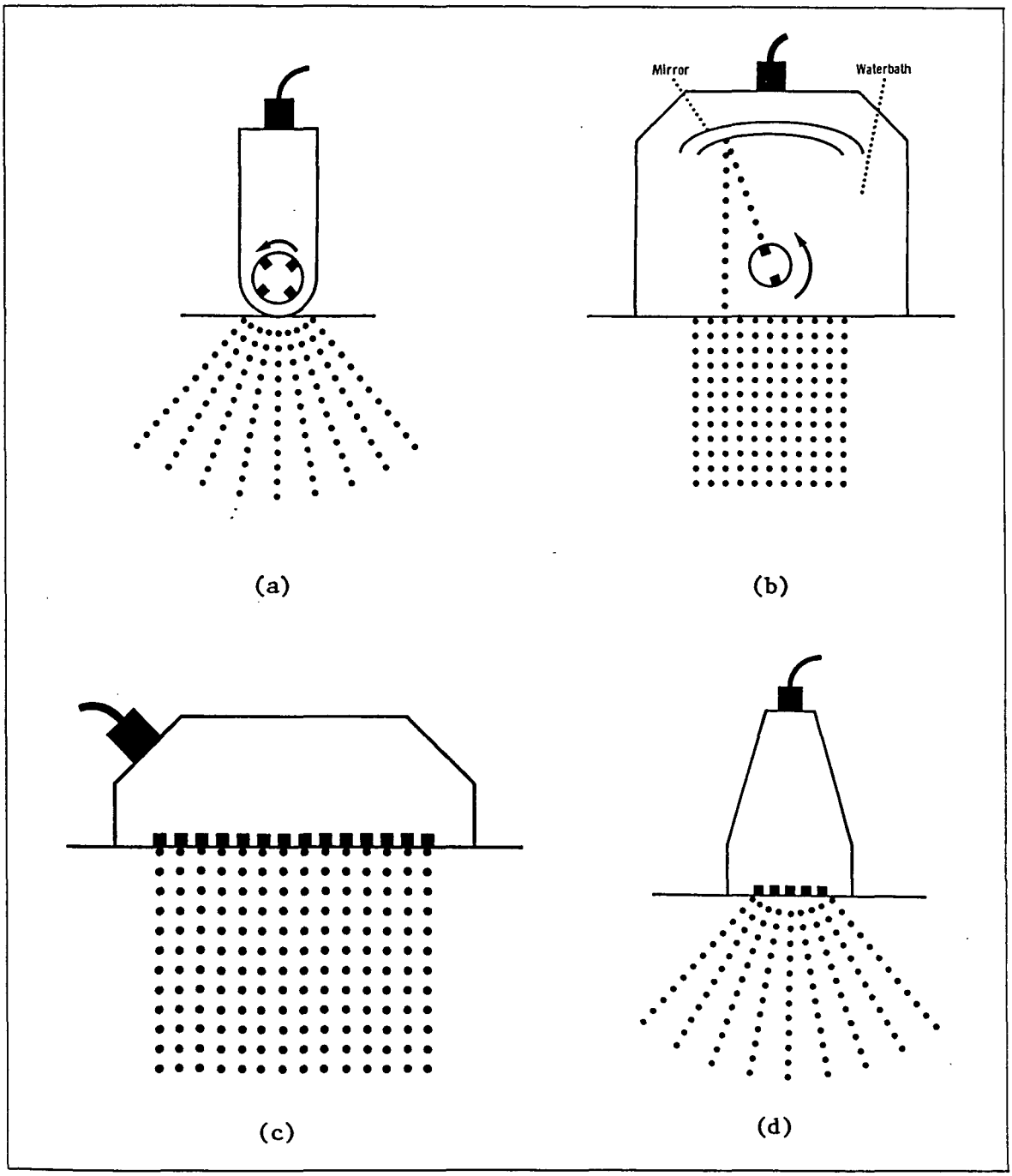

Figure 2.10: Examples of mechanical and electrical sweeping of the beam to obtain B-mode images [(a) transducers on rotating wheels, (b) oscillating transducer with reflector, (c) multi-element linear array, and (d) multi-element phased array]

industries. Recently, there has been growing interest in analyzing the composition of live animals by characterizing the tissues using ultrasound (Johnston et al., 1964; Haumschild and Carlson, 1983; Beach et al., 1983; and Miles et al., 1984).

CHAPTER 3. ULTRASONIC ATTENUATION: BACKGROUND AND LITERATURE REVIEW

As defined in the previous chapter, attenuation, in simple terms, is defined as a loss in acoustic intensity (power per unit cross-sectional area) as a transmitted ultrasound wave passes through tissue or any other medium. This chapter describes the attenuation phenomena. The data for biological tissues are given and clinical significance of some primary encouraging results are discussed. It also reviews various methods of estimating attenuation in clinical situations and their potentials in characterization of fat and muscle tissues.

Mechanisms for Attenuation

Attenuation is caused by number of processes such as absorption, scattering, reflection, refraction and wavefront divergence. In addition, when an ultrasound beam exits from tissue, additional losses may be detected that depend on the characteristics of the measurement apparatus, such as transducer aperture. For example, portions of the incident beam may be refracted or scattered and may never reach the measurement transducer.

Absorption is the fundamental tissue parameter responsible for attenuation (Linzer and Norton, 1982), although other mechanisms contribute to the observed at-

tenuation. Reflection, scattering and absorption contribute the most for measured attenuation.

Units of Measured Attenuation

By definition, attenuation can be expressed in units of intensity (watts/cm^2) or power (watts) lost per unit distance. Unfortunately, it is fairly difficult to interpret and calibrate instruments absolutely, since power levels are very low and vary with transducer selection. It is customary, therefore, to calibrate output levels by comparing them with a fixed arbitrary level using the decibel (dB) notation. Usually the output power is compared to input power for measuring attenuation of whole tissue; or recently the approach has been to compare powers at varying tissue depths for statistically better estimates of attenuation, particularly for inhomogeneous tissues. Attenuation can also be expressed as a ratio of wave echo amplitudes (pressure amplitude in voltage) in decibel notation[1]. Thus,

$$\text{Power attenuation} = 10 \log_{10}\left(\frac{P_1}{P_o}\right) \quad dB$$

$$\text{Amplitude attenuation} = 20 \log_{10}\left(\frac{A_1}{A_o}\right) \quad dB$$

where P_o, P_1 = reference and new power levels
A_o, A_1 = reference and new amplitude levels.

The replacement of factor of 10 by 20 in amplitude attenuation is related to the fact that on conversion from power to voltage, the voltage (V) appears as a square (V^2)

[1] In the literature, reference is frequently made to the *neper*; this is a logarithmic ratio defined as $\log_e(A_1/A_o)$, where A_1 and A_o are two amplitude levels. Hence, 1 neper = 8.686 dB.

and $10 \log_{10} V^2 = 20 \log_{10} V$.

When a wave is attenuated in a medium, the power levels and amplitude levels decrease at the same rate if they are measured in dB with respect to the reference level. It is therefore common practice to talk of attenuation in terms of dB per centimeter depth of tissue, without specifying whether power or amplitude is being discussed. Also, when measured thus, it is found to increase linearly with frequency, for most soft tissues; so it is expressed per unit frequency (i.e., per MHz) or at specific frequency (e.g., center frequency of transducer). Thus, the units of measured attenuation (i.e., α or $\alpha(f)$ as defined in Chapter 2) are:

Units of α :	dB cm^{-1} MHz^{-1}
or	dB cm^{-1} at 2.5 MHz

Since it is difficult to assess the individual contribution of mechanisms in routine diagnostic techniques, it is quite preferable to estimate the more relevant quantity, attenuation as a whole or **total attenuation**. In some literature, attenuation is referred to for only a single mechanism (e.g., absorption); it is recommended that these misleading terms should be avoided and the general term *attenuation* should be reserved for *total attenuation.*

Frequency Dependence of Attenuation

The importance of the various mechanisms is dependent on the wave frequency; therefore, the total attenuation is also a function of frequency. The attenuation of soft tissues increases monotonically with frequency in low MHz range. This frequency dependence of attenuation represents a useful parameter for tissue characterization

(Lele et al., 1975; Narayana and Ophir, 1983a). The frequency derivative or slope of this monotonically increasing function of frequency provides an useful index of attenuation. It has been shown that this slope is quite independent of whether or not the tissue attenuation exhibits a linear dependence on frequency (Jones and Behrens, 1981; Narayana and Ophir, 1983b).

Many investigators have worked to determine frequency dependence of attenuation for various normal and pathologic tissues. In general, for most soft tissues, this dependence is linear or almost linear (i.e., power of frequency dependence around 1) for most practical purposes. Non-linear frequency dependence has been found for blood, bone and lung tissues.

Attenuation Data for Biological Tissues

Biological tissues can be characterized ultrasonically by their attenuation, absorption, and velocity, which correlate well with the presence of major tissue components of water and protein, particularly collagen (Johnston et al., 1979). Compiled data of average attenuation for tissues by categories are shown in Table 3.1. As seen from the table, the structural tissues such as tendons and bones tend to be more attenuating than visceral organs such as liver, brain and kidney. Also, note that the frequency dependence of attenuation for blood, bone and lung is not linear, while most soft tissues exhibit a linear dependence. Increasing attenuation also correlates to decreasing water content, increasing protein content and increasing speed of sound in the tissue.

Table 3.1: Average attenuation for biological tissues by categories (data selected from Johnston et al., 1979; Dunn, 1975; and Goss et al., 1978 and 1980)

Tissue attenuation categories	Attenuation at f=1MHz (dB cm^{-1})	Tissue	Remark[a]	General trends: water content	collagen content	sound velocity
Very low	0.026	serum	-	↑ increasing H_2O content	increasing structural protein content ↓	increasing velocity of sound ↓
	0.087	blood	$f^{1.25}$			
Low	0.61	fat	@ 37^{o}C.			
Medium	0.87	brain	-			
	0.96	liver	-			
	0.7-1.4	muscle[b]	-			
	1.9	breast	-			
	2.0	heart	-			
	2.6	kidney	-			
High	4.3	tendon	-			
Very high	$\geq$ 8.7	bone	$f^{1.7}$			
	$\geq$ 34	lung	$f^{0.6}$			

[a] f^n represents the power of frequency dependence for attenuation in the power law model $\alpha(f) = \alpha_o f^n$ (spaces indicate a linear dependence, i.e., f^1).

[b] Striated muscle; attenuation along the fibers is higher than that across the fibers.

Half-value Layer Thickness: To give some appreciation of the role of attenuation in practice, the thicknesses of tissues required to reduce ultrasonic intensity by half (-3 dB) are listed in Table 3.2. Some interesting points can be noted from the table and related to practicabilities of imaging tissue structures.

1. Firstly, many soft tissues have similar attenuation characteristics, e.g., for brain and liver, the intensity of 2 MHz ultrasound is reduced by half in about 2 cm. Blood, on the other hand, is less attenuating and this helps the visualization of cardiac structures.

2. In general, fluids within the body are only weakly absorbing and are often referred to as *transonic* or *sonolucent*. Amniotic fluid, urine, aqueous humour, vitreous humour and cystic fluid allow structures lying behind them to be easily visualized. Indeed, a full bladder is standard technique for obtaining a *window*

Table 3.2: Thicknesses of biological tissues required to attenuate intensity of an ultrasound beam by half (-3 dB) (McDicken, 1976, p. 58)

Tissue/material	Thickness (in cm.) of tissue at				
	1 MHz	2 MHz	5 MHz	10 MHz	20 MHz
Aqueous humour	-	-	6	3	1.5
Air	0.25	0.06	0.01	-	-
Blood	17	8.5	3	2	1
Bone	0.2	0.1	0.04	-	-
Brain	3.5	2	1	-	-
Caster oil	3	0.75	0.12	-	-
Fat	5	2.5	1	0.5	0.25
Kidney	3	1.5	0.5	-	-
Lens of eye	-	-	0.3	0.15	0.07
Liver	3	1.5	0.5	-	-
Muscle	1.5	0.75	0.3	0.15	-
Perspex	1.5	0.7	0.3	0.15	0.07
Polythene	0.6	0.3	0.12	0.6	0.03
Soft tissues (average)	3	1.5	0.5	0.3	0.15
Vitreous humour	-	-	6	3	1.5
Water	1360	340	54	14	3.4

to the uterus. Water itself is very useful because of its extremely low absorption; for most practical purposes, water can be regarded as lossless and can therefore be used in immersion scanning with no loss of sensitivity.

3. Muscle is of special note in that it is anisotropic and a difference of a factor of 2.5 exists between the attenuation across and along its fibers.

4. The high attenuation in the bone, about 20 times that of soft tissues, creates many problems for ultrasonic scanning. B-scanning of the head is primarily difficult; bones also limit viewing access to the heart, eye and abdomen.

5. Gas bubbles in lung cause high attenuation by extremely strong scattering and absorption of the ultrasound and this makes it almost impossible to penetrate a normal lung with diagnostic ultrasound. Lung also limits examination of heart and much of the thorax.

6. A few non-biological materials also have noteworthy attenuation properties; attenuation in castor oil at low frequencies is similar to that in soft tissues, so

it is a convenient medium for constructing test and training phantoms.

7. Absorption in air is very high at diagnostic frequencies. Because of this and low acoustic impedance, transmission of ultrasound in air ceases to be practical above 0.5 MHz (McDicken, 1976, p. 59).

Clinical Significance of Attenuation

Tissue attenuation has been measured *in vitro* and *in vivo* by many investigators and some initial clinical results for several different estimation techniques have been obtained, particularly for liver, breast, eye, and uterus.

Some encouraging consistency has been noted among the results obtained using several different methods of estimation. Attenuation has been found to have potential to become a clinically measurable parameter for differential diagnosis of certain pathologies. Attenuation measurements *in vivo* and their correlation with biopsy and autopsy results has enabled separation of normal from pathologic tissues. Most investigators have chosen the liver as the target organ, primarily because of its large size, homogeneous nature of the backscatter, the ease of access and confirmation of the results through easy liver biopsy. Table 3.3 shows the attenuation data for liver pathology differentiation.

It should be noted that the ultrasonic attenuation may not serve as the only parameter for differential diagnosis, but it surely has potential to become an important, non-invasive, and relatively simple technique for soft tissue pathology differentiation.

Table 3.3: Summary of *in vivo* measurements of ultrasonic attenuation in liver using a variety of methods (Jones, 1984)

Pathology	Attenuation
Normal	• magnitude: 0.5 dB/cm @ 1 MHz (range 0.4 - 0.7) • frequency dependence[a]: 1.05 (range 0.95 - 1.15)
Cirrhosis	• 50% - 60% higher than corresponding normal • slightly greater frequency dependence
Hepatitis	• 30% - 40% lower than corresponding normal
Fatty	• high (when scattering dominates), or low (when absorption dominates) • higher frequency dependence (range 1.0 - 1.4)

[a]Represents the power, n, in the power law model $\alpha(f) = \alpha_O f^n$.

Methods of Attenuation Estimation

Ultrasonic attenuation has been measured *in vitro* by many investigators ever since the field of diagnostic ultrasound began. In last fifteen years, there has been good progress in this area and many *in vivo* methods, too, have been developed to estimate attenuation in a clinically useful manner. The goal in measurement of attenuation is to provide an objective and reliable index to quantitate the subjective, equipment-dependent estimates of attenuation that clinicians have found useful in interpreting ultrasonic images. Some uses for measurements of attenuation include:

- Improved time gain compensation for imaging (Melton and Skorton, 1981).
- Compensating backscatter measurements for the attenuation of intervening tissue (Cohen et al., 1982; and O'Donnell, 1983).
- Estimating local values of attenuation for purposes of tissue characterization (Shawker, 1984; Maklad, 1984; and Jones, 1984).
- As a long term goal, quantitate the backscatter and attenuation imaging (O'-Donnell, 1983; and Duck and Hill, 1979).

Qualitative estimation in B-mode On the standard B-mode image, the effects of attenuation are subjectively observed by ultrasonographer. Attenuation of localized lesions is judged by the appearance of the *posterior echoes*, i.e., amplitude of the returning echoes from the far side of a lesion. Terms such as *acoustic enhancement* (echo amplitude higher than the surrounding tissues) and *acoustic shadowing* (total absence of the posterior echoes) are qualitative descriptions of this posterior echo amplitude. This helps distinguish cystic and solid masses.

Attenuation in large masses or entire organs is generally estimated by the relative difficulty of *beam penetration.* This is subjectively evaluated by noting the transducer frequency, the instrument gain, and the time-gain-compensation (TCG) settings required to *penetrate* an organ or large mass, and to uniformly display the echoes in near and far fields of the transducer.

Quantitative estimation in reflection Over the past several years, several pulse echo techniques for quantitative estimation of attenuation have been developed, and some initial clinical results have been obtained, particularly for the liver. These methods can be grouped in time domain and frequency domain methods. In general, time domain methods are adaptable to real time implementations, which feature speed at the expense of flexibility. On the other hand, the frequency domain techniques allow flexibility of implementation, but tend to require off-line processing.

An excellent review of these techniques could be found in literature (Miller, 1984; and Flax, 1984). Since the part of this research was to select the best method for application to fat and muscle characterization, some methods are discussed in detail here.

Frequency Domain Methods

These methods fall generally into two main kinds: spectral difference methods and spectral shift methods. A relatively new approach of matched filter pulse compression is also considered in this category.

1. Log Spectral Difference Techniques: In these techniques, the log-power of the signal, attenuated by its path through the tissue, is compared with reference log-power. As shown in Figure 3.1, the log-power difference is plotted against frequency and *least square slope* over the transducer bandwidth is calculated. Dividing this slope by the distance the signal traveled (in cm.), gives the coefficient of attenuation in dB cm^{-1} MHz^{-1}. There are several approaches to obtain attenuated and reference spectra, as illustrated in Figure 3.2 and described below.

TRANSMISSION APPROACH: Here, a broad band pulse passes through the tissue of interest and is received by a second transducer (Figure 3.2a). The attenuation is estimated by comparing the response obtained with only water (or physiological saline) between transducers and the response obtained when tissue is substituted.

SHADOWED REFLECTOR APPROACH: This represents a slight modification of the transmission method, in which single transducer emits and receives a pulse that passes through the tissue a second time after being reflected from a flat metal or glass plate (Figure 3.2b).

BACKSCATTER APPROACH: A conceptually simple approach for estimating attenuation from backscatter signal is to compare spectra of echoes obtained from front and back tissue interfaces. This approach is impractical in most cases because

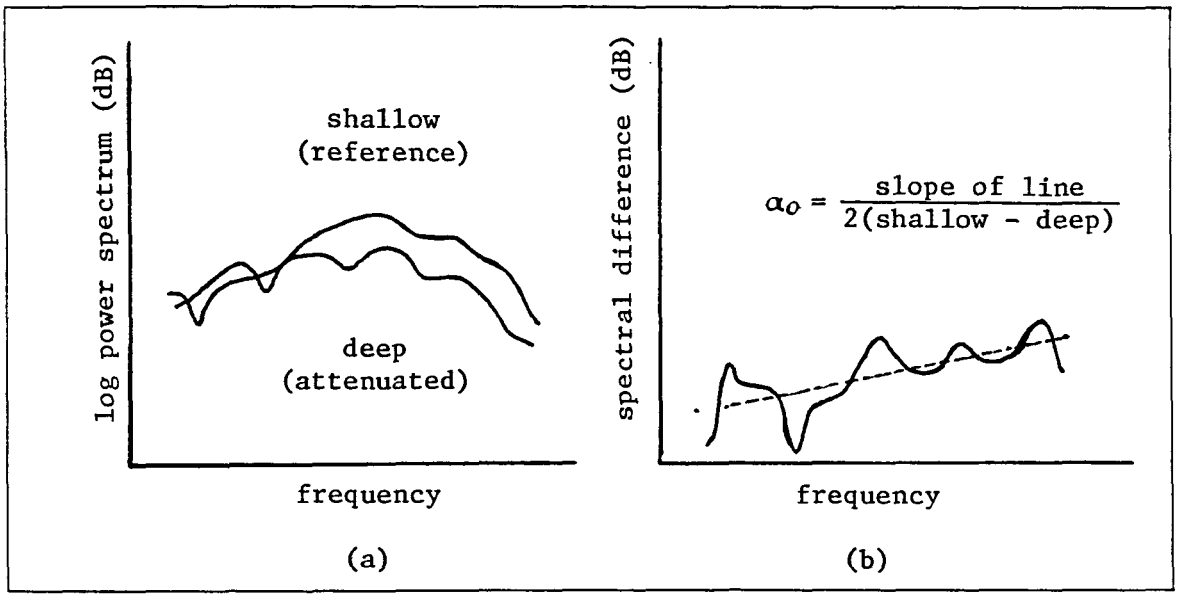

Figure 3.1: Log-spectral difference technique for estimation of attenuation [(a) reference and attenuated log-power spectra, and (b) log-spectral difference and *least square fit* to calculate the slope and coefficient of attenuation]

of the irregular shapes of the surface of organs of interest and the specular echoes that arise from tissue interfaces are highly dependent on geometrical factors that can not be controlled.

It is difficult to adapt the techniques just described to *in vivo* situations, due to the factors listed below (Ophir et al., 1984).

1. Tissue does not contain reliable reference reflectors, and therefore estimates must be made from a noisy statistical ensembles of scatterers. This limits the precision and spatial resolution obtainable in the estimate.

2. Evidence indicates that the main contribution to attenuation is from absorption and not from scattering. The attenuation estimates, however, rely heavily on the properties of the scatterers, such that small changes in these properties could readily result in erroneously large changes in the attenuation estimates.

3. Frequency dependence of attenuation may not be linear, thus reducing the spectral bandwidth of the interrogating pulse (Narayana and Ophir, 1983c).

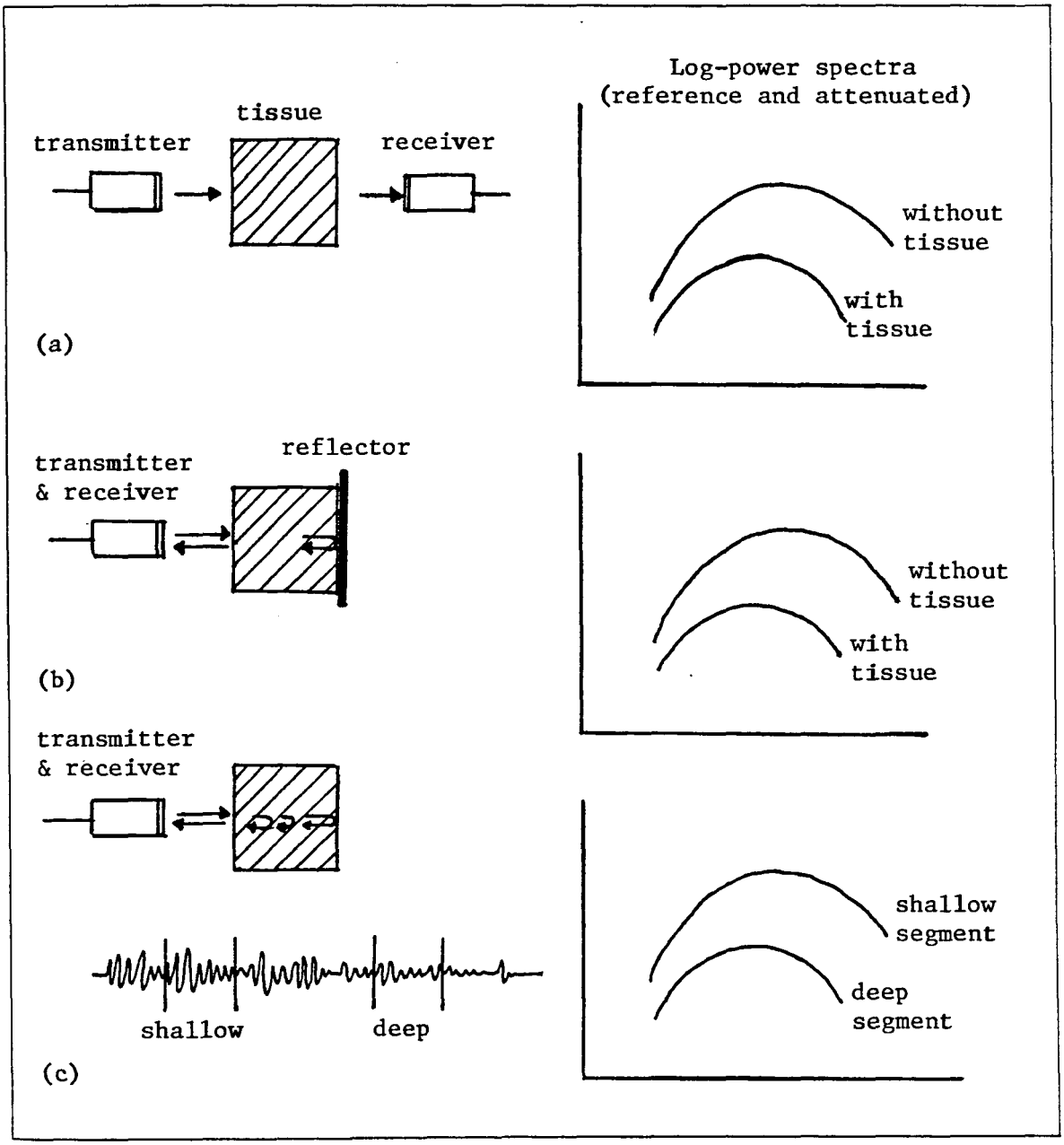

Figure 3.2: Approaches to obtain the reference and attenuated spectra for log-spectral difference technique of attenuation estimation [(a) transmission approach, (b) shadowed reflector approach, and (c) shallow and deep segments of the backscattered signal from interior of the tissue]

4. Various techniques estimate different quantities which are related to attenuation under certain assumptions (e.g., tissue model of scatterers and specular reflection). The validity of these assumptions is difficult to ascertain.
5. Transmission and shaded reflector methods can not be adapted clinically for obvious reasons.

Consequently, most of the techniques proposed for estimating attenuation in reflection concentrate on relatively weak backscattered signals emanating from the interior of the tissue. Figure 3.2c illustrates steps in this method. A shallow and a deep segment are extracted from rf A-mode signal and power spectra are obtained using appropriate method. One common approach is to take the Fourier transform using the Hanning window.

Assuming that the backscatter coefficient is the same in shallow and deep segments, log spectral difference can be obtained and attenuation coefficient (α) and slope (α_0) can be calculated as described earlier. The following points should be noted about this method.

- The mean slope exhibited by tissue volume is obtained by averaging axially (along A-mode signal) and laterally (adjacent A-mode signals). This reduces the variance (Fink et al., 1983; Lizzi and Laviola, 1976; and Kuc and Taylor, 1982).
- The optimal separation between shallow and deep pairs in rf A-mode data for axial averaging is suggested to be 2/3 of total length of the A-mode signal (Kuc et al., 1977; and Kuc and Schwartz, 1979).
- Smoothing the spectra (in frequency, autocorrelation, or cepstral domain) has some effect in improving the estimates (Robinson, 1979; and Fraser et al., 1979).

2. Spectral Shift Technique: This approach is based on the fact that soft tissues exhibit transfer characteristics of a low-pass filter (because the ultrasonic attenuation increases monotonically with frequency). This selective attenuation of the

high frequency results in a decrease, with distance travelled, in the peak frequency, the average frequency (centroid), and the bandwidth of the received signal in general. This is illustrated in Figure 3.3.

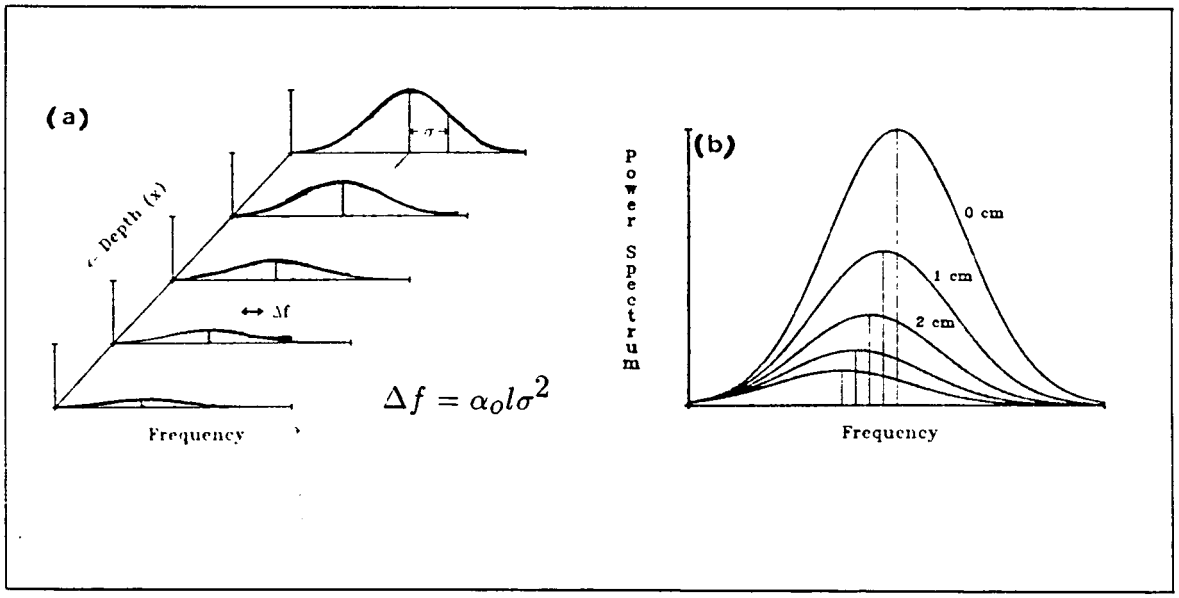

Figure 3.3: Illustration of the shift of the spectrum to lower frequencies as an ultrasonic pulse propagates through an attenuating medium

In these methods, models for the transmitted pulse shape and for the frequency dependence of attenuation are assumed to relate measured changes in the spectrum to the attenuation. Usually, the spectrum is modelled as a Gaussian with variance σ^2; then, the shape of the spectrum remains unchanged and the variance is preserved. The shift in frequency (Δf) is proportional to the slope of attenuation (α_o), the distance travelled (l) and the variance of the pulse as

$$f_c = f_o - \alpha_o l \sigma^2 \qquad or \qquad \Delta f = \alpha_o l \sigma^2 \tag{3.1}$$

where f_o is transducer center frequency and f_c is the shifted center frequency. It

has been shown that an estimate of the centroid provides a better measure of the frequency shift than an estimate based on the peak frequency. The centroid ($< f >$) can be calculated as

$$< f > = \frac{\int_{f_1}^{f_2} f|E(f)|^2 \, df}{\int_{f_1}^{f_2} |E(f)|^2 \, df}$$

where $|E(f)|^2$ is the power spectrum of the windowed rf segment.

3. Matched Filter Pulse Compression Technique: This new concept was developed by Meyer (1979 and 1982). The motivation for this approach is the limitations of time gated pulse echo ultrasound. Tissue segments from which received power spectra are computed can not be made arbitrarily short, because reducing the time windows blurs the power spectra (a trade-off between axial resolution and spectral resolution). Also, interference effects resulting from the overlap of signals emanating from adjacent regions of tissue compromise estimates of attenuation.

The matched filter pulse compression method (also called as matched filter cross-correlation method) overcomes these drawbacks. It is capable of providing results that are independent of overlaping echo wave-trains from adjacent tissue regions separated in time by $2/\Delta f$, where Δf is the system bandwidth. For example, for a bandwidth of 5 MHz, attenuation coefficient from tissue segments as small as 0.3 mm can be determined independently. This has potential of high resolution attenuation imaging. It is beyond scope of this document to discuss this method any further, but the interested reader is urged to refer the original literature (Meyer, 1979 and 1982).

This is a good point to write about terms **parametric** and **non-parametric**

for attenuation estimation techniques. A parametric method of analysis is one which requires the transmitted ultrasonic pulse to be of convenient mathematical parameters, e.g., as a Gaussian shape pulse. In contrast, a non-parametric method does not require such characteristics of transmitting pulse. For example, frequency shift method is a parametric one, while log-spectral and matched filter pulse compression methods are non-parametric ones.

Time Domain Methods

Just as the attenuation information in the frequency domain is carried in the amplitude and center frequency of the rf spectrum, so is the attenuation information in the time domain contained in the amplitude and rate of zero-crossings of the rf signal itself. The important advantage of time domain methods is the possibility of real time implementation.

1. Amplitude Difference Method: In this method, the difference in the amplitudes of backscattered echoes from two planes in the tissue is measured. This amplitude difference is related to the attenuation coefficient $\alpha(f)$.

The relationship between frequency domain and time domain attenuation is described by simple convolutional model for backscattered signal from a pulse propagating through an attenuating medium (Flax et al., 1983; and Flax, 1984). The basis for this model is given by Eq. (3.2), assuming the Gaussian spectral shape, linear frequency dependence on attenuation, negligible frequency dependence of the scatterers, and weak scattering.

$$S(f) = |\hat{A}(f)|^2 \left\{ e^{-\alpha_o l f} \right\} \left\{ e^{-(f-f_o)^2/2\sigma^2} \right\} \tag{3.2}$$

where
f = frequency
$S(f)$ = backscattered power density spectrum
$|\hat{A}(f)|^2$ = noise spectrum
α_o = attenuation coefficient (in dB cm^{-1} MHz^{-1})
l = depth of tissue traveled by ultrasound
f_o = transducer center frequency
σ = characteristic width of transducer power spectrum.

Now, the total energy contained in the signal is integral over the power density spectrum (Parseval theorem). Hence, the energy as a function attenuation and depth, $E(\alpha_o, l)$, will be

$$E(\alpha_o, l) = 2 \int_0^\infty S(f)\, df.$$

However, since the spectrum is Gaussian and does not change shape with attenuation, the energy will be simply proportional to the power density at the center frequency (f_c). Thus, the energy can be described by the proportionality

$$E(\alpha_o, l) \propto S(f_c).$$

Using Eq. (3.2), the backscattered energy is given as

$$E(\alpha_o, l) \propto A_o \left\{ e^{-\alpha_o l f_c} \right\} \left\{ e^{-(f_c-f_o)^2/2\sigma^2} \right\}$$

where A_o is the Gaussian envelop amplitude at the center frequency (f_c). Substituting Eq. (3.1) for f_c,

$$E(\alpha_o, l) \propto A_o e^{-\left\{ \alpha_o l f_o - \alpha_o^2 l^2 \sigma^2/2 \right\}}. \tag{3.3}$$

Thus, the spectral energy decays exponentially, but not as a simple linear function of α_o or l, but rather with an additional quadratic term $(\alpha_o l\sigma)^2$. However, if the pulse bandwidth is narrow such that σ^2 can be approximated as zero, then the quadratic term disappears leaving the desirable relationship

$$E(\alpha_o, l) \propto A_o e^{-\alpha_o l f_o}. \tag{3.4}$$

It is therefore possible to estimate α_o by measuring the amplitudes (or intensities) of the echoes from the backscattered signals from two planes separated by a distance l. Using a method termed **C-mode analysis**, Ophir et al. (1982) applied this narrowband relationship to estimate attenuation coefficient for human skeletal muscle *in vivo*. In this technique, a narrowband transducer and a gating mechanism are used to detect the narrowband signal located at a specified distance from the transducer face. By translating the transducer back and forth over a flat (X-Y) region, an *amplitude plane* will be defined at the gated depth, as shown in Figure 3.4. The average value of all the amplitude measurements across the plane is recorded, to reduce the effect of beam profile. Next, the transducer (or gating) is repositioned at a different axial depth and the procedure is repeated. By simply determining the amplitude change occurring with axial translation (l) between planes, and noting the transducer center frequency (f_o), the attenuation coefficient (α_o) can be readily determined from Eq. (3.4).

One of the main factors that affects the amplitude measurements is the axial beam sensitivity profile. So, a knowledge of the beam profile and appropriate corrections are necessary to determine α_o more accurately.

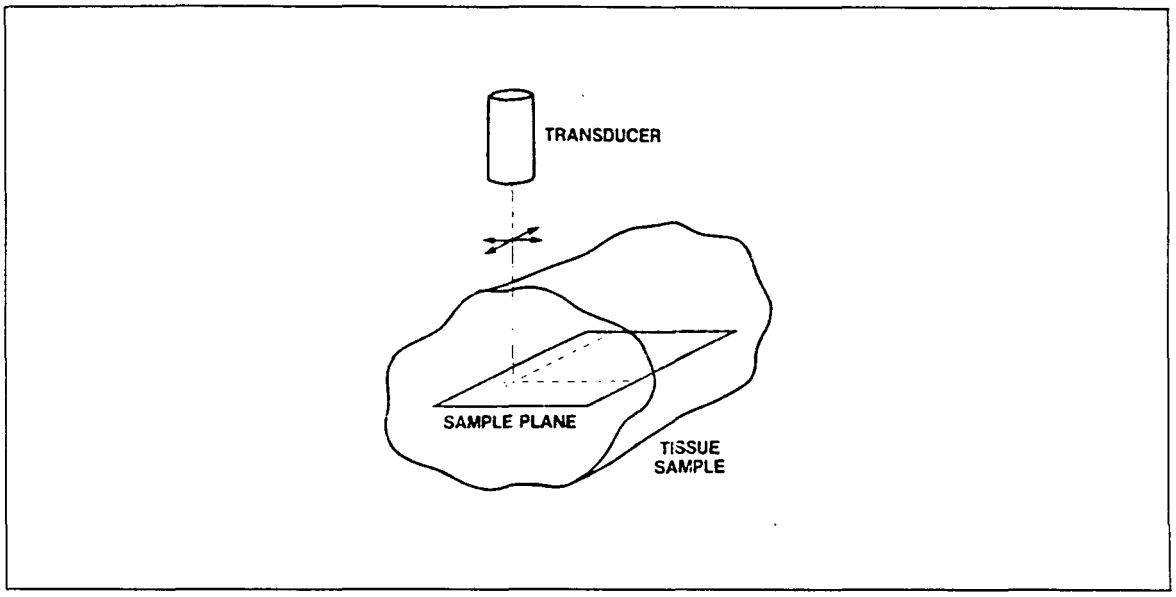

Figure 3.4: Principle of gating at a depth and measuring the signal amplitudes across the defined plane for so called *C-mode analysis*. To determine the attenuation, a second plane is measured and compared to the first (Ophir et al., 1982).

2. Zero Crossings Method: This is a time domain method which is closely related to the spectral shift method. The spectral downshift is estimated in the time domain by measuring the zero-crossing density of the rf signal (Flax et al., 1983). In order to relate the zero-crossing density and the attenuation parameters, it is necessary to assume a mathematical model for the pulse shape; commonly, a Gaussian shape for the pulse is assumed.

It has been shown that the expected density of zero-crossings found in a stochastic wave form is related to the square-root of the second moment of the power spectrum of that waveform. Because of the Gaussian spectrum assumption, this is mean frequency squared plus the bandwidth squared. Clearly, if the bandwidth is small, then the square-root of second moment is approximately equal to the mean or center frequency

(Flax, 1984). (Even if the bandwidth is not small, the bias added to the frequency estimate will remain constant, and thus, when estimating frequency shift due to attenuation, the bias will be canceled.) Thus,

$$\lambda \simeq 2 \{f_c^2 + \sigma^2\}^{\frac{1}{2}} \simeq 2f_c$$

where λ = zero-crossings estimate
f_c = center frequency
σ = bandwidth.

Making use of Eq. (3.1), we can relate the zero-crossings to the frequency shift resulting from attenuation, and thence determine the attenuation coefficient. Thus,

$$\lambda_c = \lambda_o - 2\alpha_o l\sigma^2$$

or

$$\alpha_o = \left(\frac{1}{2\sigma^2}\right)\left(\frac{\Delta\lambda}{\Delta l}\right) \tag{3.5}$$

where $\Delta\lambda$ = $\lambda_o - \lambda_c$ is difference in zero-crossings density at two depths of the tissue
Δl = depth of the tissue travelled by ultrasound.

For estimation of α_o, temporal segments at varying depths of an A-mode data are recorded and the number of zero-crossings for each segment is counted. On an average, the distal segment can be perceived to be a lower frequency waveform, but the specific number of zero-crossings occurring in a relatively short segment can be highly variable.

The zero-crossings sample period is translated through the temporal waveform and the zero-crossings density as a function depth is derived. As shown in Figure 3.5,

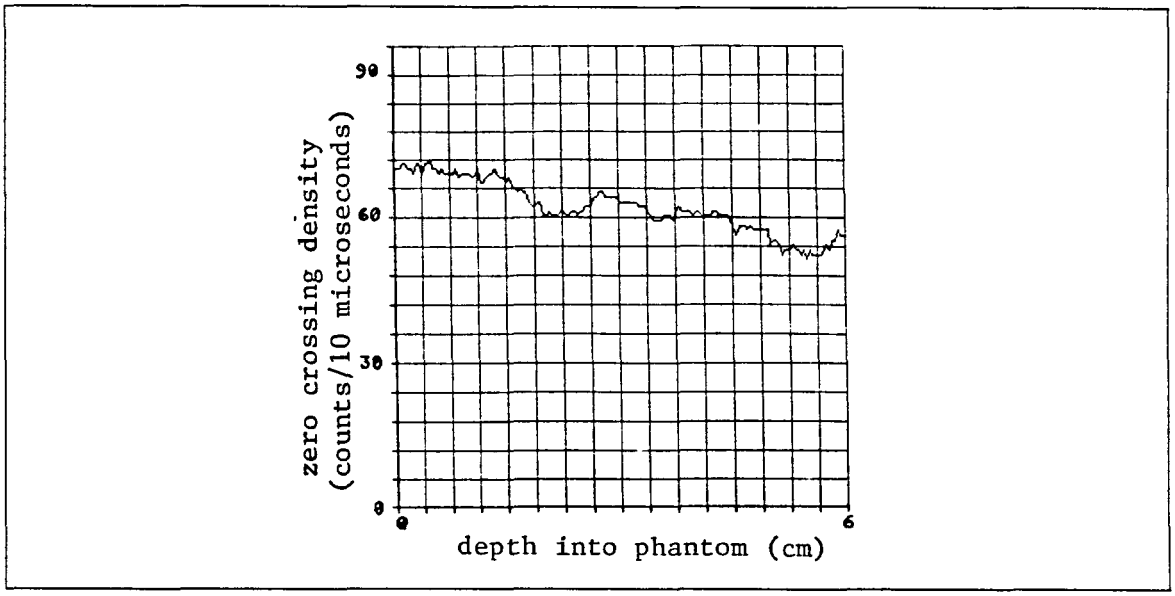

Figure 3.5: Typical graph showing decrease of zero crossings density along the depth of the tissue mimicking phantom (Flax et al., 1983)

the downshift in frequency with depth is apparent. It should be noted that stochastic variability associated with the waveform can cause significant deviations in the frequency estimate at any given depth. Averaging in time domain improves the estimation results, but it is important to make estimations over a line segment which is long enough not to be affected by the random perturbations.

Selecting a Method for Attenuation Estimation

Narayana and Ophir (1984) have reviewed the problems which are significant in the implementation of the various techniques for attenuation estimation. Some of the main factors which affect all the techniques to one degree or another are

- bandwidth of the transducer
- spectral shape
- beam profile

- center frequency
- specular reflection
- frequency dependence of tissue attenuation
- changes in tissue scattering law.

Some of these factors are experimental variables, while others are (known or unknown) tissue properties. It is therefore advisable to select a proper method by considering all possible parameters for given tissue, e.g., the center frequency and axial resolution, bandwidth, the possibility and ease of implementing the method in real-time, and nonlinear frequency dependence of attenuation for some tissues.

The log-spectral difference method was selected for study of attenuation in tissue samples (containing varying amounts of fat and muscle tissues) in this research because of several reasons. Firstly, this method has been proven useful by many workers for differentiating diffuse parenchymal diseases of liver, particularly fatty infiltration. Garra et al. (1984) compared the accuracy and precision of the frequency shift technique in the time domain (zero crossings) and the frequency domain (spectral shift). they found that the frequency domain technique yielded less variation than the time domain technique. Duerinckx et al. (1986) have shown that the zero-crossings method shows no correlation between α and fat or fibrosis in tissue (liver). Since one of the objectives in this study was to characterize the tissue by its fat/muscle content, zero-crossings method was not considered. Although the time domain amplitude difference method was successfully used by Ophir et al. (1982) for attenuation estimates of *in vivo* human muscle, it was not considered because, it requires special apparatus for scanning in planes, which, at present, has not been developed at our lab.

CHAPTER 4. SYSTEM: DATA ACQUISITION AND ANALYSIS

A personal computer based system was developed for acquisition and analysis of ultrasonic signals. The approach was to accurately collect data under experimental conditions and to analyze them for accurate, consistent, and system-independent estimates of attenuation values. The system hardware consisted of the following:

- Panametric[1] pulser/receiver model 5052PR
- Un-focused piezoelectric transducers
- Specially built scanning tank
- Heath[2] model IC-4802 computer oscilloscope
- Keithley[3] 570 data acquisition system
- Zenith[4] Z-248 personal computer

The system set-up is shown in Figure 4.1. For purpose of description, the system can be divided into data-acquisition and data analysis. The data-acquisition system includes: (1) the scanning apparatus (tank, transducer, mechanisms for controlled movement of transducer, and ultrasonic pulser/receiver); and (2) tissue samples and

[1]Panametrics, Inc., Waltham, MA, U. S. A.
[2]Heath Co., Benton Harbor, MI, U. S. A.
[3]Keithley Data Acquisition and Control, MI, U. S. A.
[4]Zenith Data Systems Corporation, St. Joseph, MI, U. S. A.

models used for this study. Software that controlled the digitization of data is described with the data-acquisition system. The data analysis system consists of the processing software routines implementing a method of extracting attenuation information from the collected data.

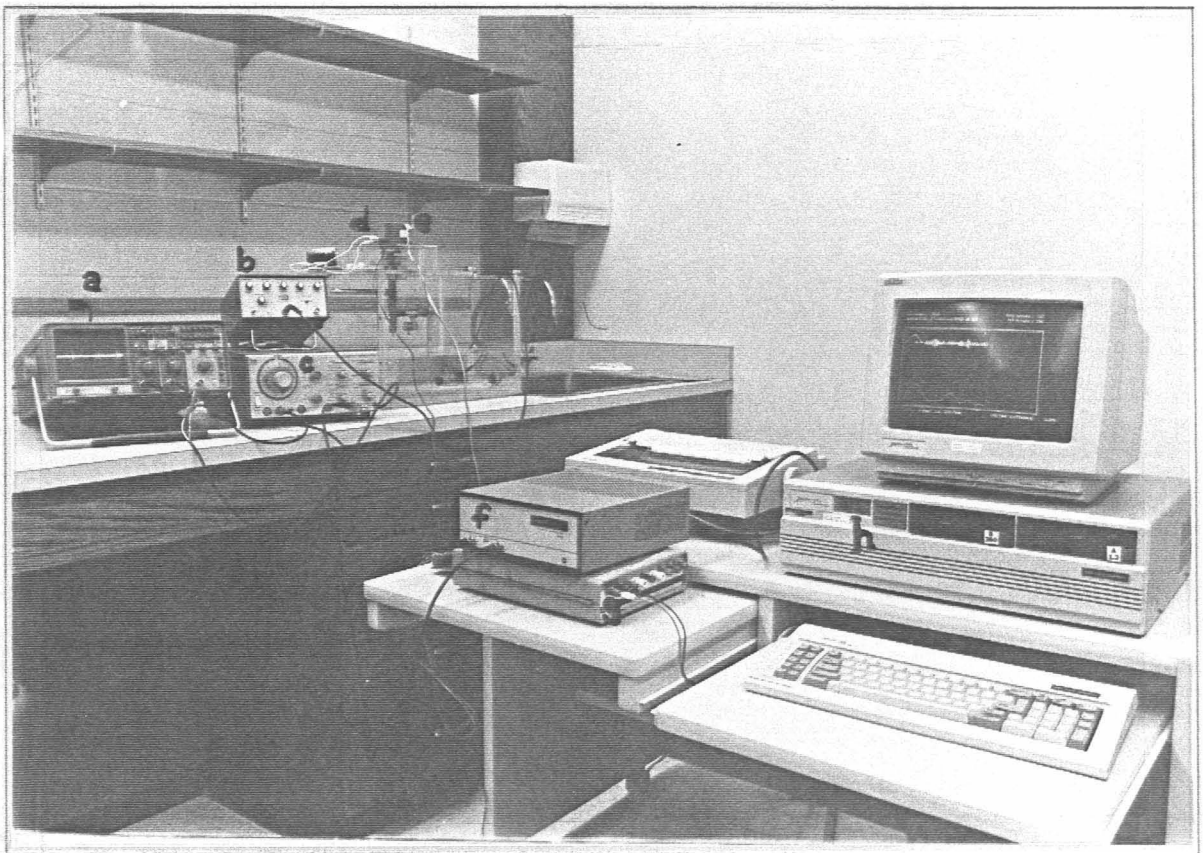

(a) Gould oscilloscope
(b) Panametric pulser/receiver
(c) Function generator
(d) Potentiometer
(e) Stepper motor
(f) Heath digitizing oscilloscope
(g) Keithley data-acquisition system
(h) Zenith Z-248 computer

Figure 4.1: System set up for ultrasonic scanning of tissue samples

Scanning Apparatus

A simple angular scan of tissue sample, using a rotating arm, was used to collect pulse-echo signals at several angles. The apparatus used for this was a specially designed scanning tank, originally developed by Brown (1986) at Iowa State University and modified by the author for automated transducer stepping and angle detection. Figure 4.2 shows front and top views of the scanning tank.

Tank

The tank was constructed of Plexiglas (3/8" thick) and had dimensions of 18" x 12" x 12". As seen in the Figure 4.2, fixed to the top of the mounting plate was a large 360 degree protractor, which allowed precise setting of transducer angles with resolution of 0.5 degree. Two copper pipes of different diameters, pierced through the center of the mounting plate, were used as shafts of transducer holding arms. This allowed the two transducers to be rotated independently. The horizontal arms had sufficient freedom to allow accurate positioning of the transducers in any desired location (distance from bottom of the tank and from center of the protractor) within its reach limits. A large gear was mounted to the top of the inner pipe, which was attached on one side to stepper motor gear, and on the other side to a small potentiometer (angle transducer) gear. This mechanism moved the transducer on an arc (via central gear) by stepper motor and detected the angular movement by the potentiometer gear. Since only one transducer was used for pulse-echo technique, only the arm connected to inner shaft was used in order for the transducer to be moved and the angle to be detected.

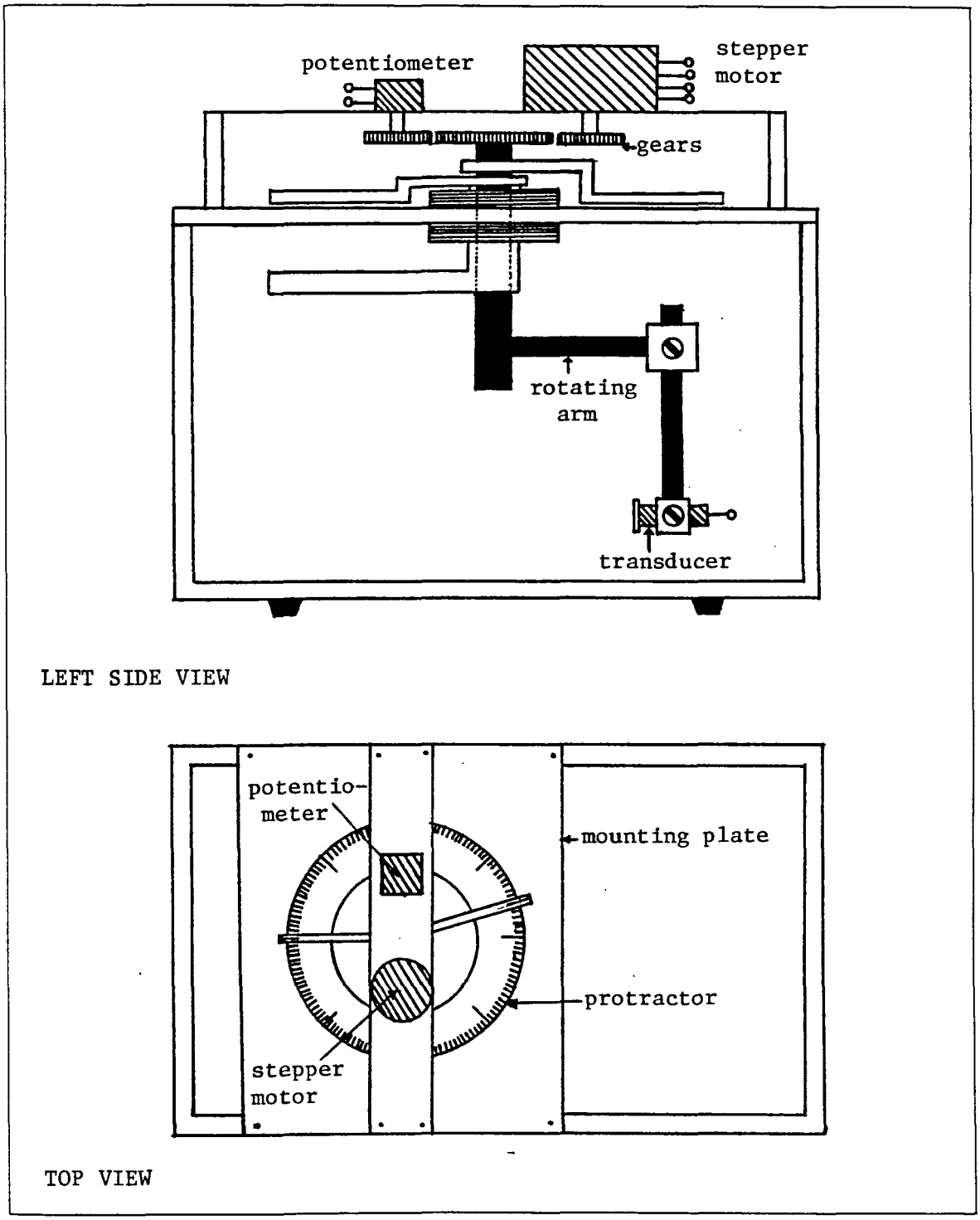

Figure 4.2: Left side view and top view of the ultrasonic scanning tank

Transducer Movement by Stepper Motor

A **stepper motor**[5] was used to rotate the transducer around the tissue/model to be scanned. Discrete pulses were used to step the motor gear sequentially. The full step resolution was about 1.3-1.4 degrees/step, and the half step resolution was about 0.6-0.7 degree/step. The pulsing pattern needed to produce full or half steps (under software control) was achieved using the Keithley relay control.

The **Keithley 570** is a personal computer based data acquisition system having several analog and digital inputs/outputs and a 16 channel relay control slot. Four channels of the relay control slot, with an additional driver circuit, were used to control the stepper motor by discrete steps.

A **potentiometer**[6] detected the gear position in about 140 degree arc and output the signal between 0 and 5 volts. This signal was digitized using one of the analog inputs to the Keithley system. The 12 bit (or 4096 step) A/D conversion of 0-5 V signal gave resolution of 1.22 mV, which was normalized to zero degree of scan and converted to the appropriate angle in degrees.

The stepper motor and angle-transducer both were under control of software.

Pulser/Receiver

Panametric pulser/receiver model 5052PR was used with a single transducer for the pulse-echo mode. This unit allowed control of following variables:

- Pulse repetition rate (200 - 5000 Hz)

[5]Slo-syn synchronous/stepping motor from Superior Electric Co., Bristol, CT, U. S. A.

[6]50 $K\Omega$ potentiometer with 5 V power supply, from Bourns, Inc., CA, U. S. A.

- Energy (14 - 94 micro Joules)
  Damping (0 - 250 ohm)
  Pulse amplitude (140 - 270 volts)
- Gain/attenuation of receiver (0 - 68 dB)
- Bandwidth (1 KHz - 35 MHz)
  High pass filter cut-off frequency (0 - 2 MHz)
- Pulse-echo/through-transmission modes

The settings were adjusted such that the received signal was displayed on an oscilloscope with least noise, good amplification for full depth of the tissue sample, and no baseline drift.

Ultrasonic Transducers

Six different transducers were tested to select for final data collection. The impulse response for each transducer was determined using an echo from thin, flat, vertically placed aluminium or Plexiglas plate. The frequency/power spectrum was calculated as a 1024 point discrete Fourier transform, using the Fast Fourier Transform (FFT) algorithm, and smoothing. Two transducers, one with a smooth, wideband spectrum, and one with narrowband spectrum were selected in order to determine effects of bandwidth and center frequency of transducer on attenuation estimates in frequency domain. The characteristics of these two transducers are shown in Figure 4.3.

Tissue Samples/Models Used

Preliminary studies for this system were done with a Plexiglas cylinder (5 cm. length and 6.3 cm. diameter). Both sides of the Plexiglas cylinder were cut flat

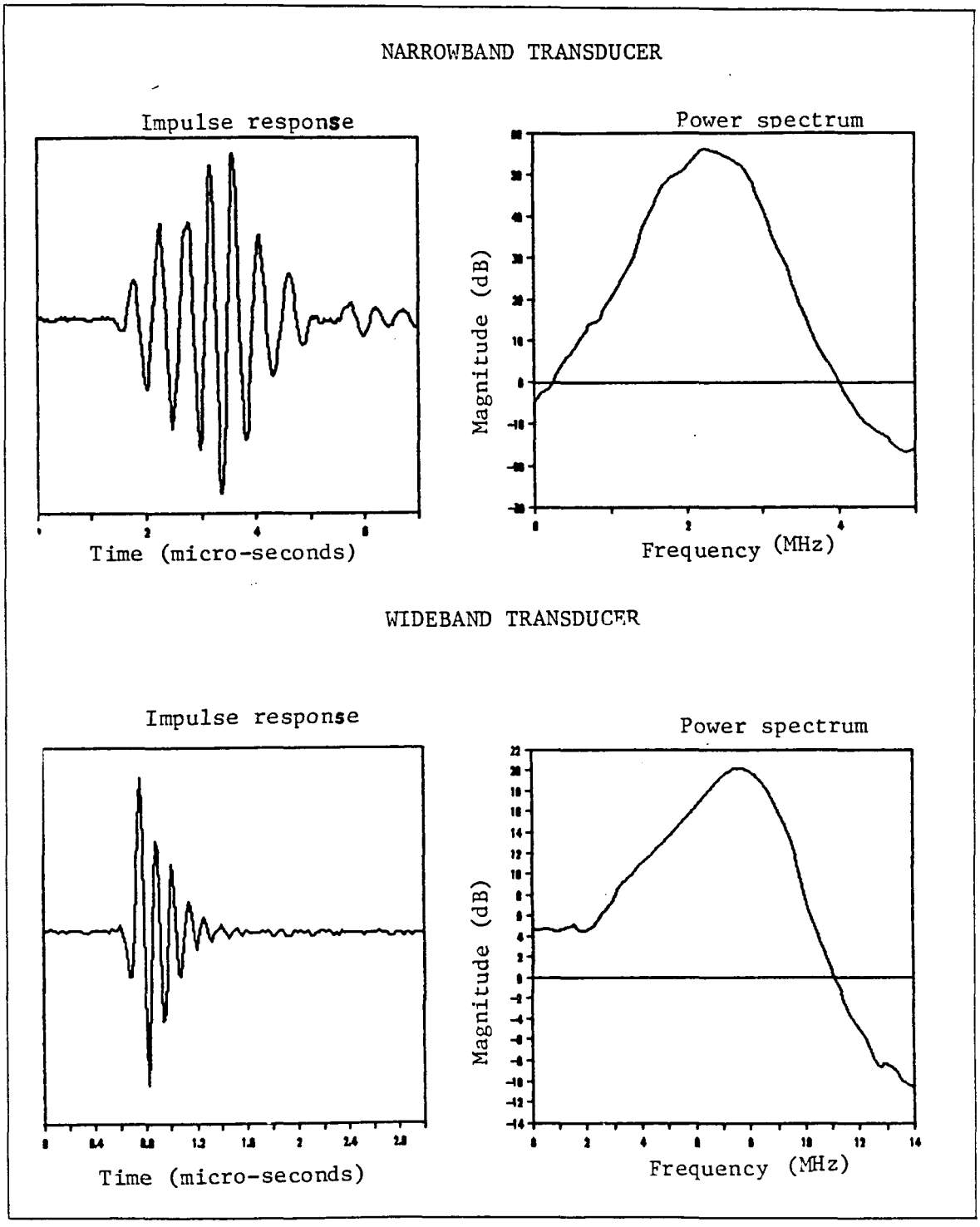

Figure 4.3: Impulse responses and power spectra of the ultrasonic transducers used in this study

and parallel to each other. The purpose was to determine all possible settings of the apparatus, and their effects, if any, on final attenuation results. For attenuation estimation in the Plexiglas, spectra of echoes from two sides of the cylinder were compared. The angle of incidence was kept perpendicular to the flat sides of the cylinder and signals were recorded for different settings of the pulser/receiver.

Porcine tissue samples with varying amounts of fat and muscle tissues were selected for this study because of their easy availability. Also, attenuation results could be roughly correlated with visible distribution of fat/muscle layers, and with quality grade of commercially available meat samples. These samples were refrigerated when purchased, and were kept refrigerated until used for scanning.

Figure 4.4 illustrates visual distribution of fat and muscle tissues in three prototype tissue samples. Note that the Sample 2 had thicker layers of muscle tissue as compared to the Samples 1 and 3.

For scanning, the meat samples were warmed in saline at $37^{o}C$ for about an hour. During the scanning, the temperature of the saline in the tank was maintained at about $37^{o}C$. The samples were handled carefully and placed in the scanning tank in front of the transducer for scanning. All visible bubbles were removed by manipulation before scanning. After scanning, the samples were immediately placed back in the refrigerator until used again.

Data Acquisition

The schematic of the data acquisition system is shown in Figure 4.5. The objective was to digitize the segments of the A-mode signals, at high MHz sampling rates,

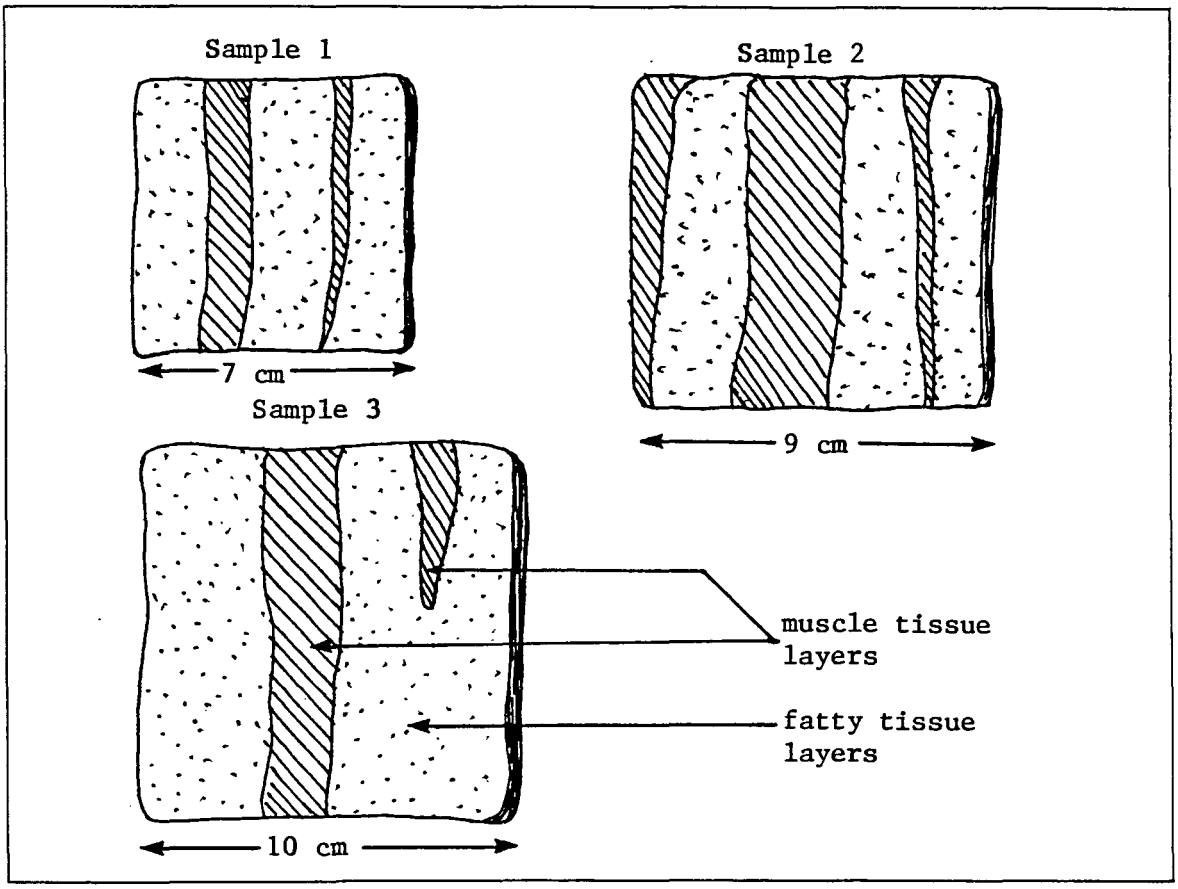

Figure 4.4: Relative fat/muscle contents and distribution for tissue samples used for attenuation measurements

and at different depths of the tissue sample.

Heath Oscilloscope

The Heath model IC-4802 Computer Oscilloscope is a versatile dual trace sampling oscilloscope, connected to a host computer via RS-232 serial port. It periodically samples analog input signals (maximum 2) and stores as digital codes (total 512 samples) in its buffer memory; this, under software control, is transmitted into the computer and displayed as waveforms on the computer's screen. The supplied software

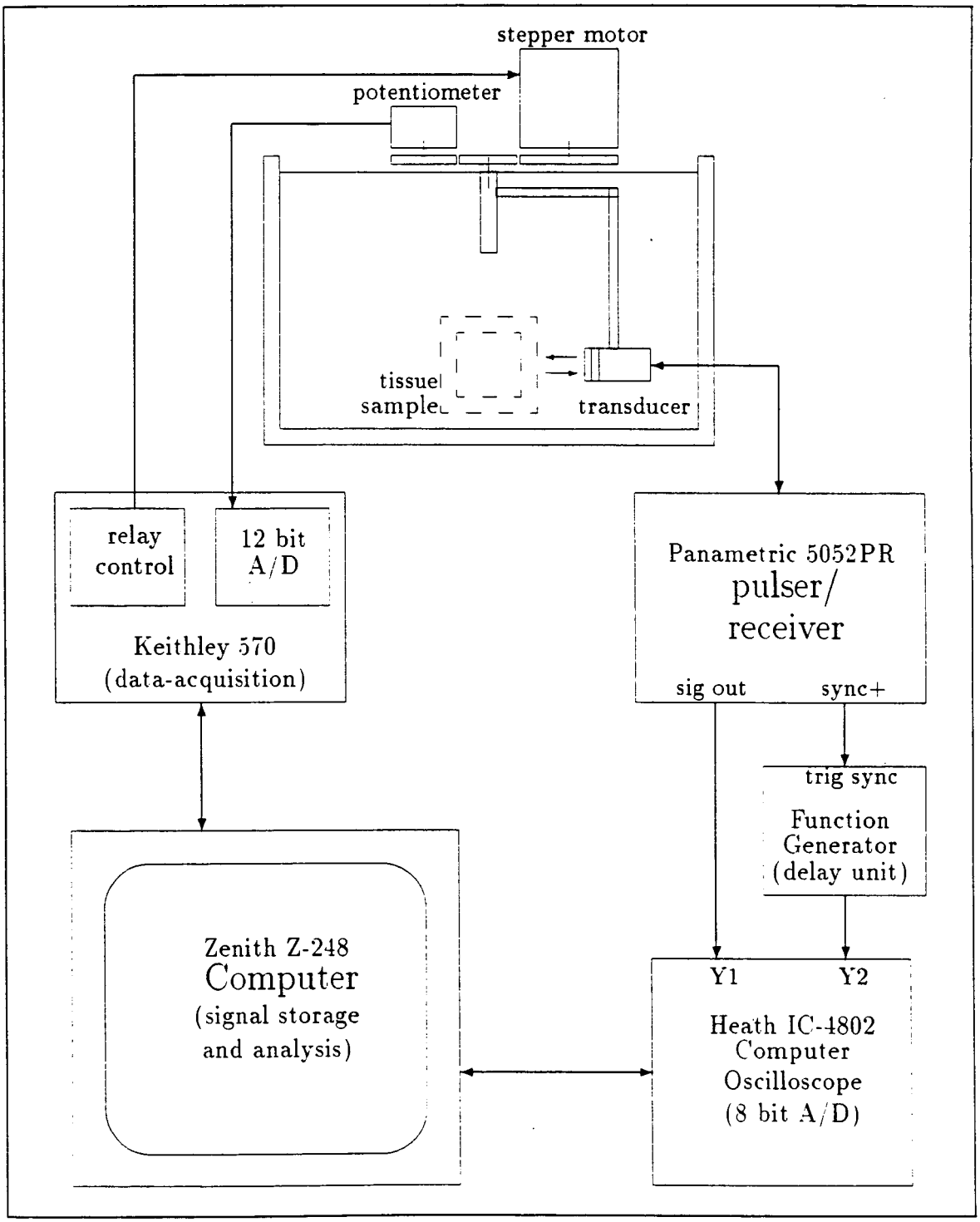

Figure 4.5: Schematic of data acquisition system

provides full control of standard oscilloscope functions from the computer keyboard. This includes controls of voltage sensitivity, time base (sampling frequency), trigger (level, slope and mode), offsets, and coupling (AC, DC). Additional features are screen display, averaging, cursor measurements of voltage and time (frequency), and disk storage of the signal. An example of the computer screen display is shown in Figure 4.6.

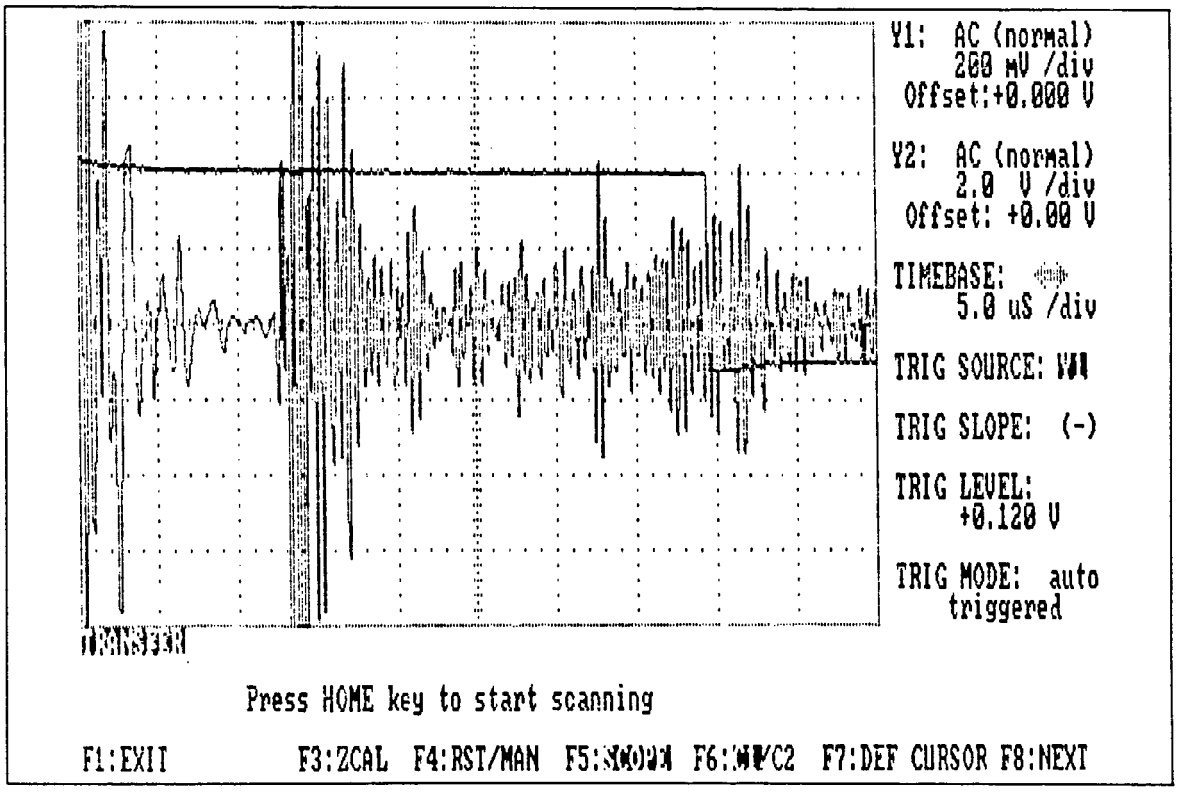

Figure 4.6: Computer Oscilloscope screen, displaying the digitized signal and controls

The oscilloscope allows sampling frequency (f_s) to be varied from 2.5 Hz to 100 KHz with real-time sampling for non-repetitive signals, and from 200 KHz to 5 GHz with equivalent time sampling for repetitive signals. According to the sampling

theorem, in order to avoid aliasing, the sampling frequency should be at least twice the greatest frequency component in the signal. So, sampling frequencies for the narrowband and wideband transducers were selected to be 10 MHz and 25 MHz, respectively. This high sampling frequency was achieved by equivalent-time sampling, where one sample was taken each time the oscilloscope was triggered, requiring 512 triggers for total 512 samples (Heath, 1986).

The oscilloscope is limited to take only 512 samples from a signal at any sampling rate; so, for the sampling frequency in MHz range, it covers only a few microsecond duration of the signal. For example, for a pulse-echo ultrasound with an average velocity of 1540 m/sec, 512 samples cover only 1.58 cm. and 3.94 cm. of tissue thicknesses, for the sampling frequencies of 25 MHz and 10 MHz, respectively. Because of this limitation, a special triggering arrangement was designed to take samples of signals coming from different depths of the tissue sample.

Near/Far Depth Triggering

As shown in Figure 4.5, the SYNC+ signal of the pulser/receiver was used to trigger a function generator[7]. The function generator settings used were:

- Mode: TRIG
- Waveform: pulse
- Output amplitude: 7 volts
- Output offset: +2 volts

These settings output a square pulse (triggering pulse) with each trigger of the pulser/receiver, i.e., synchronously with the transducer excitation pulse. The pulse

[7] F34 function generator from Interstate Electronics Corporation, U. S. A.

width could be varied by changing the frequency setting using a knob. The negative going edge of this pulse was used to trigger the oscilloscope channel Y1, to take 512 samples of the signal. The typical waveforms are shown in Figure 4.7.

Since the pulse width was adjustable, the deeper tissue signals could be digitized by moving the trigger. Of course, digitizing the whole signal as one waveform was not possible by this method, because after taking first 512 samples, the next trigger might not be adjusted exactly at the location of the 513th sample. This could cause overlap or loss of a few samples between two successive 512 sample segments, producing echo-like artifacts. So, as shown in Figure 4.7 (c and d), triggering was arranged in pairs of a near (or shallow) and a far (or deep) trigger. (The reader is cautioned not to confuse these terms with near and far fields of the transducer beam.) The near and far pulse-echo segments thus collected would later be used to calculate attenuation of the ultrasound by intervening tissue. Table 4.1 shows measured pulse width of triggering signals for various frequency settings on the function generator, and corresponding tissue depths at which the reflected signal is to be digitized.

As shown in the Table 4.1, the range of tissue depths covered by this mechanism was 7 cm. This was enough to cover the thicknesses of tissue samples used in this study. Note that these thickness values represent the differences between tissue depths at near and far triggers (considering two way travel of ultrasound).

Each A-mode signal was digitized as at least one pair of near and far segments. For some tissue samples, more than one pair were collected and re-arranged in suitable pairs for attenuation calculation; two segments were paired as a near and a far segment such that they were separated by at least 2/3 of the tissue thickness. This is shown

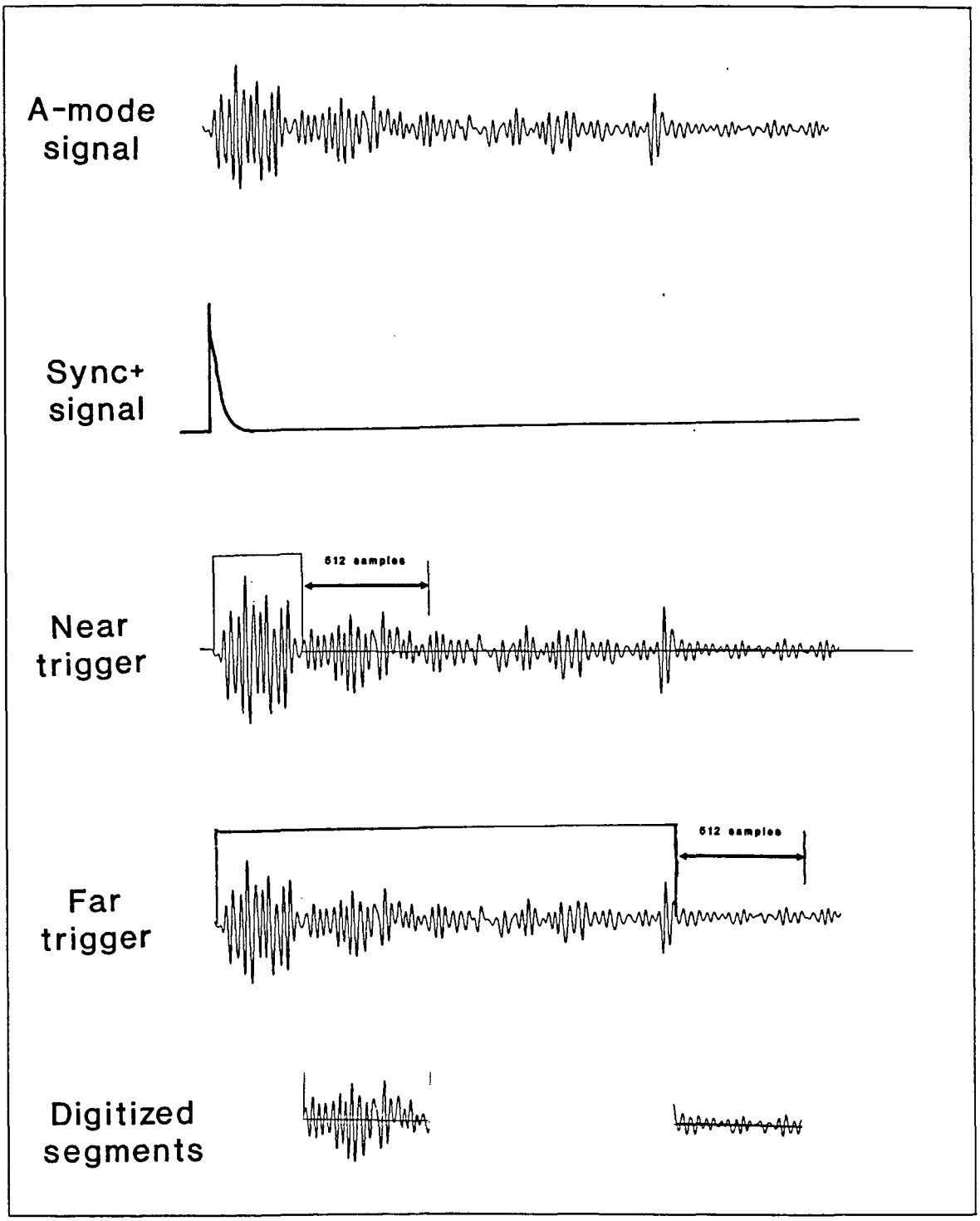

Figure 4.7: Typical waveforms at various stages of data acquisition

Table 4.1: Function generator settings for generating triggering signal, and corresponding tissue depths for digitizing a segment of echo signal

Frequency settings	Pulse-width[a] (μ sec)	Tissue-depth[b] (cm)
3.0 × 100 K	2.4	0.1848
2.0 × 100 K	2.8	0.2156
1.0 × 100 K	5.2	0.4004
0.5 × 100 K	10.0	0.7700
3.0 × 10 K	17.0	1.3090
2.0 × 10 K	26.0	2.0020
1.0 × 10 K	52.0	4.0040
0.55 × 10 K	92.0	7.0840

[a]Pulse-width of the triggering signal; falling edge of this pulse was used to trigger the sampling.

[b]Calculated from the pulse-width of the triggering signal, considering two way path for ultrasound at average velocity of 1540 m/sec.

to give better estimate of attenuation, as mentioned in the previous chapter.

A 20 MHz digital storage oscilloscope[8] was used to monitor the triggering signal and the ultrasonic signal-segment to be digitized.

Software Control of Data Acquisition

The oscilloscope Channel Y1 was connected to the received pulse-echo signal (output of the pulser/receiver) and Channel Y2 was connected to the triggering signal (output of the function generator). The potentiometer signal was input to the computer and the stepper motor activating signals were output from the computer via the Keithley system.

[8]Model OS 1420 from Gould, Poebuck Rd., Hainauit, Essex, England.

The oscilloscope data acquisition was controlled by a BASIC program (SCOPE.-BAS) supplied with the oscilloscope. This program was modified and customized. The stepper motor subroutine was added to control the transducer movement for each new A-mode and to detect the angle from the potentiometer signal. The memory subroutine was rewritten for storing the signals with appropriate file names. The flowchart of operations is shown in Figure 4.8 (see the Appendix for source codes).

To ensure accuracy of angle detection, the potentiometer was calibrated for angle detection each time a new scan was taken. This was done using a QuickBASIC[9] program called ANG-CAL.BAS (see the Appendix). The potentiometer signals, for start and end of an arc to be scanned, were detected when the user manually moved the transducer arm. The user would then enter the arc size (in degrees), and calibration number (counts/degree) would be stored in a file named ANG-CAL.DAT. This information would later be used to convert the potentiometer signal into degrees, relative to starting angle, while taking a scan.

As shown in the flow chart (Figure 4.8), the program SCOPE.BAS allowed the user to modify the Oscilloscope settings (sampling frequency, amplitude sensitivity, etc.), and when the HOME key was pressed, the user was prompted to input the scan-name (maximum 4 characters) and then actual, semi-automated scanning would begin. The program would move the transducer, detect the angle, digitize the signal and store on disk with appropriate filename, indicating the scan-name, step number and near/far trigger. For example, for a scan name MSCL, successively stored files would be MSCL1-N.DAT, MSCL1-F.DAT, MSCL2-N.DAT, MSCL2-F.DAT, etc.

[9]Microsoft QuickBASIC 4.0 by Microsoft Co., Redmond, WA, U. S. A.

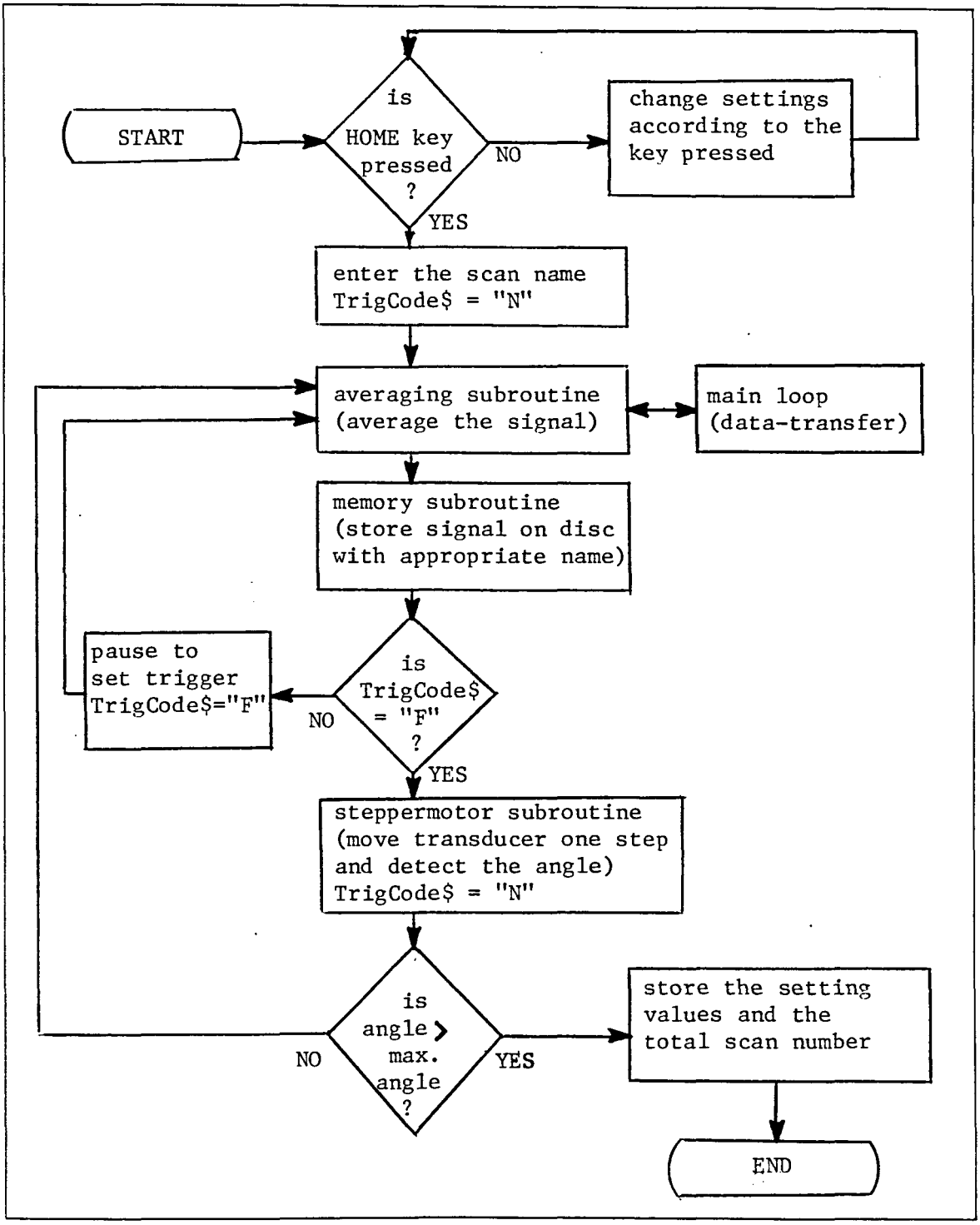

Figure 4.8: Flow-chart of data acquisition software

The data acquisition process was automated, except that the program halted at the appropriate level allowing the user to set a near or far trigger. If more than one pair of triggers were used on one A-mode signal, the data-files would be appropriately paired (by renaming) as mentioned earlier.

Data Analysis

The recorded ultrasonic data were processed, using a Zenith Z-248 personal computer, for attenuation estimations. Programs for this were developed using QuickBASIC language. The reasons for selecting QuickBASIC were its advance flow-control statements, speed, and graphics capabilities. The main program, called ATTENUAT.BAS, is listed in the Appendix.

The flow-chart of basic analysis operations is shown in Figure 4.9. The frequency domain log-spectral difference method was chosen for attenuation calculations, due to the reasons mentioned in Chapter 3. The program provided the following choices of analysis.

```
** Power spectral calculation methods
       * FFT method
       * Averaging periodogram method
            window type
            window length
            window overlap

** Attenuation coefficient calculations
       * Center frequency and bandwidth of transducer
       * Slope of attenuation coefficient over the bandwidth
       * Attenuation at the center frequency
       * Normalized attenuation over the bandwidth
```

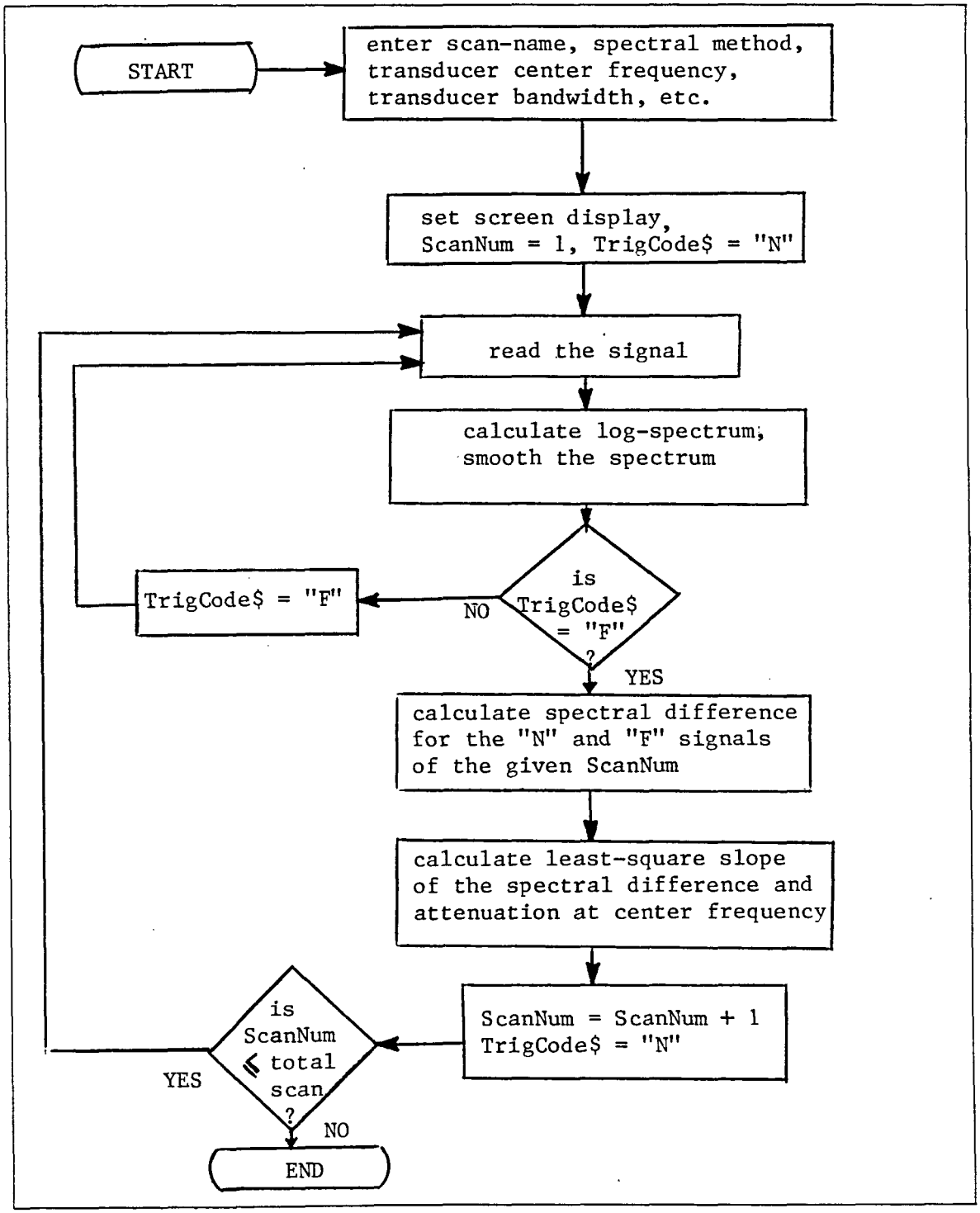

Figure 4.9: Flow-chart of data analysis for attenuation calculations

Calculation of Power Spectra

After reviewing methods of spectrum estimation, two methods were selected for this study; a simple FFT method and an averaging periodogram method. These methods give more consistent and accurate spectrum estimates as compared to other methods (Beauchamp and Yuen, 1979; and Kay, 1988).

In the FFT method, the 512-point signal was padded with 512 zeros (for better frequency resolution), and 1024 point FFT was taken. The resulting spectrum was normalized by number of FFT-points.

In the averaging periodogram method (Rabinar et al., 1979), the power spectra were calculated using short segments of data, chosen to be short enough that attenuation within the window is negligible, but long enough to adequately sample the spectrum. Windows centered around large peaks in echo signal have been suggested for this kind of study (Kuc, 1980), but the regions of tissue were deliberately chosen (by near/far triggers) to be free of large reflectors, so windows of fixed duration were used. The signal (512 samples) was windowed with 128-point Hanning windows with 64-point overlap, giving 8 segments. An FFT was taken for each segment after padding it with 128 zeros. Each spectrum was normalized, and then averaged over 8 segments, giving raw power density spectrum.

After taking the logarithm (base 10, for dB units) of the raw spectrum, the smoothing was done by a simple low pass filter (16- or 32-point moving average), to reduce *leakage* of frequencies. In notation, the final spectra would be identified as $P_N(n,\ f)$ and $P_F(n,\ f)$ for near and far triggered signals, respectively, where n represents the number of A-mode in the scan, and f represents the frequency.

Calculation of Coefficient and Slope of Attenuation

The difference between the two log-power spectra, for near and far triggered signals, was calculated and plotted over the effective bandwidth of the transducer. The *least square* slope was calculated to determine the attenuation coefficient for the tissue depth between near and far triggers. The correlation coefficient and regression analysis for slope estimates were also calculated over the bandwidth. The processing steps were repeated for all A-mode signals taken at different angles, and mean slope across the A-lines was calculated. Specifically, the steps were as following.

Attenuation $\alpha(n,\ f)$ (in dB), as a function of frequency f (in MHz), for n-th A-line of the scan was calculated as

$$\alpha(n,\ f) = P_N(n,\ f) - P_F(n,\ f).$$

If we specify this as a linear operator $\mathcal{D}$ for difference of the spectra,

$$\alpha(n,\ f) = \mathcal{D}\ \{P(n,\ f)\}.$$

Next, the least square regression was calculated over the effective bandwidth of the transducer. This gave the attenuation slope, $\alpha_O(n)$ (in dB MHz^{-1}), for the n-th A-mode of the scan.

$$\alpha_O(n) = \frac{\sum_f\ \{\alpha(n,\ f) - \overline{\alpha}(n,\ f)\}\ (f - \overline{f})}{\sum_f\ (f - \overline{f})^2},$$

where $\sum_f$ denotes summation over the frequency index, and $\overline{f}$ and $\overline{\alpha}(n,\ f)$ are mean frequency and mean attenuation within the bandwidth, respectively. This may be written in linear operator S for slope as

$$\alpha_O(n) = \mathcal{S}\ \{\alpha(n,\ f)\}.$$

This was divided by 2 l where l is the difference, in cm. of the the tissue depth, between the near and the far triggers. This gave the attenuation, for the n-th A-line, in units of dB cm^{-1} MHz^{-1}. Finally, the slopes were averaged across the A-lines, giving mean slope estimates.

$$\overline{\alpha_O} = \frac{1}{N} \sum_n \frac{\alpha_O(n)}{2\,l},$$

where N is the total number of A-lines in the scan (typically, between 10 and 20). In linear operator,

$$\overline{\alpha_O} = \mathcal{M}\ \{\alpha_O(n)\}.$$

Thus, mean attenuation slope for a scan may be expressed in terms of the spectral values $P(n,\ f)$ as

$$\overline{\alpha_O} = \frac{1}{N} \sum_n \frac{\sum_f \{P_N(n,\ f) - P_F(n,\ f)\}\ (f - \overline{f})}{2\,l\ \ \sum_f (f - \overline{f})^2}, \tag{4.1}$$

or, using the operator notation,

$$\overline{\alpha_O} = \mathcal{MSD}\{P(n,\ f)\}.$$

Note that all the operations are linear and may be written in any order to find the most efficient algorithm (Wilson, 1984). The spectral difference was taken first, since the depth of the tissue sample between the near and the far segments was not exactly same for all A-scans.

The standard deviation (S.D.) for the slope estimates was calculated as

$$\text{S.D.}\ (\alpha_O) = \left[\frac{\sum_n (\alpha_O(n) - \overline{\alpha_O})^2}{N - 1}\right]^{1/2}.$$

Since the log-spectral difference method uses the *relative* attenuation at two depths *within* the tissue, the angle dependence of backscatter should not affect attenuation estimates. This was confirmed by taking measurements for a sponge. Also, note that no efforts were made for improving the attenuation estimates by correction factors (e.g., for effects of beam pattern or transducer bandwidth), since the objective here was to compare the results for different tissue samples under consistent experimental parameters.

Summary of Data Acquisition and Analysis

To summarize, the steps in data acquisition and analysis were as following:

1. Interface all instruments properly and prepare tissue sample

2. ANG-CAL.EXE
   - calibrate the angle-transducer

3. SCOPE.BAS
   - adjust sampling frequency (f_s), amplitude sensitivity, averaging number, etc.
   - start scan and enter the scan name
   - adjust the near trigger
   - take 512 samples at specified f_s
   - average over successive signals
   - store the signal on disk with appropriate name
   - adjust the far trigger, take 512 samples, average, and store the signal
   - move the transducer and repeat the procedure

4. ATTENUAT.EXE
   - enter the parameters to be modified e.g., spectral method, bandwidth, and center frequency
   - calculate the spectra for near and far triggered signal
   - calculate the log-spectral difference (attenuation)
   - calculate least square fit over the bandwidth, calculate correlation coefficient of fit
   - calculate attenuation at the center frequency
   - repeat calculations for all A-line data
   - calculate mean and standard deviation of results across A-mode signals

CHAPTER 5. RESULTS AND CONCLUSIONS

Preliminary experiments with Plexiglas were done to determine effects of all possible settings of the apparatus on final attenuation results. Results for the muscle samples are presented and discussed in this chapter.

Preliminary Results with Plexiglas

Attenuation values were calculated for the Plexiglas cylinder. Echoes from two sides of the cylinder, using the narrowband transducer, are shown in Figure 5.1. The corresponding spectra were calculated to estimate attenuation in the cylinder. Table 5.1 shows the results at different settings of scanning apparatus.

As seen from the Table 5.1, there are no significant differences in attenuation results at higher settings of damping and attenuation on the pulser/receiver. For the damping settings higher than 6, and the attenuation settings higher than 10, the attenuation slope varies from 0.62 to 1.10 dB cm^{-1} $MHz^{-1}$with about 8% S.D. Similarly, the attenuation at center frequency (2.2 MHz) varies only from 1.26 to 1.65 dB $cm^{-1}$with 5% S.D. This consistency of the results shows that different pulse amplitude settings does not affect the attenuation estimates by the log-spectral difference method. Shore et al. (1986) also observed no significant variation in attenuation estimates, for bovine skeletal muscle, at different amplitudes of the transmitted ultrasonic

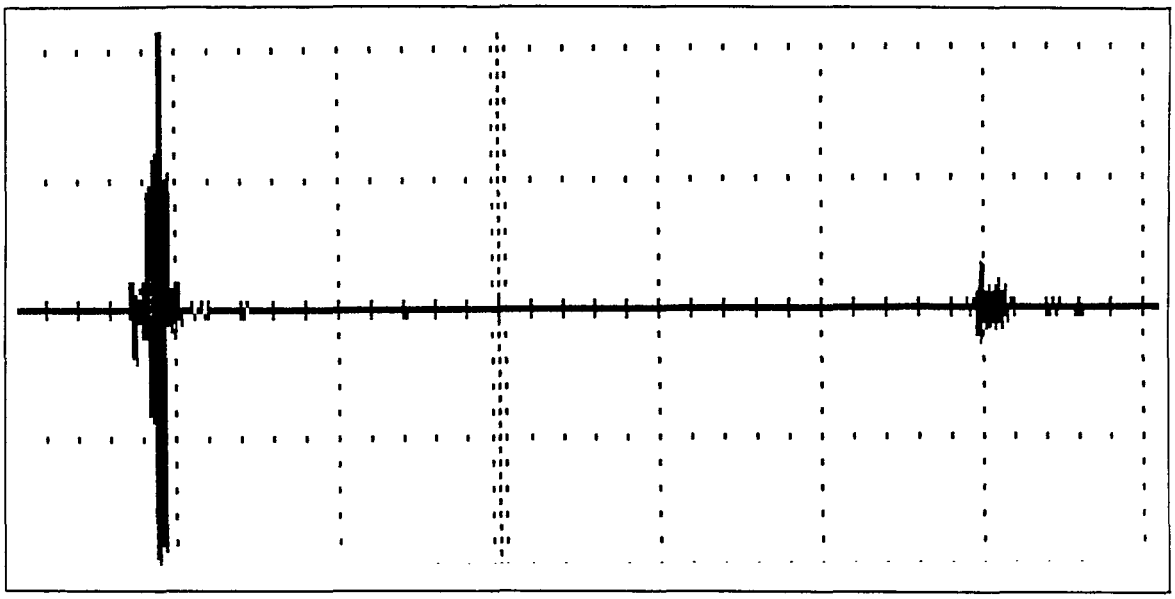

Figure 5.1: Echoes from two sides of the Plexiglas cylinder

pulse.

Unusually low values at the low settings of the damping and the attenuation could be explained by looking at what the damping and attenuation actually do to the transmitted and the received signals. At very low damping settings (0 - 4), the transmitted pulse is of very high amplitude, and when the resulting ultrasonic signal is received as a very high amplitude echo, at low settings of attenuation, it saturates the receiver amplifier. In particular, this happens for the first echo from the Plexiglas, giving unusually low estimates of attenuation.

Other reports of attenuation in Plexiglas show higher values (2.0 dB cm^{-1}at 1 MHz in Shung, 1987). Our lower results might be due to difference in Plexiglas material, or even orientation to grain structure could give different results. The actual value is not given importance, since the purpose of the preliminary experiments was

Table 5.1: Attenuation results for Plexiglas cylinder at different settings of ultrasonic pulser/receiver using the narrowband transducer

Damping[a] settings on pulser	Attenuation values for Plexiglas at different setting of attenuation[b] (dB) on receiver							
	00 dB		10 dB		20 dB		30 dB	
	slope[c]	@ f_c[d]	slope	@ f_c	slope	@ f_c	slope	@ f_c
0	-	0.26	0.23	0.63	0.62	1.30	0.92	1.57
2	-	0.28	0.26	0.63	0.65	1.33	1.03	1.60
4	-	0.37	0.25	0.84	0.85	1.46	0.89	1.31
6	0.52	0.96	0.83	1.52	0.87	1.28	0.94	1.26
8	0.97	1.49	0.90	1.59	0.99	1.26	0.97	1.28
10	1.10	1.65	0.81	1.29	0.96	1.26	0.85	1.29

[a] Affects damping of the signal transmitted from pulser, to excite the transducer; higher number indicates increased damping.

[b] Affects linear amplification of received echoes in the receiver; actual amplification is determined by combined effects of the gain and the attenuation settings.

[c] Slope of attenuation in dB cm^{-1} MHz^{-1} calculated within bandwidth (1.4 - 3.0 MHz) of the narrowband transducer.

[d] Attenuation at center frequency, f_c = 2.2 MHz, for the narrowband transducer.

to check the effects of the system parameters on the consistency of the results.

These preliminary results help in determining the characteristics of the system. Using these results, it becomes possible to compare the results of scans taken at different settings of the pulser/receiver (damping higher than 4 and attenuation higher than 10), although all scans for a particular sample were taken at one setting only.

Also, it is observed that attenuation at a particular frequency (i.e., at the center frequency of the transducer) is a better and consistent quantity than the slope of attenuation, particularly for narrowband transducer.

The method used in this study for measuring ultrasound is relative rather than

absolute. So, as predicted, the results for different angles show no significant variations. It is obvious that the reflection and scattering depend on the angle of ultrasound incidence; so, the received backscatter power might differ at different angles. But, in the spectral difference method, the powers at different depths of tissue are compared, so the bias for the angle dependence is cancelled. This was confirmed by taking scans of a sponge at different angles. For this, several A-mode signals at different angles were digitized and attenuation coefficients were calculated. The results were found to be consistent for all practical purposes.

Consistency of the results at different pulse amplitudes and angles allows us to compare results across A-mode signals of the same sample, and for the different samples, too.

Attenuation in the Tissue Samples

For the tissue samples, typical plots of the A-mode signal, spectra for near and far segments of the signal, and the coefficient and slope of attenuation are shown in Figure 5.2.

Table 5.2 shows attenuation slope (α_0) results for the tissue samples, using the narrowband transducer and two methods of spectrum calculation. The corresponding results for the wideband transducer are shown in Table 5.3. Similarly, results for the attenuation ($\alpha(f)$) at specific frequency (f) in the bandwidth of the transducers are given in Table 5.4 and Table 5.5. Typically, the mean and standard deviation (S.D.) calculations include 8 - 15 scans after discarding the minimum and the maximum estimates.

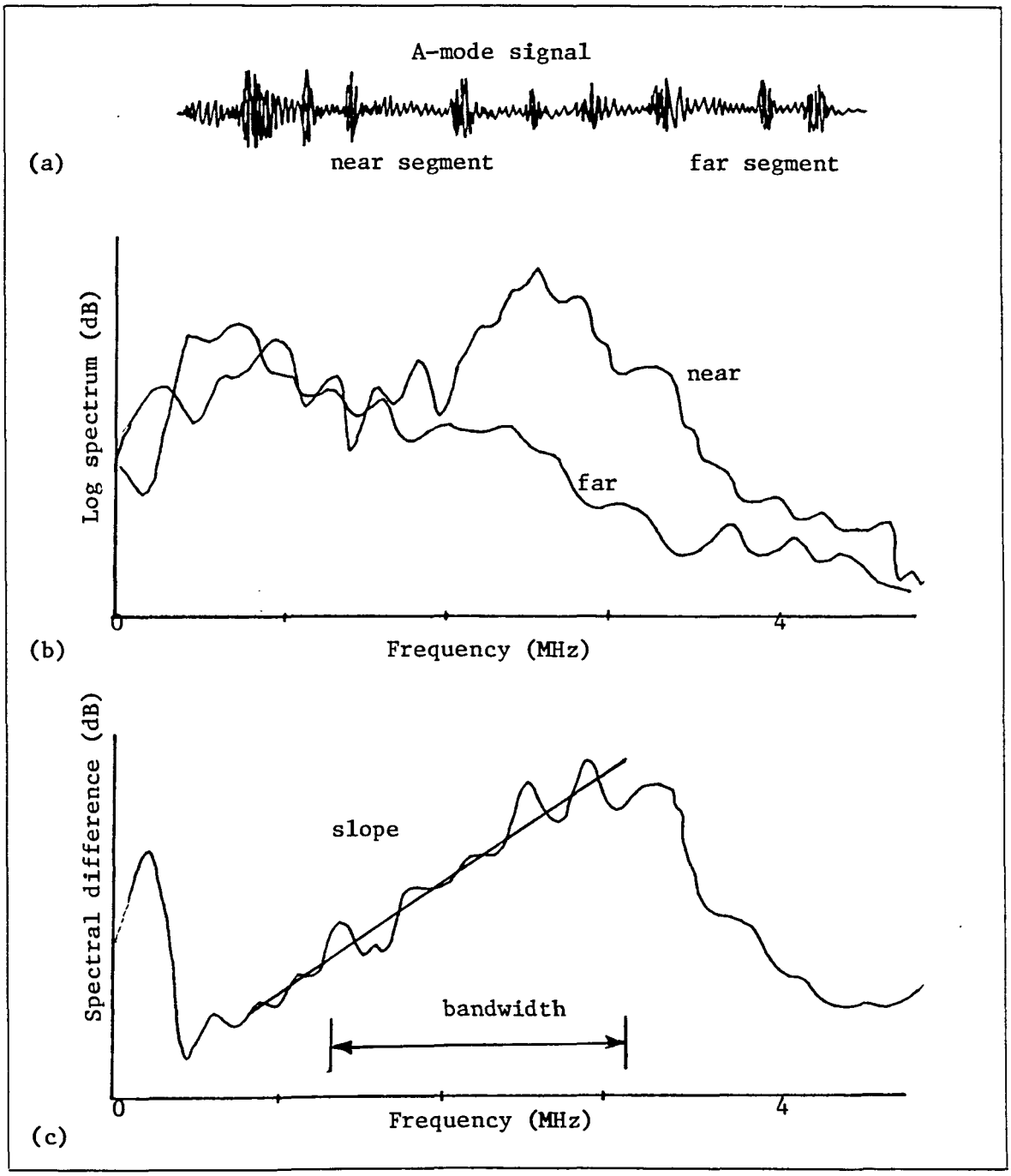

Figure 5.2: Typical plots for calculation of attenuation in the tissue samples [(a) A-mode signal, (b) spectra for near and far segments of the signal, and (c) spectral difference and the *least square* slope]

Table 5.2: Attenuation slope values for tissue samples using the **narrowband transducer** (mean ± standard deviation)

Tissue sample	Attenuation slope (dB cm^{-1} MHz^{-1})	
	FFT method	Periodogram method
Sample 1	1.52 ± 0.32 (21%) (range: 1.01 - 1.89)	1.32 ± 0.18 (13%) (range: 1.12 - 1.68)
Sample 2	2.14 ± 0.39 (18%) (range: 1.6 - 2.59)	2.31 ± 0.29 (12%) (range: 2.02 - 2.77)
Sample 3	1.18 ± 0.29 (25%) (range: 0.86 - 1.52)	1.39 ± 0.16 (11%) (range: 1.17 - 1.56)

Table 5.3: Attenuation slope values for tissue samples using the **wideband transducer** (mean ± standard deviation)

Tissue sample	Attenuation slope (dB cm^{-1} MHz^{-1})	
	FFT method	Periodogram method
Sample 2	2.42 ± 0.33 (14%) (range: 2.19 - 2.93)	2.45 ± 0.23 (10%) (range: 2.20 - 2.82)
Sample 3	1.03 ± 0.24 (23%) (range: 0.74 - 1.37)	1.12 ± 0.11 (10%) (range: 0.89 - 1.36)

In general, the results for the wideband transducer showed more consistent results than with the narrowband transducer. Also, there were slight differences among two methods of spectral estimation. The averaging periodogram method showed fewer variations for slope estimates.

Other reports of attenuation of ultrasound in skeletal muscles range from 1.25 to 3.2 dB cm^{-1} MHz^{-1}along the fibers and from 0.75 to 3.11 dB cm^{-1} MHz^{-1}across the fibers. Also, recall that the attenuation in the fat is usually between 0.5 and 1.0 depending upon the temperature and treatment of the tissue (e.g., freezing). The results for the commercially available meat samples used in this study are within this

Table 5.4: Attenuation at particular frequency (f_C = 2.2 MHz) for tissue samples using the **narrowband transducer** (mean ± standard deviation)

Tissue sample	Attenuation @ f_C = 2.2 MHz (dB cm^{-1})	
	FFT method	Periodogram method
Sample 1	3.41 ± 0.40 (12%) (range: 2.98 - 4.09)	3.57 ± 0.44 (12%) (range: 2.80 - 4.07)
Sample 2	4.79 ± 0.71 (15%) (range: 3.66 - 5.54)	4.85 ± 0.36 (7%) (range: 4.48 - 5.34)
Sample 3	3.95 ± 0.28 (7%) (range: 3.45 - 4.21)	4.37 ± 0.33 (7%) (range: 3.96 - 4.83)

Table 5.5: Attenuation at particular frequency for tissue samples using the **wideband transducer** (mean ± standard deviation)

Tissue sample	Attenuation (dB cm^{-1})	
	FFT method	Periodogram method
Sample 2 (@ f = 7.0 MHz)	17.40 ± 1.13 (7%) (range: 16.12 - 19.24)	17.52 ± 0.41 (2%) (range: 16.87 - 18.03)
Sample 3 (@ f = 6.5 MHz)	9.12 ± 1.02 (11%) (range: 7.53 - 10.55)	8.60 ± 0.46 (5%) (range: 7.92 - 9.05)

range. In general, the measurements were across the muscle fibers (in between the fat layers); of course, this might not be true in strict sense, because the muscle fibers may not be quite parallel to each other, and changing the angle of incidence changes the relative orientation.

The significant difference in results for muscle samples possibly reflects the relative proportion of fat and muscle layers. Recalling the facts that

- the Sample 2 had thicker layers of the muscle tissue and fewer layers of the fat as compared to the Sample 1 (recall Figure 4.4),
- the spectral measurements were made for the signals from the first and last

thirds of the sample thickness, thus covering 2/3 of the tissue thickness for the attenuation calculations, and

- normal muscle has higher attenuation than normal fat,

it was predicted that the overall attenuation for Sample 2 would be higher. In fact, this is the result seen. This shows potential to differentiate and determine relative contents of fat and muscle using only A-mode signals.

Effects of Transducer Characteristics

Since two transducers with different center frequencies and bandwidths were used, it was possible to see the effects of transducer characteristics on attenuation estimates. The wideband transducer shows more consistent results for attenuation. Since the slope of attenuation was measured within the bandwidth, the interrogating pulse with wider range of frequency components allowed more frequency components to be included in calculations and so, frequency selective attenuation in the tissue could be more precisely determined. For the narrowband transducer, average attenuation over the bandwidth was found to give consistent results. Attenuation at mean frequency rather than center frequency was found a better quantity to represent attenuation, particularly when the spectral shape is not Gaussian.

Effects of Spectral Estimation Method

Comparing the results for the two methods of spectral estimation, the averaging periodogram method is found to give better and consistent estimates of attenuation. Since the log-spectral difference method of attenuation estimation was used, the results largely depend on consistency and accuracy of power spectrum calculations. It

has been proven that the averaging periodogram method gives better estimates of spectrum than simple FFT method. Also, the smoothing of raw spectrum definitely affects the attenuation estimates. In this study, simple low-pass filtering was used to smooth the spectra; other smoothing methods might give slightly better results. From this, it is concluded that the better spectral estimation method gives more consistent results for attenuation.

Attenuation Along the Tissue Thickness

By taking several signal segments along one A-line, the attenuation was seen increasing with depth of the tissue, as expected. The plot of depth vs. attenuation coefficient (α) for the Sample 3 is shown in Figure 5.3.

An effort was made to correlate the attenuation along the thickness of the sample with the visual distribution of the fat and muscle layers. As shown in the figure, relatively higher slope of the attenuation in the middle of Sample 3 could be due to thick muscle layer. This could be properly modified and used to create gross images of the tissues using attenuation parameter.

Conclusions

Ultrasonic attenuation was found to have potential for fat/muscle differentiation. The log-spectral difference method was chosen for estimation of attenuation in tissue samples using A-mode signals. A simple, personal computer based system was developed to take several A-scans of a tissue sample. This pulse echo system included automated stepping of transducer, angle detection, digitizing the signal at

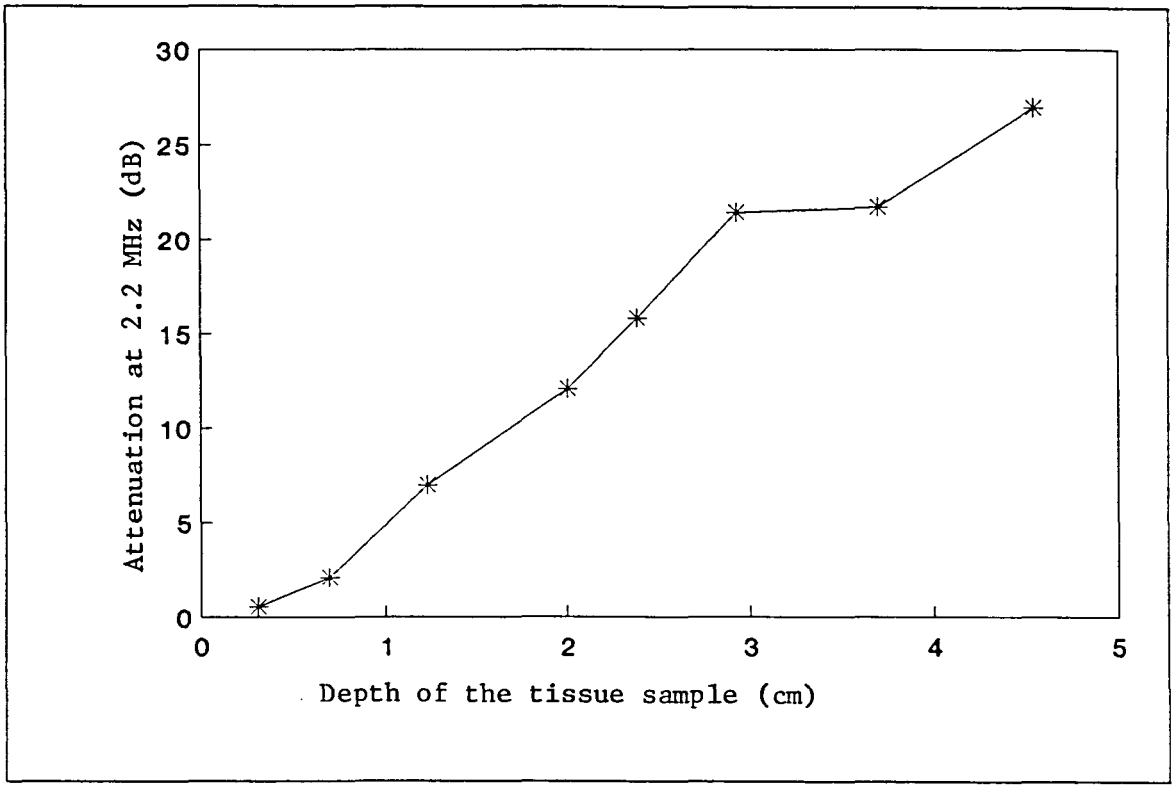

Figure 5.3: Plot of tissue thickness vs. attenuation, showing increase in attenuation as the signal travels deeper in the tissue

high MHz sampling rates and at varying depths of the tissue sample, and storing it on a disk. Software was developed for off-line signal processing to calculate the attenuation coefficient and slope from the stored signal.

The system was tested using a Plexiglas cylinder at different pulse amplitude settings and a sponge at different angles. Since the log-spectral difference method calculates attenuation by comparing the echo signal from *within* the tissue, the transducer angle or amplitude settings does not significantly affect the attenuation estimates.

Several scans of commercially available meat sample were taken using a narrow-band and a wide-band transducer. The attenuation estimates were calculated using

two different methods of power spectrum estimation, i.e., simple FFT method and so-called averaging Periodogram method. The broadband transducer gives better estimates of the slope of the attenuation coefficient, while for the narrow-band transducer, attenuation at center frequency is more consistent quantity. The averaging Periodogram method gives more consistent estimates of attenuation than simple FFT method. This simply reflects the better power spectrum estimates by the Periodogram method.

The attenuation estimation method shows potential in differentiating and determining relative contents of fat and muscle in a given tissue sample. With more scanning and chemical analyses of the tissues, if attenuation results can be correlated with the tissue contents, this can be used as a criterion in ultrasonically differentiating tissues or organs, and possibly some pathologies, too. In the meat industry, this approach could be applied to objectively grade the meat samples by ultrasonically estimating the contents and marbling of fat.

CHAPTER 6. RECOMMENDATIONS FOR FURTHER STUDIES

The system could be improved to digitize the full depth of the backscatter signal by modifying the the trigger mechanism and increasing buffer memory of the digitizing Computer Oscilloscope. The scanning apparatus could be improved to include mechanisms for linear movement of the transducer so that the signal from a single plane of the tissue depth could be received. The broadband transducer with Gaussian spectral shape could improve the results. Better power spectral estimation methods, e.g., with better smoothing in autocorrelation or cepstral domain, could also improve consistency of the results. Even other methods of attenuation estimation, e.g., amplitude difference method as used by Ophir et al. (1982), could be tried once the scanning apparatus is improved suitably.

To prove the potential of the attenuation method in meat grading, more samples would have to be scanned and attenuation results would have to be correlated with results of chemical analyses of tissue contents. If the method proves to be useful by statistically reliable and consistent experiments and results, the next step would be to take measurements in live animals. For this, modifications in the scanning apparatus would be required so that it can be easily operated in the field. The final stage would be to design a cost-effective and easy-to-use ultrasonic instrument with a built-in microprocessor that can be used in the field to non-invasively grade the

meat in live animals. This could revolutionize the subjective meat grading system presently employed.

In the medical field, this method could be tested for differentiating fatty from normal liver, diseased from normal skeletal muscle, ischemic from normal myocardium, and many more pathologies if there happens to be significant difference in acoustic properties of the tissues.

BIBLIOGRAPHY

Beach, A. D., D. L. Tuck, R. J. Twizell. 1983. Ultrasonic equipment for the measurement of backfat on unshorn live sheep. *Ultrasonics* 21:184-187.

Beauchamp, H. G., and Yuen C. K. 1979. Digital Methods for Signal Analysis. George Allen & Sons, London. 316 pp.

Brown, L. F. 1986. Design of wideband ultrasound instrumentation for tissue characterization. M. S. Thesis. Iowa State University. 120 pp.

Christensen, D. A. 1988. Ultrasonic Bioinstrumentation. John Wiley & Sons, New York. 235 pp.

Cohen, R. D., J. G. Mottley, J. G. Miller, P. B. Kurnik, and B. E. Sobel. 1982. Detection of ischemic myocardium *in vivo* through the chest wall by quantitative ultrasonic tissue characterization. *American Journal of Cardiology* 50:838-843.

Duck, F. A., and C. R. Hill. 1979. Acoustic attenuation reconstruction from back-scattered ultrasound. Pages 137-148 in *Proceedings of IFIP TC-4 working conference on computer aided tomography and ultrasonics in medicine.* North Holland Publ. Co., New York.

Duerinckx, A. J., L. A. Ferrari, J. C. Hoefs, P. V. Sankar, D. Fleming, and C. Cole-Bueglet. 1986. Estimation of acoustic attenuation in liver using one megabyte of data and the zero-crossings technique. *Ultrasonics* 24:325-332.

Dunn, F. 1975. Ultrasonic attenuation, absorption, and velocity in tissues and organs. Pages 21-28 in M. Linzer, ed. *Ultrasonic Tissue Characterization.* National Bureau of Standards Publication 453. U. S. Government Printing Office, Washington, D.C.

Fink, M., F. Hottier, and J. F. Cordoso. 1983. Ultrasonic signal processing for *in vivo* attenuation measurement: short time Fourier analysis. *Ultrasonic Imaging* 5:117-135.

Flax, S. W. 1984. Non-frequency domain attenuation estimation techniques. Pages 366-375 in J. Ophir et al., Attenuation estimation in reflection: progress and prospects. *Ultrasonic Imaging* 6:349-395.

Flax, S. W., N. J. Pelc, G. H. Glover, F. D. Gutmann, and M. McLachlan. 1983. Spectral characterization and attenuation measurements in ultrasound. *Ultrasonic Imaging* 5:95-116.

Fraser, J., G. S. Kino, and J. Birnholz. 1979. Cepstral signal processing for tissue signature analysis. Pages 287-295 in M. Linzer, ed. *Ultrasonic Tissue Characterization II.* National Bureau of Standards Special Publication 525. U. S. Government Office, Washington, D.C.

Garra, B. S., T. H. Shawker, M. Nassi, M. A. Russell. 1984. Ultrasound attenuation measurements of the liver *in vivo* using a commercial sector scanner. *Ultrasonic Imaging* 6:396-407.

Goss, S. A., R. L. Johnston, and F. Dunn. 1978. Comprehensive compilation of empirical ultrasonic properties of mammalian tissues. *Journal of Acoustic Society of America* 64:423-457.

Goss, S. A., R. L. Johnston, and F. Dunn. 1980. Comprehensive compilation of empirical ultrasonic properties of mammalian tissues. *Journal of Acoustic Society of America* 68:93-108.

Greenleaf, J. F., and S. A. Johnson. 1975. Algebraic reconstruction of spatial distributions of refractive index and attenuation in tissues from time-of-flight and amplitude profiles. Pages 109-119 in M. Linzer, ed. *Ultrasonic Tissue Characterization.* National Bureau of Standards Publication 453. U. S. Government Printing Office, Washington, D.C.

Hagen-Ansert, S. L. 1983. Textbook of Diagnostic Ultrasonography. 2nd ed. C. V. Mosby Co., St. Louis. 683 pp.

Haumschild, D. J., and D. L. Carlson 1983. An ultrasonic Bragg scattering technique for the quantitative characterization of marbling in beef. *Ultrasonics* 21:226-233.

Heath *Zenith.* 1986. Computer Oscilloscope Model IC-4802 Operation/Service Manual. Heath Co., Benton Harbor, Michigan, U. S. A.

Javanaud, C. 1988. Applications of ultrasound to food systems. *Ultrasonics* 26:117-123.

Johnston, E. K., R. L. Hiner, R. H. Alsmayer, L. E. Campbell, W. T. Platt, and J. C. Webb. 1964. Ultrasonic pulse-echo measurement of livestock physical composition. *Transactions of ASAE* 7(3):246-249.

Johnston, R. L., S. A. Goss, V. Maynard, J. K. Brady, L. A. Frizzell, W. D. O'Brien, Jr., and F. Dunn. 1979. Elements of tissue characterization. Part I. Ultrasonic propagation properties. Pages 19-27 in M. Linzer, ed. *Ultrasonic Tissue Characterization II.* National Bureau of Standards Special Publication 525. U. S. Government Printing Office, Washington, D.C.

Jones, J. P. 1984. Summary of current results. Pages 382-386 in J. Ophir et al., Attenuation estimation in reflection: progress and prospects. *Ultrasonic Imaging* 6:349-395.

Jones, J. P., and M. Behrens. 1981. *In vivo* measurement of frequency-dependent attenuation in normal liver, pancreas, and spleen. *Ultrasonic Imaging* 3:205. (abstract only)

Kay, M. S. 1988. Modern Spectral Estimation: Theory and Applications. Prentice Hall, Englewood Cliffs, New Jersey. 543 pp.

Kuc, R. 1980. Clinical application of an ultrasound attenuation coefficient estimation technique for liver pathology characterization. *IEEE Transactions on Biomedical Engineering* BME-27: 312-319.

Kuc, R., and K. J. W. Taylor. 1982. Variation of acoustic attenuation coefficient slope for *in vivo* liver. *Ultrasound in Medicine and Biology* 8:403-412.

Kuc, R. B., and M. Schwartz. 1979. Estimating the acoustic attenuation slope for liver from reflected ultrasound signals. *IEEE Transactions on Sonics and Ultrasonics* SU-26: 353-362.

Kuc, R., M. Schwartz, N. Finby, and F. Dain. 1977. Variance reduction in the characterization of liver using reflected ultrasonic signals. Pages 219-222 in *IEEE ULtrasonics Symposium Proceedings* (IEEE Cat. No. 77CH 1264-1SU).

IEEE, New York.

Lele, P. P., and J. Namery. 1974. A computer based ultrasonic system for the detection and mapping of myocardial infarcts. Page 121 in *1974 San Diego Biomedical Symposium Proceedings 13.* IEEE publications, New York.

Lele, P. P., A. B. Mansfield, A. I. Murphy, J. Namery, and N. Senapati. 1975. Tissue characterization by ultrasonic frequency-dependent attenuation and scattering. Pages 167-196 in M. Linzer, ed. *Ultrasonic Tissue Characterization.* National Bureau of Standards Special Publication 453. U. S. Government Printing Office, Washington, D.C.

Levi, S., and J. Keuwez. 1975. Tissue characterization *in vivo* by differential attenuation measurements. Pages 121-124 in M. Linzer, ed. *Ultrasonic Tissue Characterization II.* National Bureau of Standards Special Publication 525. U. S. Government Printing Office, Washington, D.C.

Linzer, M., and J. E. Norton. 1982. Ultrasonic tissue characterization. *Annual Review of Biophysics and Bioengineering* 2:303-329.

Lizzi, F. L., and M. A. Laviola. 1976. Tissue signature characterization utilizing frequency domain analysis. Pages 714-719 in *1976 IEEE Ultrasonics Symposium Proceedings* (IEEE Cat. No. 76CH 1120-5SU). IEEE, New York.

Maklad, N. F. 1984. Priliminary clinical results and challenges. Pages 356-360 in J. Ophir et al., Attenuation estimation in reflection: progress and prospects. *Ultrasonic Imaging* 6:349-395.

McDicken, W. N. 1976. Diagnostic Ultrasonics: Principles and Use of Instruments. John Wiley and Sons, New York. 320 pp.

Melton, H. E., Jr., and D. J. Skorton. 1981. Rational-gain-compensation for attenuation in ultrasonic cardiac imaging. Pages 607-611 in *1981 IEEE Ultrasonics Symposium Proceedings* (IEEE Cat. No. 81CH 1689-9). IEEE, New York.

Metreweli, C. 1978. Practical Abdominal Ultrasound. William Heinemann Medical Books Ltd., London. 121 pp.

Meyer, C. R. 1979. An iterative parametric spectral estimation technique for high-resolution pulse-echo ultrasound. *IEEE Transactions on Biomedical*

Engineering BME-26:207-212.

Meyer, C. R. 1982. Preliminary results on a system for wideband reflection-mode ultrasonic attenuation imaging. *IEEE Transactions on Sonics and Ultrasonics* SU-29:12-17.

Miles, C. A., and G. A. J. Fursey. 1976. Measurement of the fat content of meat using ultrasonic waves. *Food Chemistry* 2:107-118.

Miles, C. A., G. A. J. Fursey, and R. W. R. York. 1984. New equipment for measuring the speed of ultrasound and its application in the estimation of body composition of farm livestock. Pages 93-105 in D. Lister, ed. *In vitro Measurement of Body Composition in Meat Animals.* Elsevier Applied Science, London.

Miller, J. G. 1984. Frequency domain techniques for the estimation of attenuation in reflection. Pages 360-366 in J. Ophir et al., Attenuation estimation in reflection: progress and prospects. *Ultrasonic Imaging* 6:349-395.

Narayana, P. A., and J. Ophir. 1983a. On the frequency dependence of attenuationm in normal and fatty liver. *IEEE Transactions on Sonics and Ultrasonics* SU-30:379-383.

Narayana, P. A., and J. Ophir. 1983b. On the validity of the linear approximation in parametric measurement of attenuation in tissues. *Ultrasound in Medicine and Biology* 9:357-361.

Narayana, P. A., and J. Ophir. 1983c. A closed form method for the measurement of attenuation in nonlinearly dispersive media. *Ultrasonic Imaging* 5:17-21.

Narayana, P. A., and J. Ophir. 1984. Attenuation estimation: Problems and tradeoffs. Pages 375-382 in J. Ophir et al., Attenuation estimation in reflection: progress and prospects. *Ultrasonic Imaging* 6:349-395.

O'Donnell, M. 1983. Quantitative volume backscatter imaging. *IEEE Transactions on Sonics and Ultrasonics* SU-30:26-36.

Ophir, J., N. F. Maklad, and R. H. Biglow. 1982. Ultrasonic attenuation measurements of *in vivo* human muscle. *Ultrasonic Imaging* 4:290-295.

Ophir, J., T. H. Shawker, N. F. Maklad, J. G. Miller, S. W. Flax, P. A. Narayana,

and J. P. Jones. 1984 Attenuation estimation in reflection: Progress and prospects. *Ultrasonic Imaging* 6:349-395.

Rabinar, L. R., R. W. Schafer, and D. Dlugos. 1979. Periodogram method for power spectrum estimation. Pages 2.1-1 - 2.1-10 in Digital Signal Processing Committee, IEEE Acoustic, Speech, and Signal Processing Society, editors. *Programs for Digital Dignal Processing.* IEEE Press, New York.

Robinson, D. E. Computer spectral analysis of ultrasonic A-mode echoes. 1979. Pages 281-286 in M. Linzer, ed. *Ultrasonic Tissue Characterization II.* National Bureau of Standards Special Publication 525. U. S. Government Printing Office, Washington, D.C.

Shawker, T. H. 1984. Clinical significance of attenuation. Pages 351-356 in J. Ophir et al., Attenuation estimation in reflection: progress and prospects. *Ultrasonic Imaging* 6:349-395.

Shore, D., M. O. Woods, and C. A. Miles. 1986. Attenuation of ultrasound in *post rigor* bovine skeletal muscle. *Ultrasonics* 23:81-87.

Shung, K. Kirk. 1987. General Engineering Principles in Diagnostic Ultrasound. *IEEE Engineering in Medicine and Biology Magazine* 6:7-13.

Wells, P. N. T. 1977. Biomedical Ultrasonics. Academic Press, London.

Wilson, L. S., D. E. Robinson, and B. D. Doust. 1984. Frequency domain processing for ultrasonic attenuation measurement in liver. *Ultrasonic Imaging* 6:278-292.

Woods, M. O., and C. A. Miles. 1986. Ultrasound speed and attenuation in homogenates of bovine skeletal muscle. *Ultrasonics* 24:260-266.

ACKNOWLEDGEMENTS

I would like to express my gratitude to my major professor, Dr. David Carlson, for his excellent guidance and help, especially for setting up the system. Thanks for your confidence in me and saying, "You can do it; think about it "! This helped me a lot in creating confidence in myself for solving engineering problems. I am also thankful to Dr. Donald Young and Dr. Frederick Hembrough for readily serving on my committee. I am appreciative of the Biomedical Engineering Department for helping support my research. I would like to thank all the faculty and students in the department for directly or indirectly teaching me the first principles of biomedical engineering.

I would most like to thank my parents for their undying support and confidence in me. I am also deeply indebted to my brothers and sister-in-law (*bhabhi*) for their encouragement and love. I am very proud and fortunate to have all of them in my life. I dedicate this work to my grandmother (*ba*), who would have been the first person I would have wanted to see after my graduation, but unfortunately is no longer among us. Mere words can not express my admiration, love and gratitude for her, but her encouragement for higher education will always inspire me to strive for excellence.

APPENDIX

Data Acquisition Programs

```
'*********************************************************************
'* Program: ANG-CAL.BAS                          Language: QuickBASIC  *
'* Auther:  Viren R. Amin                                              *
'* Date:    June 15, 1989                                              *
'*               To calibrate the angle-transducer                     *
'*********************************************************************

OPEN "A:\DATA-ACQ\ANG-CAL.DAT" FOR OUTPUT AS #1
CLS : SCREEN 9: COLOR 3

'initialization of Keithley system
Keithley:
   'for relay control slot
    DEF SEG = &HCFF8
    POKE 1, 6

   'for ANALOG-IN from angle-transducer
    DEF SEG = &HCFF8
    POKE 1, 6: POKE 10, 0: POKE 26, 0'ANALOG CHANNEL 0, 1x GAIN

ScreenDisplay:
    LOCATE 3, 20: COLOR 12: PRINT "CALIBRATION OF ANGLE TRANSDUCER"
    COLOR 3
    LOCATE 5, 16: PRINT "Make sure Keithley is set for 0 TO 5 volt"
    LOCATE 7, 19: PRINT "Make sure power supply is plugged in"
    LOCATE 12,15:  PRINT "ARE YOU READY TO BEGIN CALIBRATION (Y/N) ?"
    DO
        A$ = INKEY$: LOCATE 12, 60: PRINT A$
```

```
    LOOP UNTIL (A$ = "y" OR A$ = "Y")
    CLS
    LOCATE 3, 1: PRINT "SET TRANSDUCER AT ANGLE ZERO FOR SCAN"
    LOCATE 4, 1: PRINT "Press any key when done"
    LOCATE 3, 50: COLOR 12: PRINT "POSITION IS  "

111 DO
       AA = PEEK(3): BB = PEEK(2): B =256 *(AA - 240)+ BB
       POKE 24, 0
       LOCATE 3, 62: PRINT B
    LOOP WHILE INKEY$ = ""
    ZeroAngle = B

    COLOR 3
    LOCATE 7, 1 : PRINT "SET TRANSDUCER AT MAXIMUM ANGLE FOR SCAN"
    LOCATE 8, 1: PRINT "Press any key when done"
    LOCATE 7, 50: COLOR 12: PRINT "POSITION IS  "

222 DO
       AA = PEEK(3): BB = PEEK(2): B = 256 * (AA - 240) + BB
       POKE 24, 0
       LOCATE 7, 62: PRINT B
    LOOP WHILE INKEY$ = ""
    MaxAngle = B

    COLOR 3: LOCATE 11, 1
    INPUT "ENTER NUMBER OF DEGREES BETWEEN ZERO AND MAX. ANGLES:  ";
          DiffDeg
    Resolution = ABS(MaxAngle - ZeroAngle) / DiffDeg
    COLOR 12: LOCATE 14, 1
    PRINT "1 DEGREE = "; Resolution, "(Resolution = ";
          Resolution; "/"; "degree)"
    COLOR 7

    PRINT #1, ZeroAngle, MaxAngle, DiffDeg, Resolution
    LOCATE 19, 20: PRINT "  Move transducer back to ZeroAngle"
    LOCATE 20, 20: PRINT "Make sure the stepper motor is powered"
    LOCATE 21, 20: PRINT "    and press any key to continue"
    DO :  LOOP WHILE INKEY$ = ""
```

```
END
```

```
'*****************************************************************
'* Program: SCOPE.BAS                              Language: BASICA  *
'* Date:    June 03, 1989                                            *
'*       Originally provided with Heath Computer Oscilloscope       *
'*   Modified to customize the data-acquisition for this research   *
'*       Only modified or added subroutines are included here       *
'*               Original line numbers are preserved                *
'*****************************************************************

1 'VERSION 2.0
2 'COMPUTER OSCILLOSCOPE - HEATH/ZENITH COMPUTER BASED INSTRUMENTS
4 'REVISED BY BARB ERWIN
5 'MODIFIED BY VIREN R. AMIN (JULY 07,1989)

10 'clear memory above 45000 for Assembly language routines
90 'DEFINE CONSTANTS ************************************************
190 '
191 'for Keithley ... get angle-transducer calibration data
195 OPEN "A:\data-acq\ang-cal.dat" FOR INPUT AS #2
197 INPUT #2, ZEROANGLE, MAXANGLE, DIFFDEG, RESOLUTION!
199 '
200 'DEFINE COMMANDS *************************************************
280 'DEFINE STRING ARRAYS AND FUNCTION POINTER LOCATIONS ***********
510 'BRING IN ASSEMBLY LANGUAGE ROUTINES ***************************
530 ' "MAP.BIN", "UARTINI.BIN", "PLOT.BIN", "GRAT.BIN", "REQ.BIN",
550 ' "REQFRT.BIN", "SEND.BIN", "CKUART.BIN","AVG.BIN",
580 '
590 'MAKE REVERSE VIDEO BLOCKS AND MESSAGES************************
780 'SHOW INTRO SCREEN, HELP MESSAGE,SET BAUD RATE AND COM: CHANNEL*
1110 'INITIALIZE UART **********************************************
1150 'INITIALIZE SCREEN ********************************************
1190 '
1194 MEMORYFLAG = -1
1379 '
1380 '*********** START OF MAIN LOOP ********************************
1390 '
1400 COUNT = 0: COMAND = 0: EROR = 0: FAST = FALSE: I = FRE(""):
     IF WATE = TRUE THEN GOTO 1420
1410 IF Y1Y2>0 AND MODE<4 THEN CALL SEND!(REQMEM,COMM):WATE=TRUE
```

```
1420 CALL CKUART!(COMAND,COMM,EROR)
1423 IF MEMORYFLAG = -1 THEN LOCATE 23, 14:
     PRINT "Press HOME key to start scanning"
1424 IF AVGFLAG = 1 THEN AVGFLAG = 0: AVGCNT = 0:
     GOTO 6270 'store after averaging
1430 IF COMAND = 114 AND WATE = TRUE THEN GOTO 1460
1440 IF COMAND = 115 AND WATE = TRUE THEN COMAND = 0:
     PUT (0, 161), S, PRESET
1450 IF COMAND <> 0 OR EROR <> 0 THEN COMAND = 0: GOTO 1200
     ELSE X$ = "": GOTO 1530
1460 WATE = FALSE: PUT (0, 161), T, PRESET
1470 CALL REQ!(Y1(0),Y2(0),Y1Y2,TRIG,COMM,BAUD,EROR):
     PUT(0,161),BLANK8,PRESET
1480 IF EROR = FALSE THEN GOTO 1490 ELSE GOTO 1530
1490 IF TRIG = 1 THEN MODE = MODE AND 7
1500 PUT (0, 161), BLANK8, PRESET: IF AVGY1 = TRUE OR AVGY2 = TRUE
     THEN GOTO 1690
1505 'LOCATE 22, 43: PRINT "Main loop "; MAINLOOP:
     MAINLOOP = MAINLOOP + 1
1510 X$ = "": GOSUB 3270: GOSUB 1790
1520 ' CHECK FOR COMMANDS AND CLEAR KEYBOARD BUFFER
1530 GOSUB 3270: IF X$ = "" THEN GOTO 1630
1540 IF LEN(X$) <> 2 THEN GOTO 1610
1550 X = ASC(RIGHT$(X$, 1)) - 58

1556 'if HOME is pressed, start SCAN  (go to 10000)
1558 'otherwise allows the settings to be changed
1560 ON X GOSUB 4400, 7040, 5210, 5250, 4980, 4465, 4535, 4900, 2170,
     2170, 7040, 7040, 10000, 2350, 7040, 7040, 3330, 7040, 3320,
     7040, 7040, 2360
1570 IF X = 13 AND PNT = 3 THEN OFFSETY1 = 0: GOSUB 1790:
     COMAND = Y1ZERO: GOTO 1620
1580 IF X = 13 AND PNT = 7 THEN OFFSETY2 = 0: GOSUB 1790:
     COMAND = Y2ZERO: GOTO 1620
1590 IF X = 13 AND PNT = 8 THEN HOFFSET = 0: GOSUB 1790:
     X$ = "": GOTO 1220
1600 IF X = 13 AND PNT = 12 THEN COMAND = TRGZERO: GOTO 1620:
     ELSE X$ = "": GOTO 1530
1610 IF X$ = "?" OR X$ = "/" THEN GOTO 800 ELSE X$ = "": GOTO 1530
```

```
1620 CALL SEND!(COMAND,COMM):EROR=FALSE:COMAND=0:X$="":GOTO 1220
1630 IF Y1Y2 = 0 THEN GOSUB 1790: Y1Y2 = -1
1640 IF Y1Y2 = -1 THEN GOSUB 1860
1650 IF EROR = TRUE THEN EROR = FALSE: GOTO 1200:     ELSE GOTO 1400
1660 '
1670 '********** END OF MAIN LOOP ***********************************
1680 '
1690 AVGCNT = AVGCNT + 1: IF AVGCNT <= AVGNUM THEN GOTO 1710
1700 WATE = TRUE: GOTO 1530
1710 LOCATE 23, 71: PRINT "(avg#"; AVGCNT; ")"
1720 IF AVGY1=TRUE THEN CALL AVG!(Y1(0),Y1SUM(0),AVGCNT)
1730 IF AVGY2=TRUE THEN CALL AVG!(Y2(0),Y2SUM(0),AVGCNT)
1740 IF AVGCNT = AVGNUM THEN WATE = TRUE: AVVGY1 = FALSE:
     AVGFLAG = 1      'avg off
1750 GOTO 1510
1760 '
1770 '***** PLOT SCREEN SUBROUTINE ********************************
2150 '***** F9/F10 SELECT SUBROUTINES ******************************
2330 '***** UP/DOWN ARROW SUBROUTINES ******************************
3300 '***** LEFT/RIGHT ARROW SUBROUTINES ****************************
3730 '***** REQUEST FRONT PANEL SUBROUTINE ***************************
4310 '***** LINE/DOT  GRAT ON/OFF  SUBROUTINES **********************
4450 '***** CURSOR CONTROL SUBROUTINE ******************************
4520 '***** CURSOR SETUP SUBROUTINE ********************************
4880 '***** CHANGE MENU SUBROUTINE *********************************
4950 '***** SCOPE ON/OFF SUBROUTINE ********************************
5040 '***** PRINT MENU SUBROUTINE **********************************
5190 '***** RE-ZERO  MANUAL TRIGGER/RESET SUBROUTINES ***************
5410 '***** RIGHT SIDE SUBROUTINE ***********************************

5600 '***** MEMORY SUBROUTINE ***************************************
5610 '
5620 'KEEP THIS LINE NUMBER .... FOR GOSUB AND GOTO 5620
5622 GOTO 6270
5651 IF MEMORYFLAG > 0 THEN GOTO 6270
6260 LOCATE 23, 1: PRINT SPC(54); : LOCATE 23, 1:
     PRINT "FILENAME? A:\DATA-ACQ\ (4 char max, no extension) "; :
     LINE INPUT DATAFL$: DATAFILE$ = "a:\DATA-ACQ\" + DATAFL$
6262 OPEN "O", 3, (DATAFILE$ + "info.dat")
```

```
6264 PRINT #3, Y1SEN, RATE, INVERTY1, OFFSETY1, HOFFSET: CLOSE #3
6266 LOCATE 23, 1: PRINT SPC(54); : MEMORYFLAG = 0
6267 RETURN
6269 '
6270 IF TRIGCODE$ = "N" THEN MEMORYFLAG = MEMORYFLAG + 1:
     IF MEMORYFLAG < 10 THEN N = 1 ELSE N = 2
6272 LOCATE 23, 59: PRINT (DATAFL$ + "-" + RIGHT$(STR$(MEMORYFLAG),
     N) + TRIGCODE$ + ".dat")
6274 OPEN "O", 1, (DATAFILE$ + "-" + RIGHT$(STR$(MEMORYFLAG), N) +
     TRIGCODE$ + ".dat")
6300 PRINT #1, USING "###.#"; ANGLE!  'angle, relative to start
6310 FOR I = 0 TO 511: PRINT #1, Y1(I); : NEXT I
6320 CLOSE #1: ON ERROR GOTO 0
6380 LOCATE 23, 1: PRINT SPC(54);
6390 GOTO 10000                        'go for next angle


6720 '************ AVERAGING SUBROUTINE ****************************
6730 '
6740 PUT (0, 161), BLANK8, PRESET    'keep this line for calls
6750 LOCATE 21, 10: PRINT SPC(65); : GOSUB 1790:  WATE = FALSE
6844 AVGY1 = TRUE: AVGY2 = FALSE: AVGFLAG = 0
6930 AVGNUM = 9                'no. of averages
6960 ON ERROR GOTO 0: WATE = FALSE     '': GOSUB 5430: GOTO 4710
6967 GOTO 4710
7800 '
7810 '*** TIMER ROUTINE
7820 LOCATE 25, 1: PRINT "<press any key to continue>";
7830 XTX$= INKEY$: T! = TIMER: IF (T! < MT!) AND (XTX$= "") THEN 7830
7840 RETURN

10000 '************************************************************
10002 '**********  STEPPER MOTOR ROUTINE  **************************
10004 ' subroutine for stepper motor and angle transducer
10010 'initialization of Keithley system
10012 IF MEMORYFLAG = -1 THEN GOSUB 6260        'get file name
10014 LOCATE 23, 10:
      PRINT "             Adjust trigger                "
10015 WHILE INKEY$ = "": WEND: LOCATE 23, 20:
```

```
      PRINT "                          "
10017 IF TRIGCODE$ = "N" THEN TRIGCODE$ = "F" ELSE TRIGCODE$ = "N"
10018 IF TRIGCODE$ = "F" THEN GOTO 10400  'do not step for far trig
10020 DEF SEG = &HCFF8: POKE 1, 6    ''for relay control slot

10030 'for ANALOG-IN from angle-transducer
10040 DEF SEG = &HCFF8: POKE 1, 6: POKE 10, 0: POKE 26, 0
      'ANALOG CHANNEL 0, 1x GAIN
10052 LOCATE 22, 64: PRINT "ANGLE "
10054 LOCATE 23, 77: PRINT "0"              'AVG# = 0
10100 STEPPER = STEPPER + 1: IF STEPPER = 4 THEN STEPPER = 0:
      STP = STP + 1
10110 P = 31 - 2 ^ STEPPER: POKE 12, P
10120 XX = STP * 4 + STEPPER
      'check     PRINT USING "###"; XX     'step no.

10129 'angle detection
10130 'delay before detecting the angle
10140  TIME$ = "00": WHILE TIMER < .2: WEND
10160  POKE 24, 0: AA! = PEEK(3): BB! = PEEK(2)    'discard old data
10170  B! = 256 * (AA! - 240) + BB!: POKE 24, 0
10180     ANGLE! = (B! - ZEROANGLE) / RESOLUTION!
10210     LOCATE 22, 70: PRINT USING "###.#"; ANGLE!    ''ANGLE
10250 DEF SEG    'resume original segment .... very important
10320 IF ABS(ANGLE!) > (ABS(DIFFDEG) + 3) THEN
      OPEN "O", 3, "A:\data-acq\fileinfo.dat": PRINT #3, DATAFL$:
      PRINT #3, MEMORYFLAG: CLOSE #3: GOTO 4400
10400 STEPPERFLAG = 1: GOTO 6740    'to avg and then goto main loop
```

Data Analysis Programs

```
'*********************************************************************
'* Program:  ATTENUAT.BAS                Language: QuickBASIC 4.0  *
'* Auther:   VIREN R. AMIN                                         *
'* Date:     July 10, 1989                                         *
'*                                                                 *
'* Main Features: spectrum calculations (two methods)              *
'*                attenuation calculations                         *
'*                                                                 *
'*********************************************************************

'declaration of subroutines and subprograms
DECLARE SUB Plot (PTS() AS SINGLE, Num, Xoff, Yoff, Xmag, Ymag, Clr)
DECLARE SUB FFT (N!, A!(), B!(), INV!)
DECLARE SUB FindSlope (y() AS SINGLE, SamplFreq!)
DECLARE SUB SpctFFT ()
DECLARE SUB SpctAvgPer (DumySig!(),WindowSize!,Overlap!,WindowType!)

'declaration of data types and array dimensions
DIM SHARED Sig(1 TO 1024)  AS SINGLE
DIM SHARED Imag(1 TO 1024), Temp(1 TO 512), Zero(1 TO 512)  AS SINGLE
DIM SHARED SpectrumN(1 TO 512), SpectrumF(1 TO 512)  AS SINGLE
DIM SHARED Mag(1 TO 1024), SpctAvg(1 TO 512) AS SINGLE

DIM SHARED LowFreq, HighFreq, CenterFreq AS SINGLE
DIM SHARED TimeBase, ScanNum AS INTEGER
DIM SHARED WS, WT, OL, LastPoint, Yoffset, Yscale, Xscale

'define F1 for emergency exit
KEY(1) ON: ON KEY(1) GOSUB EndProg

'make sure about proper directories and files
CLS : SCREEN 9: COLOR 2
LOCATE 5, 1: COLOR 3
PRINT "Make sure DIR A: contains:": PRINT
PRINT "\data-acq\*.DAT  as input (signal) files"
PRINT "\spct-FFT\      for spectrum by FFT method (512*2 point FFT)"
PRINT "\spct-win\      for spectrum by averaging Periodograms"
PRINT
```

```
PRINT "output files will be:"
PRINT "         \*.MAG  for spectrum"
PRINT "         \*.DIF  for spectral difference (attenuation)"
PRINT "         \*.SLP  for slope and simple statistics"
LOCATE 23, 20: COLOR 7: PRINT "< Press any key to continue >"
DO WHILE INKEY$ = "": LOOP
CLS

'enter choices and parameters to be changed
INPUT "Do you want to store the results <NO> "; WriteAns$
       WriteAns$ = UCASE$(WriteAns$)
PRINT : PRINT : COLOR 3
PRINT "FOR CALCULATING SLOPE OF ATTENUATION IN BANDWIDTH"
INPUT "Enter lower cut-off frequency of bandwidth <1.00 MHz> ";
       LowFreq
       IF LowFreq = 0 THEN LowFreq = 1.0
INPUT "Enter upper cut-off frequency of bandwidth <3.00 MHz> ";
       HighFreq
       IF HighFreq = 0 THEN HighFreq = 3.0
PRINT
PRINT "FOR CALCULATING ATTENUATION AT CENTER FREQUENCY"
INPUT "Enter the center frequency <2.0> "; CenterFreq
       IF CenterFreq = 0 THEN CenterFreq = 2.0

PRINT : PRINT : COLOR 2
PRINT "Enter choice for SPECTRUM ESTIMATION METHOD <1>"
    PRINT " 1) FFT method  (512*2 point FFT)                  "
    PRINT " 2) averaging periodogram method (with windowing)"
    LOCATE 12, 50: INPUT SpctChoice
    IF SpctChoice = 0 THEN SpctChoice = 1
    IF SpctChoice = 2 THEN
         LOCATE 16, 1: COLOR 3

         PRINT "Do you want to change window parameters <NO> "
         PRINT "(128 point HANNING window with 64 point overlap)"
         LOCATE 16, 48: INPUT WinAns$
         WinAns$ = UCASE$(WinAns$)
              IF WinAns$ = "Y" THEN
                   LOCATE 19, 1
```

```
                INPUT "Window type: 1=R 2=Hm 3=Hn          "; WT
                INPUT "Window size: 2 to 256 (power of 2)  "; WS
                INPUT "Overlap:     0 to 192               "; OL
            ELSE
                WT = 3: WS = 128: OL = 64
            END IF
    ELSE
            WS = 512
    END IF
    Xscale = 512 / WS: MovAvg = WS / 32

'enter the scan-name
CLS : COLOR 7
INPUT "Scan name:     "; ScanF$: ScanF$ = UCASE$(ScanF$)
      IF ScanF$ = "" THEN
           OPEN "I", 3, "A:\DATA-ACQ\FILEINFO.DAT"
           INPUT #3, ScanF$: CLOSE #3    ''ScanF$ = "PRX2"
      END IF
LOCATE 1, 15: ScanF$ = UCASE$(ScanF$): PRINT ScanF$ + SPACE$(8)
OPEN "I", 1, "A:\DATA-ACQ\" + ScanF$ + "INFO.DAT"
      INPUT #1, AmplBase, TimeBase, Junk3, Junk4, Junk5, TotalAscan
CLOSE #1
Yscale = 40

'set amplitude and time bases of the signal
SELECT CASE AmplBase
       CASE 0: Sensitivity = .005        '0 = 5 mV/div
       CASE 1: Sensitivity = .01         '1 = 10 mV/div
       CASE 2: Sensitivity = .02         '2 = 20 mV/div
       CASE 3: Sensitivity = .05         '3 = 50 mV/div
       CASE 4: Sensitivity = .1          '4 = 100 mV/div
       CASE 5: Sensitivity = .2          '5 = 200 mV/div
       CASE 6: Sensitivity = .5          '6 = 500 mV/div
       CASE 7: Sensitivity = 1           '7 = 1 V/div
       CASE 8: Sensitivity = 2           '8 = 2 V/div
       CASE 9: Sensitivity = 5           '9 = 5 V/div
       CASE ELSE: PRINT "Vertical Sensitivity (volt) is not in range"
              GOTO EndProg
END SELECT
```

```
SELECT CASE TimeBase
       CASE 8: SamplFreq = 10            '8=5us/div = 10MHz
       CASE 7: SamplFreq = 25            '7=2us/div = 25MHz
       CASE ELSE: PRINT "Sampling freq. is not 10 or 25 MHz; Enter ";
                  INPUT SamplFreq: LOCATE 2, 1: PRINT SPACE$(50)
END SELECT
ScanNum = 1:   Trigcode$ = "N": Yoffset = 70

'set up screen for signal, spectrum
'and spectral difference display
VIEW (2, 50)-(540, 300), 0, 14
WINDOW SCREEN (-10, -5)-(798, 405)
LINE (-5, 0)-(517, 400), 12, B: PAINT (100, 100), 8, 12
LINE (527, 0)-(793, 400), 12, B: PAINT (600, 100), 8, 12
LOCATE 23, 13: PRINT "SIGNAL  and  SPECTRUM"
LOCATE 23, 48: PRINT "SPECTRAL DIFFERENCE"
LOCATE 23, 70: PRINT "ATTEN:sl/Fc"
LOCATE 23, 1: COLOR 2: PRINT "F1:EXIT"

'read the data-file
GetFile:
    IF ScanNum < 10 THEN N = 1 ELSE N = 2
    DataFl$ = "A:\data-acq\" + ScanF$ + "-" +
              RIGHT$(STR$(ScanNum), N) + Trigcode$ + ".DAT"
    LOCATE 2, 1: COLOR 7: PRINT "Reading file: ";
                 COLOR 12: PRINT DataFl$
    OPEN DataFl$ FOR INPUT AS #1: INPUT #1, Angle
    IF WriteAns$ = "Y" THEN LOCATE 3, 1:  COLOR 7:
                            PRINT "Writing file: " ReadingFile:

i = 0: SumSig = 0
DO: i = i + 1: INPUT #1, Sig(i)
    '128 is offset for 0 volt
    'convert in voltage according to A/D oscilloscope formula
     Sig(i) = (1 / 25) * (Sig(i) - 128) * Sensitivity
    'Sig(i) = (Sig(i) - 128)      'can use this (will give dB offset)
     SumSig = SumSig + Sig(i)
LOOP UNTIL EOF(1)
```

```
CLOSE #1

'remove mean noise from the signal
LastPoint = i
LOCATE 2, 15: COLOR 7: PRINT DataFl$
LOCATE 1, 51: COLOR 7: PRINT "Data-points ="; LastPoint
AvgSig = SumSig / LastPoint
FOR i = 1 TO LastPoint: Sig(i) = Sig(i) - AvgSig: NEXT

'Plot the signal
CALL Plot(Sig(), 512, 1, Yoffset, 1, Yscale, 3)

'calculate the spectrum
IF SpctChoice = 1 THEN
    CALL SpctFFT
ELSE
    CALL SpctAvgPer(Sig(), WS, OL, WT)
END IF

'calculate dB power
FOR i = 1 TO WS
    IF Mag(i) = 0 THEN Mag(i) = .000001
    Mag(i) = 10 * (LOG(Mag(i)) / LOG(10#))  'log base 10
NEXT
CALL Plot(Mag(), WS, 1, 270, Xscale, 2, 0)

'low-pass filter for spectral smoothing
'taking averages of neighbouring values in | X(f)^2 |
'i.e.  32 point moving average ... for smoothing
'      (32 is approximately the number of degrees of freedom)
'MovAvg = WS/2       (-15 ... 0 ... +16 = 32)
MovAvg2 = MovAvg / 2
FOR i = 1 TO WS
     Temp = 0: Temp(i) = 0
     xx = i - MovAvg2 + 1: yy = i + MovAvg2: zz = MovAvg
     IF i <= MovAvg2 THEN xx = 1: yy = MovAvg2+i:  zz = MovAvg2+i
     IF i > (WS - MovAvg2) THEN xx = i - MovAvg2 + 1: yy = WS:
                                zz = MovAvg2 + WS - i
```

```
     FOR j = xx TO yy: Temp = Temp + Mag(j): NEXT
     Temp(i) = Temp / zz
     IF Trigcode$ = "N" THEN SpectrumN(i) = Temp(i)
                        ELSE SpectrumF(i) = Temp(i)
NEXT
CALL Plot(Temp(), WS, 1, 270, Xscale, 2, 10)

'store the spectrum if choosen to
WritingFile:
    IF WriteAns$ = "Y" THEN
         SpectrumFl$ = "A:\spct-FFT\" + ScanF$ + "-" +
                        RIGHT$(STR$(ScanNum), N) + Trigcode$ + ".MAG"
         LOCATE 3, 15: COLOR 12: PRINT SpectrumFl$
         OPEN "O", 3, SpectrumFl$
               FOR i = 1 TO WS: PRINT #3, Temp(i): NEXT
         CLOSE #3
         LOCATE 3, 15: COLOR 7: PRINT SpectrumFl$
    END IF

'log-spectral difference,
'if both near and far spectra are calculated
IF Trigcode$ = "F" THEN
    ERASE Temp
    FOR i = 1 TO WS: Temp(i) = SpectrumN(i) - SpectrumF(i):  NEXT

   'Plot the spectrum-difference in the right window
    CALL Plot(Temp(), WS, 532, (20 + 20*ScanNum), Xscale/2, 1, 10)

    IF WriteAns$ = "Y" THEN
         SpctDiffFl$ = "A:\spct-FFT\" + ScanF$ + "-" +
                        RIGHT$(STR$(ScanNum), N) + ".DIF"
         LOCATE 3, 15: COLOR 12: PRINT SpctDiffFl$ + " "
         OPEN "O", 5, SpctDiffFl$
             FOR i = 1 TO WS: PRINT #5, Temp(i): NEXT
         CLOSE #5
         LOCATE 3, 15: COLOR 7: PRINT SpctDiffFl$ + " "
    END IF
    CALL FindSlope(Temp(), SamplFreq)
```

```
   'clear the left window for new signal
    LINE (-5, 0)-(517, 400), 12, B: PAINT (100, 100), 8, 12
    PAINT (100, 70), 8, 12: PAINT (100, 170), 8, 12
    PAINT (100, 220), 8, 12: PAINT (100, 270), 8, 12
    PAINT (100, 320), 8, 12: PAINT (100, 370), 8, 12
    ScanNum = ScanNum + 1: Trigcode$ = "N": Yoffset = 70
ELSE
    Trigcode$ = "F": Yoffset = 170
END IF

IF ScanNum <= TotalAscan THEN GOTO GetFile
PALETTE 8, 0     'clear the background color for print screen

'end if done, or if F1 is pressed
EndProg: DO WHILE INKEY$ = "": LOOP
END
```

```
'*****************************************************************
'* Subroutine   FFT                                              *
'* Implements the discrete Fourier transform of a complex signal *
'*        using radix-2 Fast Fourier Transform algorithm         *
'*               with decimation-in-time approach                *
'*                                                               *
'*****************************************************************
SUB FFT (N, A(), B(), INV)
        'A() = real part
        'B() = imaginary part
        'N   = size of FFT (power of 2: N=2**M, M=1,2,...,15)
        'INV = -1 for direct DFT
        '    =  1 for inverse DFT

        DIM UA(N), UB(N)
        PI = 3.141592653#: M = LOG(N) / LOG(2)        'N = 2^M
        LOCATE 2, 52: COLOR 12: PRINT "FFT-Points ="; : PRINT N

BitReversal:
        N1 = N - 1: N2 = INT(N / 2): j = 1
        FOR i = 1 TO N1
                IF i >= j THEN GOTO Fft100
                TA = A(j):       TB = B(j)
                A(j) = A(i):     B(j) = B(i)
                A(i) = TA:       B(i) = TB
Fft100:         k = N2
Fft200:         IF k >= j THEN GOTO Fft430
                j = j - k: k = INT(k / 2)
                GOTO Fft200

Fft430:         j = j + k
        NEXT i

FFTLoop:
        FOR L = 1 TO m        ' (N=2^K)
            LE = 2 ^ L: L2 = INT(LE / 2)
            UA(1) = 1:    UB(1) = 0
            WA = COS(PI / L2): IF ABS(WA) < 1E-08 THEN WA = 0
            WB = INV * SIN(PI / L2): IF ABS(WB) < 1E-08 THEN WB = 0
```

```
            FOR G = 1 TO L2
                FOR H = G TO N STEP LE
                        IP = H + L2
                        VA = A(IP) * UA(G) - B(IP) * UB(G)
                        VB = B(IP) * UA(G) + A(IP) * UB(G)

                        A(IP) = A(H) - VA
                        B(IP) = B(H) - VB
                        A(H) = A(H) + VA
                        B(H) = B(H) + VB
                NEXT H
                UA(G + 1) = UA(G) * WA - UB(G) * WB
                UB(G + 1) = UB(G) * WA + UA(G) * WB
            NEXT G
        NEXT L
        IF INV = 1 THEN  '(i.e., inverse FFT)
            FOR i = 1 TO N
                A(i) = A(i) / N
                B(i) = B(i) / N
            NEXT
        END IF
        FOR i = 1 TO N: Mag(i) = (1 / N) * (A(i)^2 + B(i)^2): NEXT

       'CALL Plot(MAG(), N / 2, 10, 250, 2, 1 / 50, 9)
       'FOR PHASE ...   add here
        LOCATE 2, 52: COLOR 7: PRINT "FFT-Points ="; : PRINT N
END SUB
```

```
'*****************************************************************
'* Subroutine   FindSlope                                        *
'* Calculates least square slope of the log-spectral difference, *
'*    attenuation at center frequency, and related quantities    *
'*                                                               *
'*****************************************************************
SUB FindSlope (y() AS SINGLE, SamplFreq AS SINGLE)
       '      Y() = log-spectral difference
       'SamplFreq = sampling frequency
       'discrete frequencies for 512 samples are calculated
       'from sampling frequency

        SHARED ScanNum AS INTEGER, WriteAns$, ScanF$, N, WS
        SHARED LowFreq AS SINGLE, HighFreq, CenterFreq AS SINGLE
        DIM x(1 TO WS) AS SINGLE

        z = (SamplFreq / 2) / WS                    'freq resolution

'bandwidth cut-off frequencies
       '1.0 MHz to 3.0 MHz default  (CINT for rounding)
        LowPoint = CINT(LowFreq / z): HighPoint = CINT(HighFreq / z)
        COLOR 5
        LINE ((532 + LowPoint * Xscale / 2), 1)-
             ((532 + LowPoint * Xscale / 2), 398), 0
        LINE ((532 + HighPoint * Xscale / 2), 1)-
             ((532 + HighPoint * Xscale / 2), 398), 0
        LOCATE 1, 72: PRINT LowPoint: LOCATE 3, 72: PRINT HighPoint

'calculate attenuation at center frequency
        CenterPoint = CenterFreq / z
        LOCATE 2, 72: PRINT CenterPoint
        COLOR 5
        LINE ((532 + CenterPoint * Xscale / 2), 1)-
             ((532 + CenterPoint * Xscale / 2), 398), 0

        CenterAtten = 0
        FOR i = (CenterPoint - 3) TO (CenterPoint + 3)
            CenterAtten = CenterAtten + y(i)    ': LPRINT y(i)
        NEXT
```

```
        CenterAtten = CenterAtten / 7
       'LPRINT : LPRINT : LPRINT CenterAtten
        COLOR 2 :  LOCATE 11 + ScanNum, 69: PRINT ScanNum;
        LOCATE , 72: PRINT ")";: PRINT USING "+##.####"; CenterAtten


'calculate least square slope of the attenuation
        SumX = 0: Sumy = 0
        sumx2 = 0: sumy2 = 0: sumxy = 0
        FOR i = LowPoint TO HighPoint
                x(i) = i * z
                SumX = SumX + x(i): sumx2 = sumx2 + (x(i) ^ 2)
                Sumy = Sumy + y(i): sumy2 = sumy2 + (y(i) ^ 2)
                sumxy = sumxy + (x(i) * y(i))
        NEXT

       'for average over bandwidth
        yyy = Sumy / (HighPoint - LowPoint + 1)
        LOCATE 17 + ScanNum, 69: PRINT ScanNum;
        LOCATE , 72: PRINT ")";
        PRINT USING "+##.####"; yyy

        NP = HighPoint - LowPoint + 1: Meanx = SumX / NP:
                                       Meany = Sumy / NP
        xx = sumx2 - ((SumX ^ 2) / NP)
        yy = sumy2 - ((Sumy ^ 2) / NP)
        xy = sumxy - ((SumX * Sumy) / NP)

        Slope = xy / xx
        Intercept = Meany - (Slope * Meanx)
        Corr = xy / SQR(xx * yy)
        'Devx = SQR(sumx2 - ((SumX ^ 2) / NP))
        'Varx = Devx ^ 2
        'Devy = SQR(sumy2 - ((Sumy ^ 2) / NP))
        'Vary = Devy ^ 2

        LOCATE 4 + ScanNum, 69: PRINT ScanNum;
        LOCATE , 72: PRINT ")";
        PRINT USING "+##.####"; Slope
```

```
'write the results in appropriate file
        IF WriteAns$ = "Y" THEN
            SlopeFl$ = "A:\spct-FFT\" + ScanF$ + "-" +
                        RIGHT$(STR$(ScanNum), N) + ".SLP"
            LOCATE 3, 15: COLOR 12: PRINT SlopeFl$; "    "
            OPEN "O", 7, SlopeFl$

            PRINT #7, SlopeFl$: PRINT #7, "------------------------"
            PRINT #7, "Bandwidth LOW  (freq, points) = "; LowFreq,
                                                          LowPoint
            PRINT #7, "Bandwidth HIGH (freq, points) = "; HighFreq,
                                                          HighPoint
            PRINT #7,
            PRINT #7, "Mean (freq, power)  = "; Meanx, Meany
            PRINT #7, "Dev  (freq, power)  = "; Devx, Devy
            PRINT #7, "Var (freq, power)   = "; Varx, Vary
            PRINT #7, "Corrrelation        = "; Corr
            PRINT #7,
            PRINT #7, "Slope               = "; Slope
            PRINT #7, "Intercept           = "; Intercept
            CLOSE #7
            LOCATE 3, 15: COLOR 7: PRINT SlopeFl$
        END IF

END SUB
```

```
'*****************************************************************
'* Subroutine   Plot                                             *
'*    Plots the signal with specified length and magnification   *
'*                                                               *
'*****************************************************************
SUB Plot (PTS() AS SINGLE, Num, Xoff, Yoff, Xmag, Ymag, Clr)
        'PTS() = signal points
        'Num   = number of points
        'Xoff  = X-axis offset (vertical position on the screen)
        'Yoff  = Y-axis offset (horizontal position on the screen)
        'Xmag  = X-axis magnification
        'Ymag  = Y-axis magnification
        'Clr   = COLOR number (1 to 15)

         DIM xx(Num), yy(Num)
         xx(0) = Xoff + INT(1 * Xmag)
         yy(0) = Yoff - INT(PTS(1) * Ymag)
         FOR i = 1 TO Num
             xx(i) = Xoff + INT(i * Xmag)
             yy(i) = Yoff - INT(PTS(i) * Ymag)
             LINE (Xoff, Yoff)-(Xoff + Num * Xmag, Yoff), 4  'X-axis
             LINE (xx(i - 1), yy(i - 1))-(xx(i), yy(i)), Clr
         NEXT
END SUB


'*****************************************************************
'* Subroutine   SpctFFT                                          *
'*          spectrum calculation by simple FFT method            *
'*                                                               *
'*****************************************************************
SUB SpctFFT
         FOR i = 1 TO 1024: Imag(i) = 0: NEXT
         FOR i = 513 TO 1024: Sig(i) = 0: NEXT
         CALL FFT(1024, Sig(), Imag(), -1)        'direct FFT
         CALL Plot(Mag(), 512, 1, 270, 1, 50, 0)
END SUB
```

```
'*****************************************************************
'* Subroutine   SpctAvgPer                                       *
'*     spectrum calculation by averaging Periodogram method      *
'*                                                               *
'*****************************************************************
SUB SpctAvgPer (DumySig!(), WindowSize!, Overlap!, WindowType!)
        'DumySig()   = signal points
        'WindowSize = size of window ( or segment)
        'Overlap    = Number of overlaping points
        'WindowType = 1 for Rectangular window
        '           = 2 for Hamming window
        '           = 3 for Hanning window

    DIM spectrum(10, 256) AS SINGLE
    DIM Hwindow(1 TO WindowSize)
    SHARED WS, OL, WT

    IF WindowType > 1 THEN
       TwoPI = 8! * ATN(1!)
       IF WindowType = 2 THEN aa=.54: bb = .46 ELSE aa = .5:  bb = .5
       FOR i = 1 TO WindowSize
           Hwindow(i) = aa - bb * COS(TwoPI * (i-1) / (WindowSize-1))
       NEXT
       CALL Plot(Hwindow(), WindowSize,1, Yoffset, 1, Yscale, 13)
    END IF

    NumWindows = LastPoint / (WindowSize - Overlap)
    NumWindows = INT(NumWindows)
   'PRINT "Number of Windows = "; NumWindows

SegmentingLoop:
    FOR k = 1 TO NumWindows - 1              'discard last window
                                             'k=window number
        j = 0                                'j=segment-data subscript
        Start = (k - 1) * (WindowSize - Overlap) + 1
        Finish = Start + WindowSize - 1

        FOR i = Start TO Finish              'i=signal-data subscript
            j = j + 1
```

```
        IF i > LastPoint THEN           'if no more points, then
            Temp(j) = 0                 'pad with zeros
        ELSE
            IF WindowType > 1 THEN
               Temp(j) = DumySig(i) * Hwindow(j)
            ELSE
               Temp(j) = DumySig(i)
            END IF
        END IF
     NEXT i
    'check by Ploting
     CALL Plot(Temp(), WindowSize, Start, Yoffset, 1, Yscale,
               13 + k MOD 2)

    'pad 128-point segment with 128-point zeros
    'so, FFT spectra contain 128 points for positive frequencies
     FOR m = WindowSize + 1 TO WindowSize * 2: Temp(m)=0: NEXT

     ERASE Zero                              'clear imag. part
     CALL FFT(WindowSize * 2, Temp(), Zero(), -1)  'direct FFT
    'CALL Plot(Mag(), WindowSize, Start, Yoffset,1,Yscale, 12)

     FOR i = 1 TO WindowSize: spectrum(k, i) = Mag(i): NEXT i

NEXT k

IF WritePrompt$ = "Y" THEN
   OPEN "A:\segments\WIN-INFO.DAT" FOR OUTPUT AS #3
       PRINT #3, "Total data-points", LastPoint
       PRINT #3, "Window type (1=R, 2=Hm, 3=Hn)", WindowType
       PRINT #3, "Window-Size (points)", WindowSize
       PRINT #3, "Overlapping points", Overlap
       PRINT #3, "Total segments generated", NumWindows
   CLOSE #3
END IF

'calculate the average of windowed spectra.
'SpctAvg(i) contains the average power spectrum
FOR i = 1 TO WindowSize
```

```
        Accumulator = 0
        FOR k = 1 TO NumWindows - 1    ' discard last window
           'SpctAvg(k, I) = Spectrum(k, I) + Spectrum(k + 1, I)
            Accumulator = Accumulator + spectrum(k, i)
        NEXT k
        SpctAvg(i) = Accumulator / (NumWindows - 1)
        Mag(i) = SpctAvg(i)
    NEXT i
   'CALL Plot(SpctAvg(), WindowSize, 300, 320, 2, 50, 14)

END SUB
```

```
'*****************************************************************
'* Program:  STDDEV.BAS                                          *
'* calculates mean and standard deviation across A-line results  *
'*                                                               *
'*****************************************************************
        DIM x(25)
        CLS : PRINT "Enter the values one by one <0 to end> "
        i = 1

Start:  PRINT i; ")  "; : INPUT x(i)
        IF x(i) <> 0 THEN i = i + 1:   GOTO Start
        N = i - 1: PRINT "N = "; N

        Sum = 0
        FOR i = 1 TO N: Sum = Sum + x(i): NEXT
        Avg = Sum / N

        FOR i = 1 TO N
            sumx = sumx + (x(i) - Avg) ^ 2
        NEXT
        StdDev = SQR(sumx / (N - 1))
        PRINT : PRINT
        PRINT "Mean      = "; Avg
        PRINT "Std. Dev. = "; StdDev

End:    END
```